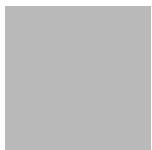



PAUL SCHERRER INSTITUT



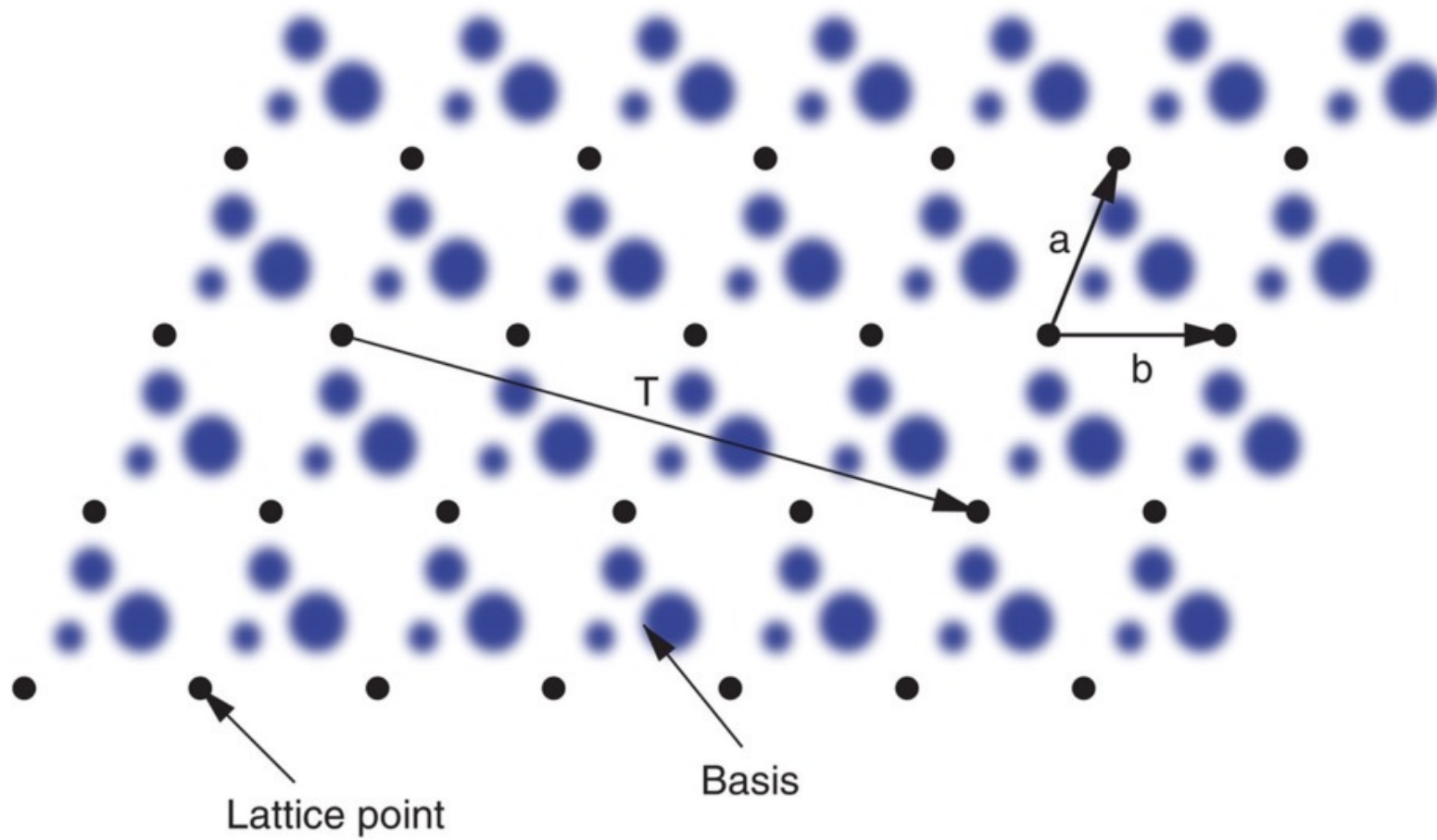
Materials Science at Large Scale Facilities

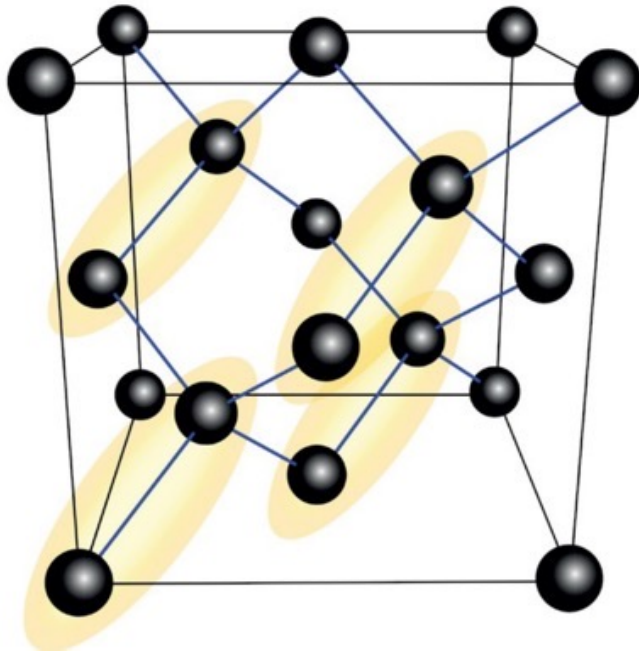
Diffraction



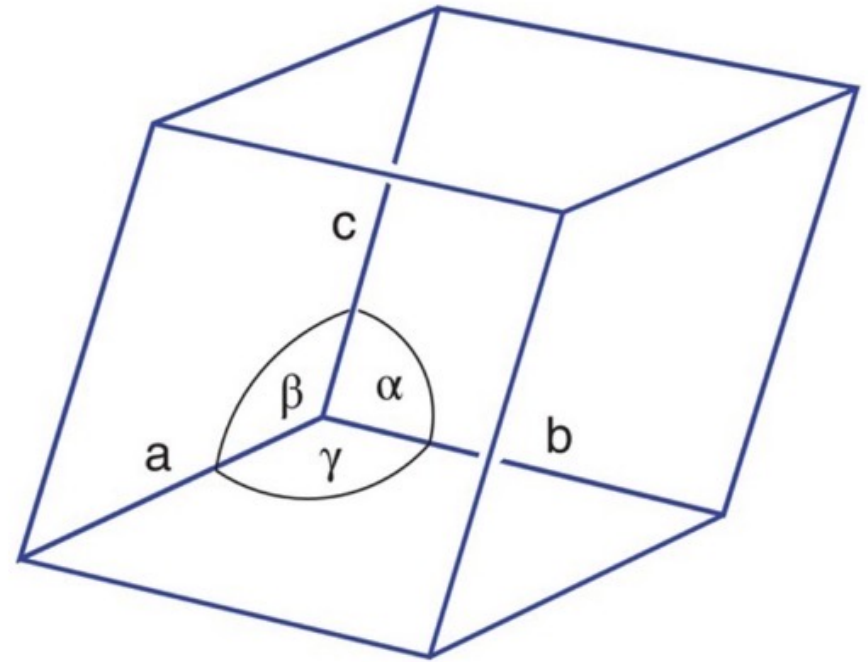
- 
- A bit of crystallography
 - Diffraction basics
 - Diffraction methods + applications
 - Laue / rotating crystal
 - Powder diffraction
 - Pair distribution function
 - Energy dispersive
 - Neutron time-of-flight
 - Surface x-ray diffraction

Crystal structure



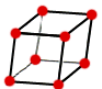
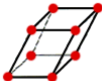
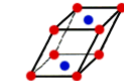
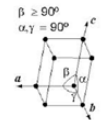
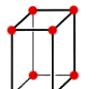
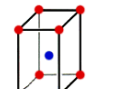
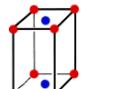
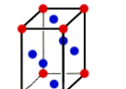
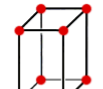
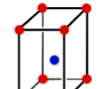


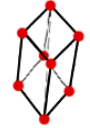
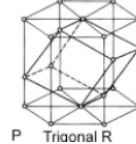
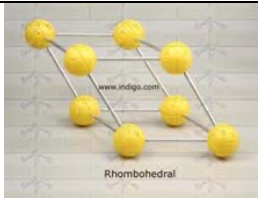
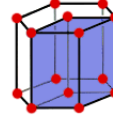
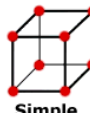
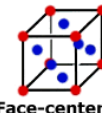

The crystal structure of diamond



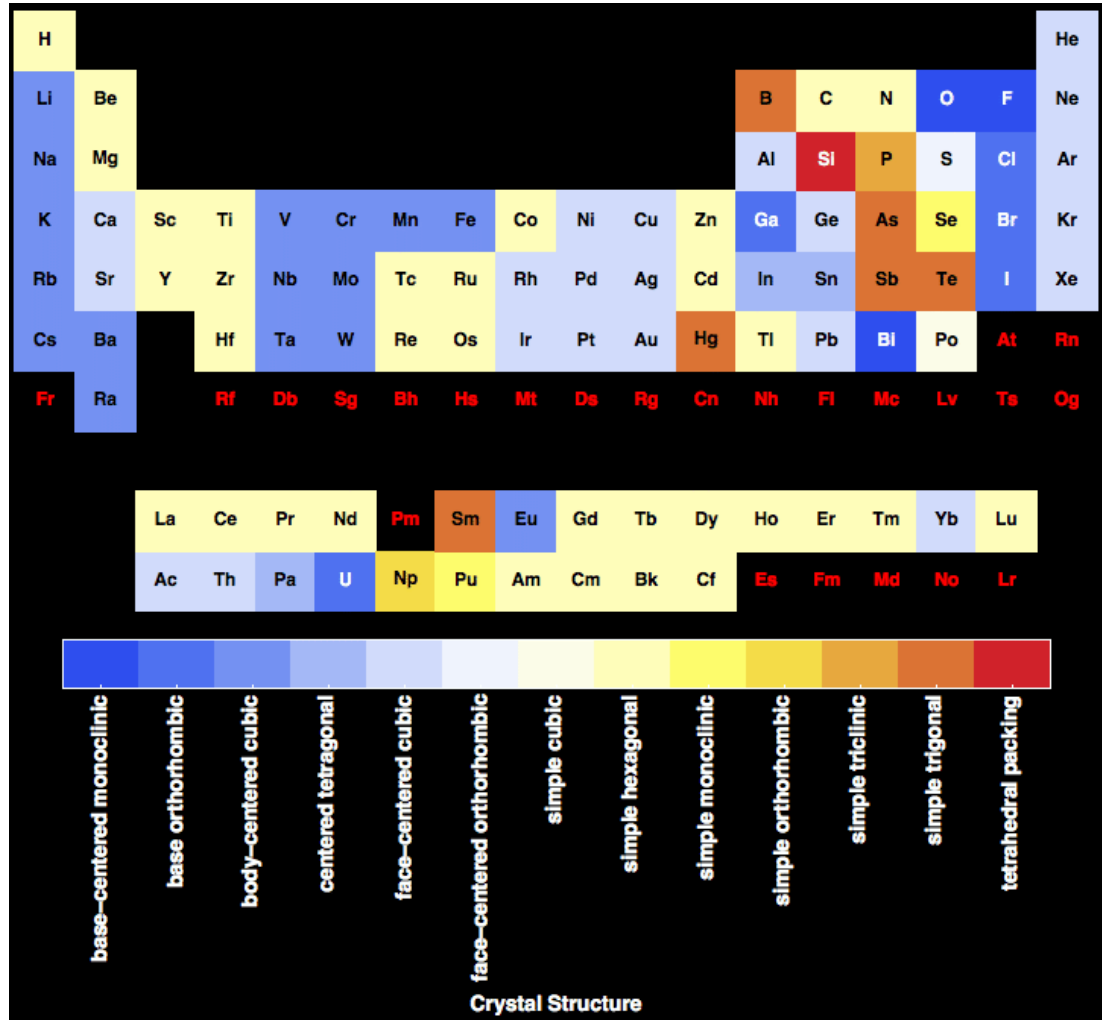
Crystal unit cell

Crystal structure – Bravais lattices

Crystal system	The 14 Bravais lattices	Defining symmetry
Triclinic $a \neq b \neq c$ $\alpha \neq \beta \neq \gamma \neq 90^\circ$	 Triclinic	1-fold axis
Monoclinic $a \neq b \neq c$; $\alpha = \gamma = 90^\circ$; $\beta \neq 90$	 Simple Monoclinic  Base-centered monoclinic 	2-fold axis
Orthorhombic $a \neq b \neq c$ $\alpha = \beta = \gamma = 90^\circ$	 Simple orthorhombic  Body-centered orthorhombic  Base-centered orthorhombic  Face-centered orthorhombic	3 x 2 fold axis
Tetragonal $a = b \neq c$ $\alpha = \beta = \gamma = 90^\circ$	 Simple tetragonal  Body-centered tetragonal	4-fold axis

Rhombohedral (trigonal) $a = b = c$ $\alpha = \beta = \gamma \neq 90^\circ$	 Rhombohedral  P Trigonal R  Rhombohedral	3-fold axis
Hexagonal $a = b \neq c$ $\alpha = \beta = 90^\circ, \gamma = 120^\circ$	 Hexagonal	6-fold axis
Cubic $a = b = c$ $\alpha = \beta = \gamma = 90^\circ$	 Simple cubic  Face-centered cubic  Body-centered cubic	4 x 3-fold axis

Crystal structure – Bravais lattices

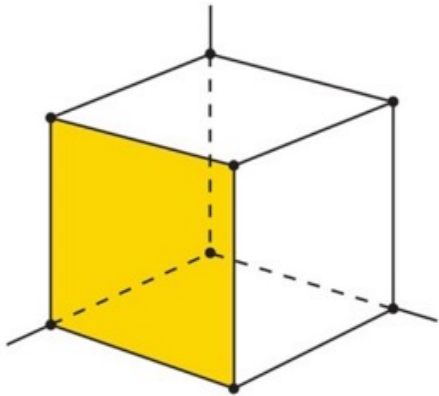


- Volume unit cell:

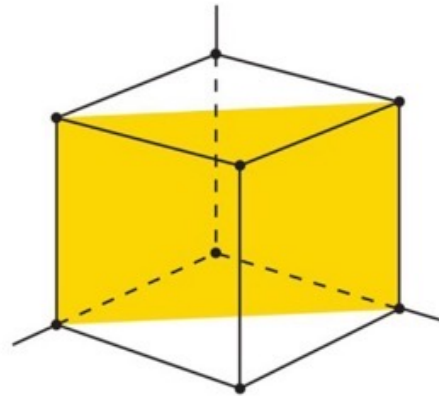
$$V_c = |\mathbf{a} \cdot \mathbf{b} \times \mathbf{c}|.$$

$$V_c = abc(1 + 2 \cos \alpha \cos \beta \cos \gamma - \cos^2 \alpha - \cos^2 \beta - \cos^2 \gamma)^{1/2}.$$

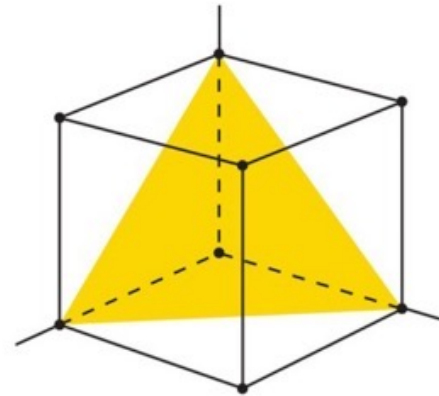
Miller indices - planes



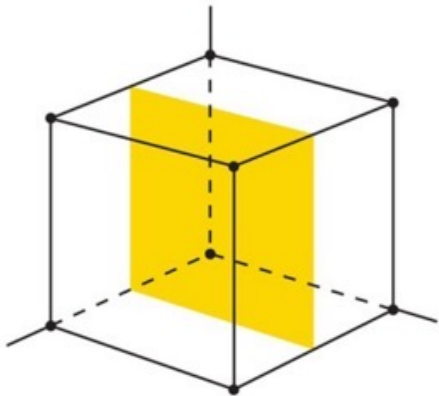
(100)



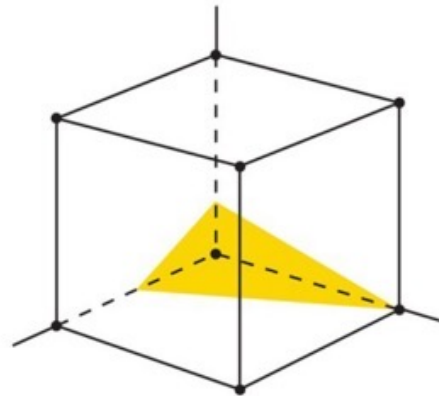
(110)



(111)

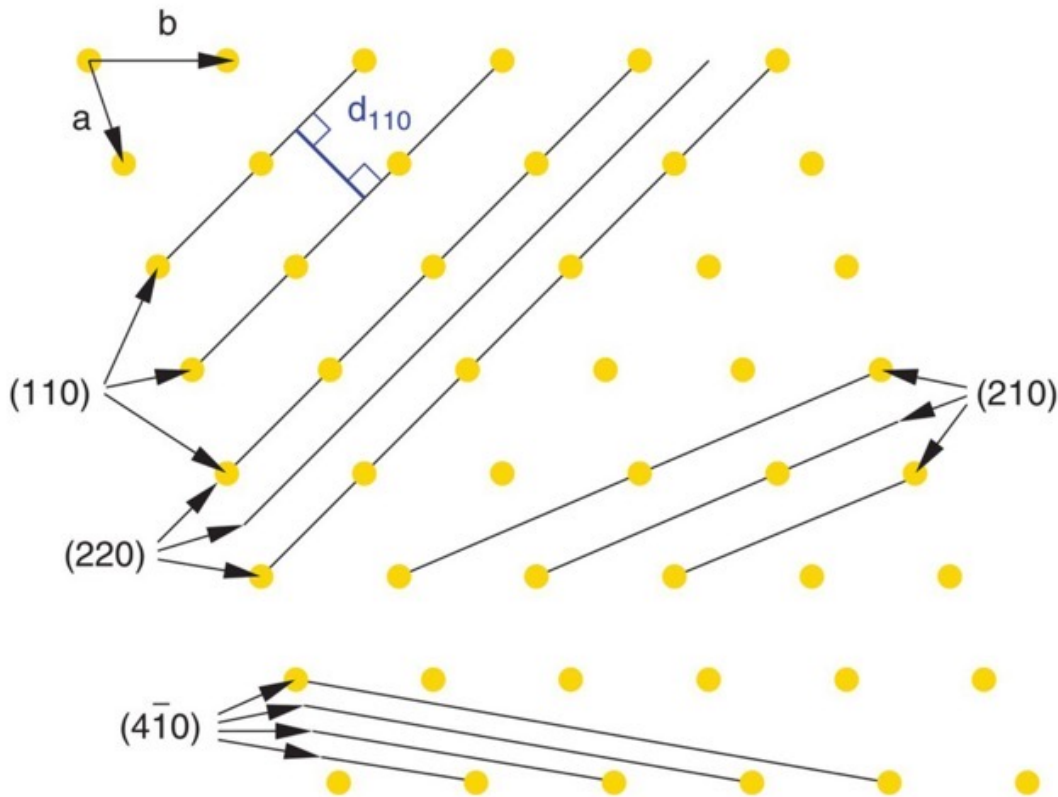


(200)



$$\frac{h}{a}x + \frac{k}{b}y + \frac{l}{c}z = C$$

Miller indices - planes



General case

$$d_{hkl} = \frac{X}{Y},$$

$$X = [1 - \cos^2\alpha - \cos^2\beta - \cos^2\gamma + 2 \cos\alpha \cos\beta \cos\gamma]^{1/2}$$

$$Y = \left[\left(\frac{h}{a}\right)^2 \sin^2\alpha + \left(\frac{k}{b}\right)^2 \sin^2\beta + \left(\frac{l}{c}\right)^2 \sin^2\gamma - \frac{2kl}{bc} (\cos\alpha - \cos\beta \cos\gamma) - \frac{2lh}{ca} (\cos\beta - \cos\gamma \cos\alpha) - \frac{2hk}{ab} (\cos\gamma - \cos\alpha \cos\beta) \right]^{1/2}.$$

Cubic unit cell

$$d_{hkl} = \frac{a}{\sqrt{h^2 + k^2 + l^2}}$$

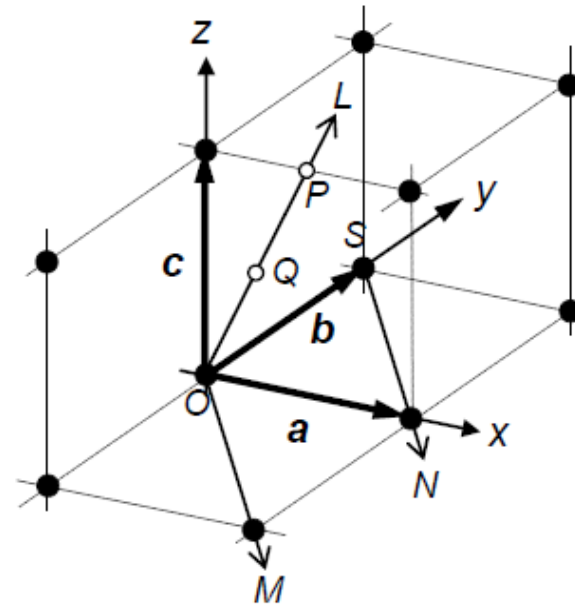
Miller indices - multiplicity

- Miller indices of the set of all planes that are equivalent by symmetry of the lattice: $\{hkl\}$
- Be careful! The multiplicity depends on the symmetry, so on the crystal system
- Example:
 - multiplicity of $\{100\}$ plane in cubic system = 6
(100), (010), (001), (-100), (0-10), (00-1)
 - multiplicity of $\{001\}$ plane in tetragonal system = 2
(001), (00-1)
 - multiplicity of $\{100\}$ plane in tetragonal system = 4
(100), (-100), (010), (0-10)

Miller indices - directions

*Direction OP:*Coordinates point P: $\frac{1}{2}, 0, 1$ Vector $OP = \frac{1}{2} \mathbf{a} + \mathbf{c}$ or $[\frac{1}{2} 0 1]$ or $[1 0 2]$ Coordinates point Q: $\frac{1}{2}, 0, \frac{1}{2}$ Vector $OQ = \frac{1}{4} \mathbf{a} + \frac{1}{2} \mathbf{c}$ or $[\frac{1}{4} 0 \frac{1}{2}]$ or $[1 0 2]$ *Direction SN*

consider OM which is parallel to SN

Coordinates OM: $1, -1, 0$ Vector $OM = \mathbf{a} - \mathbf{b}$ Direction SN and OM: $[1-10]$ 

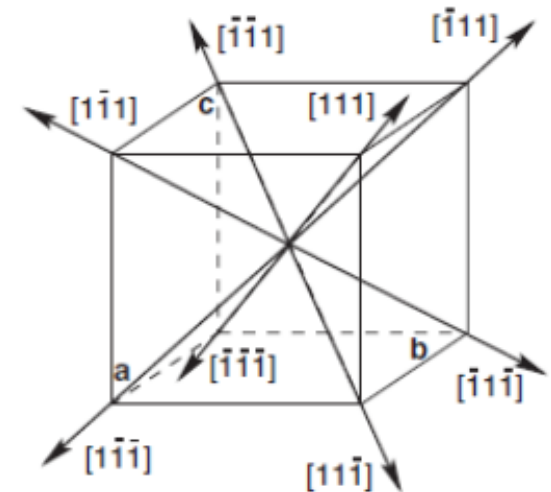
Miller indices - directions

Due to the symmetry of crystal systems, different directions can be equivalent. e.g. For cubic crystals, the directions $[1\ 0\ 0]$, $[-1\ 0\ 0]$, $[0\ 1\ 0]$, $[0\ -1\ 0]$, $[0\ 0\ 1]$, $[0\ 0\ -1]$ are all equivalent by symmetry. There is a special notation for directions of the same form: $\langle 100 \rangle$, which in this case means the family made of the three basis axis **a, b, c**

Similarly, there are 8 equivalent $\langle 111 \rangle$ directions in a cubic system. The number of equivalent directions is called the multiplicity of the direction.

The angle between the directions $[u_1\ v_1\ w_1]$ and $[u_2\ v_2\ w_2]$ is:

$$\cos \vartheta = \frac{u_1 u_2 + v_1 v_2 + w_1 w_2}{\sqrt{u_1^2 + v_1^2 + w_1^2} \cdot \sqrt{u_2^2 + v_2^2 + w_2^2}}$$



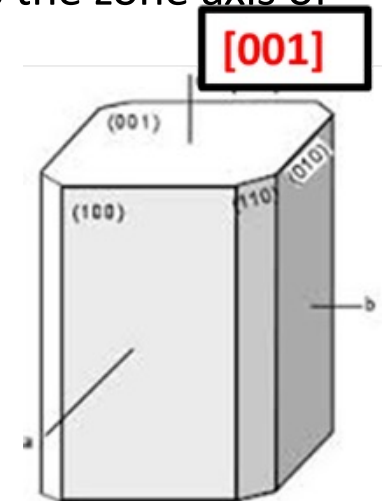
Miller indices – directions/planes

In the cubic system the (hkl) plane and the vector $[hkl]$ are normal to one another but this characteristic is unique to the cubic crystal system and does not apply to crystal systems of lower symmetry.

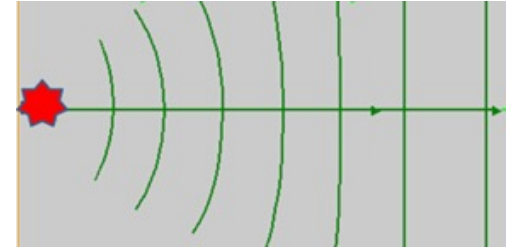
A zone is defined as “a set of planes in a crystal whose intersections are parallel”. The common direction of the intersections is called the zone axis. Therefore, one often has to calculate the intersection of two planes. For instance, the $[001]$ direction is the zone axis of the $\{100\}$ and $\{110\}$ family of planes.

The bright diffraction spots you see correspond to lattice planes (hkl) that belong to the zone axis of observation. Example:

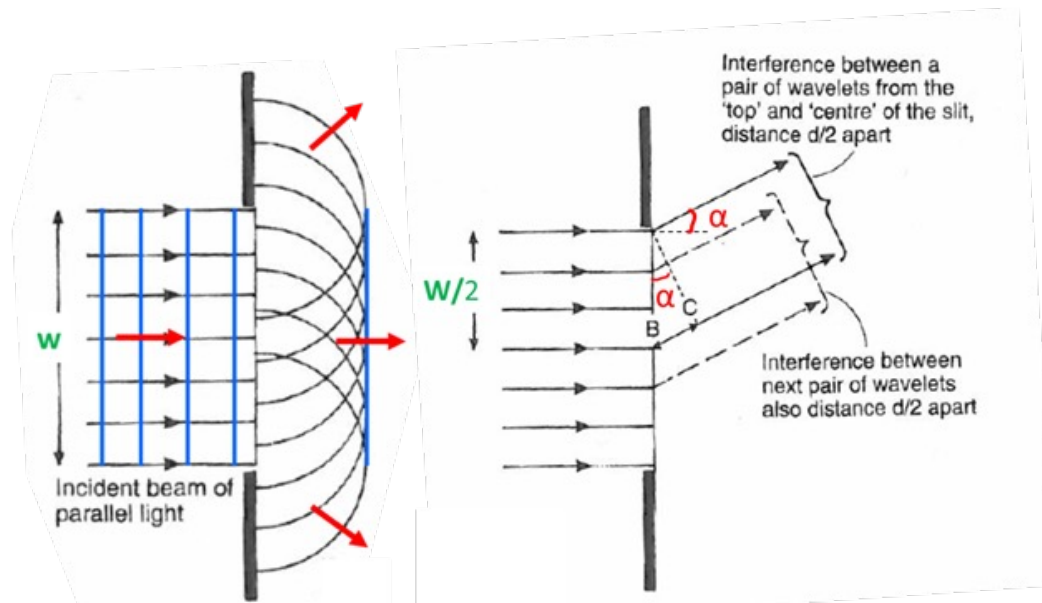
If you align the crystal so that the electron beam is along $[001]$, you get a $[001]$ zone axis pattern. It shows reflections $(hk0)$, because those planes are perpendicular to $[001]$.



Interference



- Electromagnetic wave far away from the source: flat wavefront
- Single slit (Huygens' Principle)
 - Every point on a wavefront acts as a source of secondary spherical wavelets.
 - The new wavefront is the tangent envelope of all these wavelets.
 - Explains reflection, refraction, diffraction, and interference.
 - Basis for Fresnel diffraction and the concept of scattering in crystallography.



Destructive interference when:

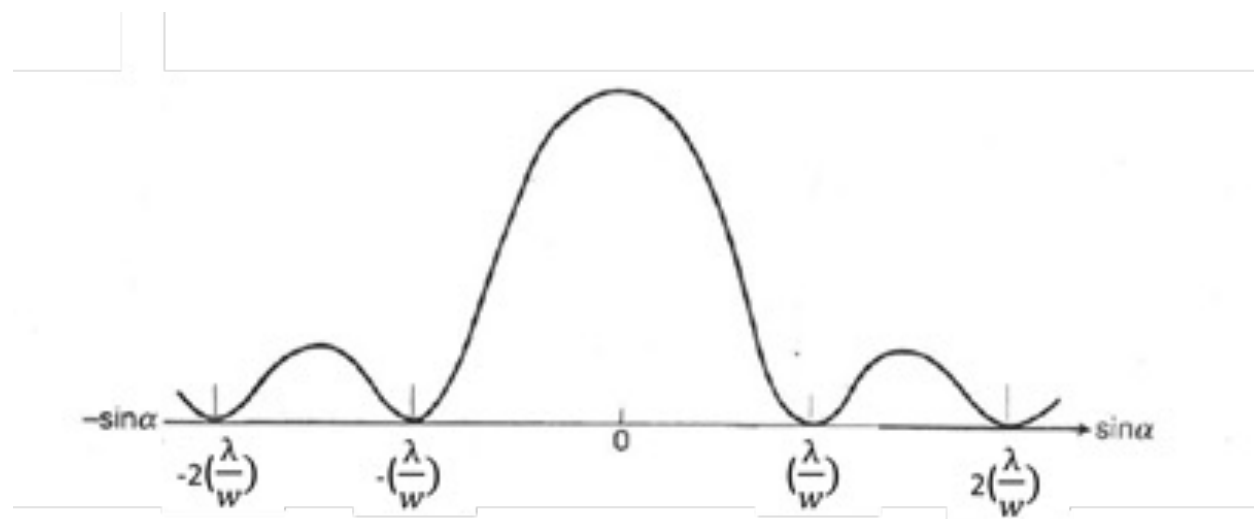
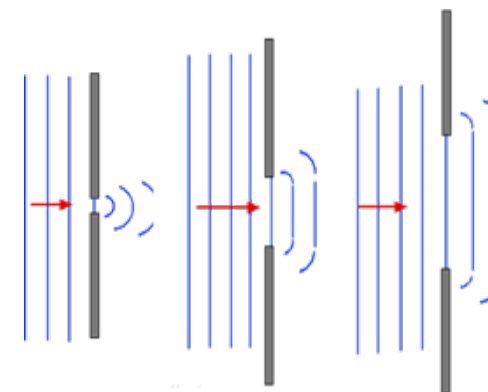
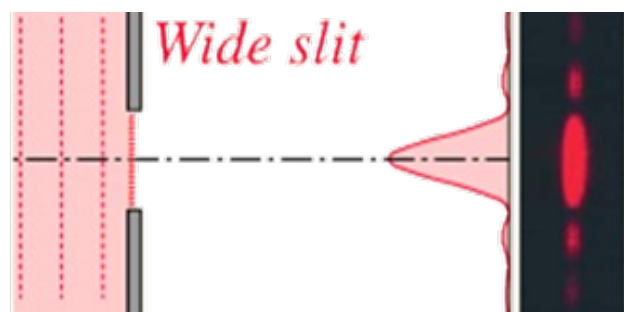
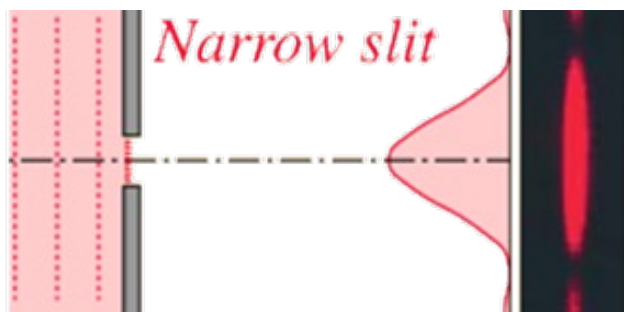
$$BC = \lambda/2 = (w/2) \sin\alpha$$

or

$$\sin\alpha = \lambda/w, 2\lambda/w, 3\lambda/w, \dots$$

Diffraction pattern depends strongly on ratio

$$\frac{\lambda}{\text{width slit}}$$

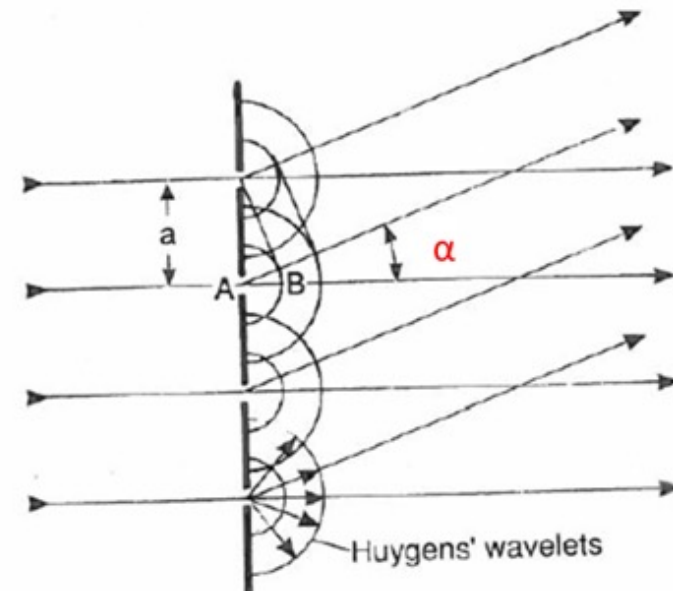


Diffraction from a grating

In 1803, Thomas Young showed in a two-slit experiment that the distance between the maximum of a detector and the center of the pattern was proportional to the reciprocal of the distance between the slits.

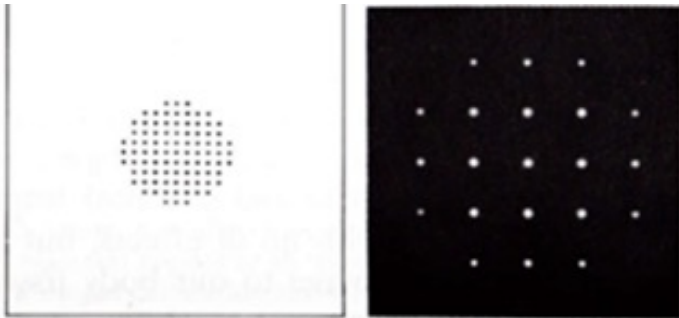
The conditions for constructive interference are very similar as for diffraction at one gap, but here the path difference is a function of the distance a between the openings in the diffraction grating:

$$a \sin \alpha = n \lambda \text{ where } n \text{ is an integer}$$



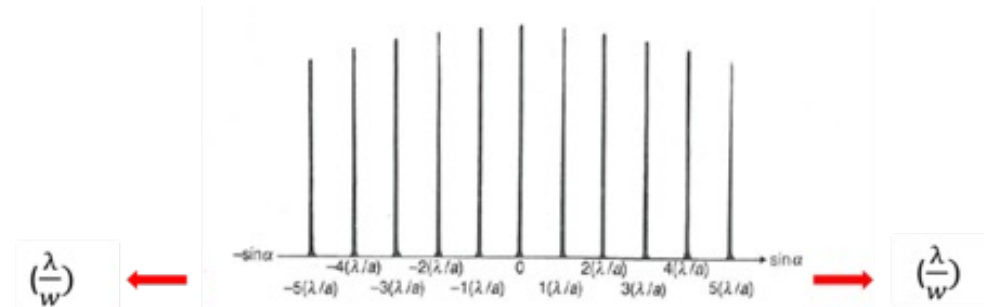
Diffraction from grating

- To have constructive interference among slits $n\lambda \leq a$ (distance between slits). This means that we need a wavelength of the order of the distance between the slits. If the wavelength is much smaller, the maxima will be very close to the forward direction i.e. the interference fringes will be very close to each other.
- When the width w of the slit is smaller than λ and $w < a$, the envelope function becomes broader and the first min induced by the width of the slit might not be visible. The pattern will look like



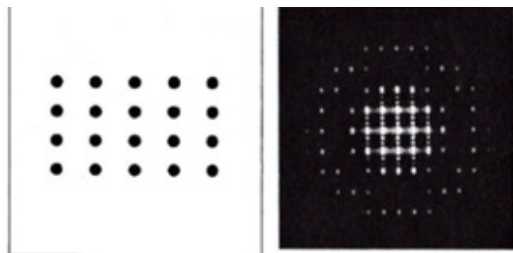
$$w < a$$

$$w < \lambda$$



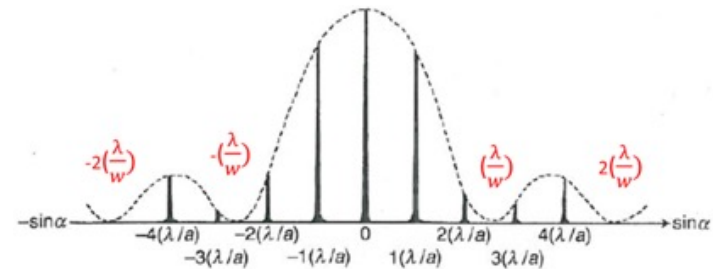
Diffraction from grating

- When w is of the order of λ but still $w < a$, the diffraction pattern will look like



$w < a$

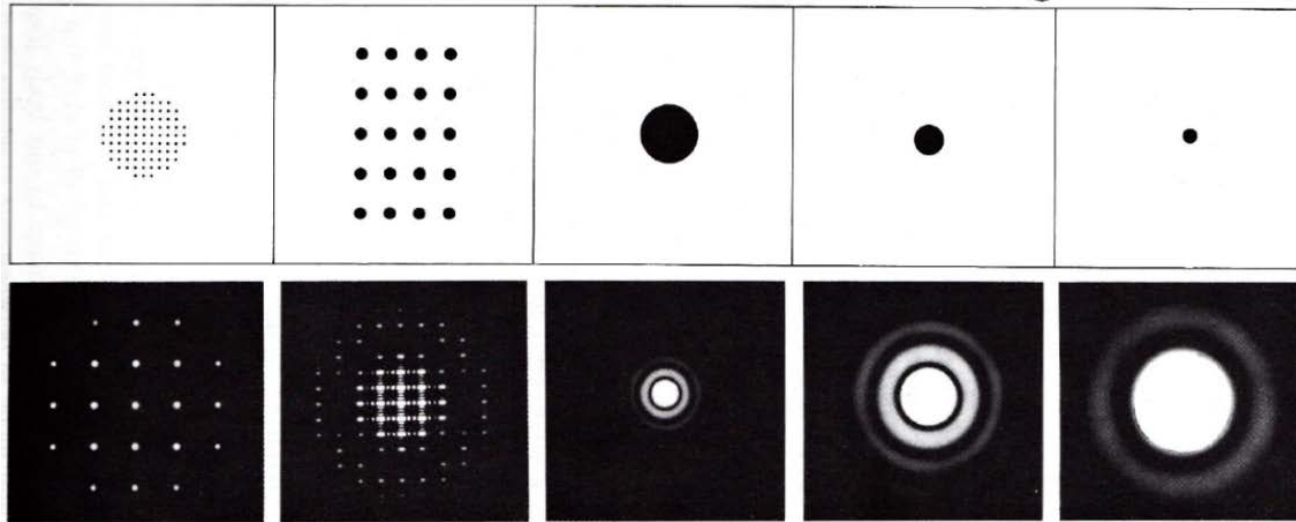
w of order
of λ



- The diffraction angles are invariant under scaling; that is, they depend only on the ratio of the wavelength to the size (w) of the diffracting object
- While diffraction occurs whenever propagating waves encounter slits, its effects are generally most pronounced for waves whose wavelength is roughly similar to the dimensions of the diffracting objects

Diffraction from grating

- The pictures below show the diffraction patterns for a planar diffracting grating consisting of circular openings.



Diffraction from crystal lattice

- Classical diffraction theory at a series of line slits (2D aperture grating) can be extended to diffraction at a 3D crystal lattice. That is in principle the contribution of Max von Laue and William Lawrence and William Henry Bragg (father and son). In 1912 Von Laue had the idea to send a beam of X-rays through a copper sulfate crystal and showed that there were diffraction spots surrounding the central spot of the primary beam. Around the same time, crystallographers were becoming convinced of the lattice-like construction of crystals.
- If one derives it from an analogy with the slits, the distance between the atoms is the grating distance and the size of the atoms is the width of the slit.
- Distance between atoms is of the order of 10^{-10} m, size of the atoms is smaller
⇒ This means that $w < a$, so one can have constructive interference.

Which radiation?

- X-rays, neutrons and electrons can be used. Typical wavelengths are:

	Energy	Wavelength
Neutrons	1 – 5 meV (cold)	9 – 4 Å
	25 – 50 meV (thermal)	1.8 – 1.3 Å
X-rays	100 keV	0.12 Å (hard X-rays)
	40 keV	0.31 Å
	5 keV	2.48 Å (soft X-rays)
Electrons	200 keV	0.025 Å

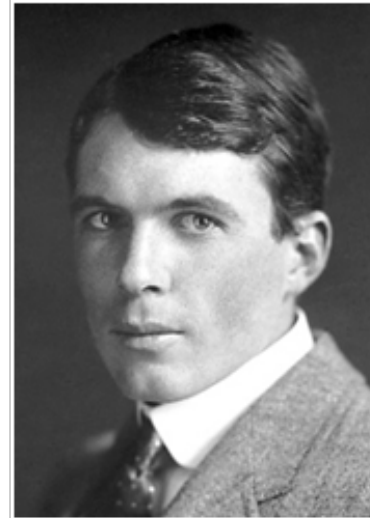
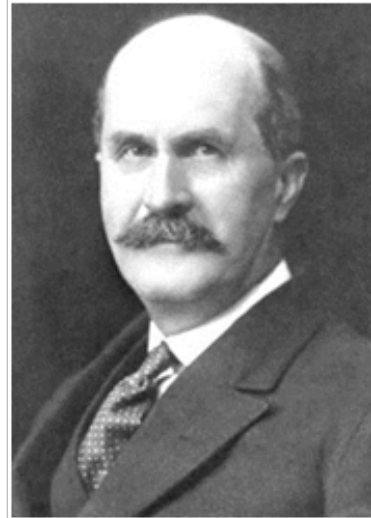
- X-rays and electrons fulfill the conditions for the relations between a , w and λ , the diffraction patterns will however differ i.e. the relation between λ and θ will differ. For instance, when one uses hard X-rays, the angle at which one will see constructive interference will be smaller than when using soft X-rays. Cold neutrons have a too large wavelength for diffraction from typical metals.

Historical figures

Max von Laue



William Lawrence Bragg William Henry Bragg



The discoveries of von Laue and Bragg gave birth to two new sciences, X-ray crystallography and X-ray spectroscopy, and two Nobel Prizes in physics: Max von Laue “for his discovery of the diffraction of X-rays by crystals” in 1914 and to Bragg and his father, Sir William Henry Bragg, “for their services in the analysis of crystal structure by means of X-rays” in 1915. William was then 25 years old! Max von Laue made already in 1912 the analogy between grating interference and diffraction at crystals but he took the 3D crystal as an ensemble of rows of atoms. His theory did not become immediately popular because it was rather complex. Father (W.H. Bragg) and son (W.L.) Bragg explained these patterns as layers of planes of atoms which behave as reflecting planes.

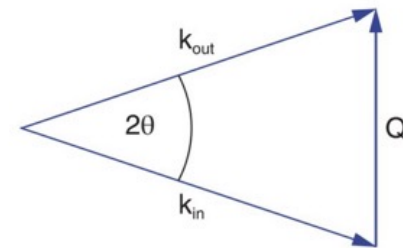
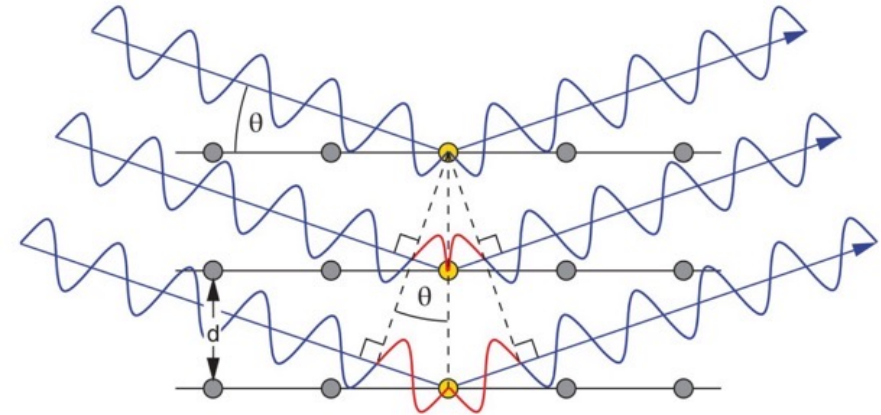
Bragg law

- Within a year of the discovery that X-rays diffract at crystals, father and son Bragg, have exploited the phenomenon to solve the first crystal structure and determined the rule governing a diffraction

$$m\lambda = 2d \sin \theta.$$

$$\sin \theta = \frac{6.1992}{d_{hkl}[\text{\AA}] E[\text{keV}]}$$

- *The scattering vector \mathbf{Q} always lies perpendicular to the scattering planes, or in other words, the angle subtended by $|\mathbf{k}_{in}| = \frac{2\pi}{\lambda}$ (or \mathbf{k}_{out}) and the scattering planes is θ .*



Bragg law defines on a purely geometrical basis for which angles constructive interference can occur

- Reciprocal lattice:

$$\mathbf{a}^* = 2\pi \frac{\mathbf{b} \times \mathbf{c}}{\mathbf{a} \cdot (\mathbf{b} \times \mathbf{c})}$$

$$\mathbf{b}^* = 2\pi \frac{\mathbf{c} \times \mathbf{a}}{\mathbf{b} \cdot (\mathbf{c} \times \mathbf{a})}$$

$$\mathbf{c}^* = 2\pi \frac{\mathbf{a} \times \mathbf{b}}{\mathbf{c} \cdot (\mathbf{a} \times \mathbf{b})}$$

- A geometric lattice is an infinite, regular array of vertices (points) in space
- The **reciprocal lattice** represents the Fourier transform of this lattice
- It exists in the space of spatial frequencies, known as reciprocal space or **k** space, where **k** refers to the wave vector

Each point in reciprocal space corresponds to a **set of planes** in real space.

The position of that point (its reciprocal-lattice vector **G**) is **perpendicular to those planes**, and its magnitude is **inversely proportional to their spacing** ($|G| = 2\pi/d$).

The reciprocal lattice provides a **natural language for describing diffraction**, because constructive interference of waves (X-rays, neutrons, electrons) occurs when the scattering vector equals a reciprocal-lattice vector — the **Laue or Bragg condition**.



Intuitive analogy (Fourier / sound domain)

Think of a crystal lattice like a repeating musical rhythm in time.

Its Fourier transform gives you the frequencies present in that rhythm.

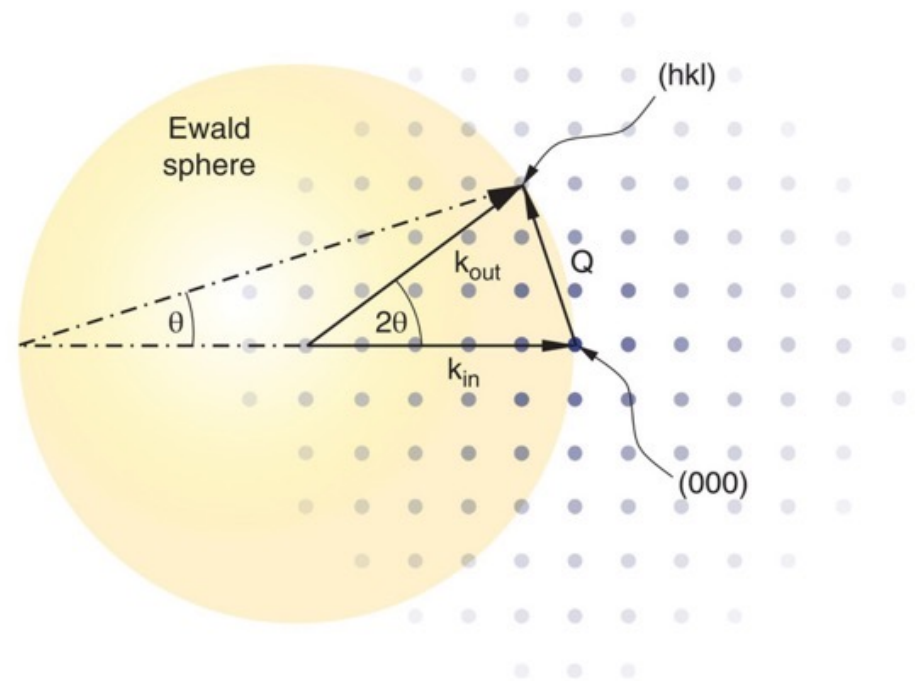
Likewise, a repeating pattern in space produces spatial frequencies — that's the reciprocal lattice.

- Large distances in real space \rightarrow small spacing in reciprocal space (low frequency).
- Small distances in real space \rightarrow large spacing in reciprocal space (high frequency).

So, the reciprocal lattice is to the crystal what a spectrum is to a sound — it tells you which frequencies (wavevectors) can produce constructive interference.

Ewald sphere

The incident wavevector \mathbf{k}_{in} must end, and the scattering vector $\Delta\mathbf{k} = \mathbf{Q}$, must begin at the (000) diffraction spot of the direct beam, while, for constructive interference to occur, \mathbf{Q} and \mathbf{k}_{out} must end at another diffraction maximum (a 'reciprocal-lattice point'). As x-ray diffraction is an elastic process, this means that these two points must lie on the surface of a sphere (the 'Ewald sphere') of radius $|\mathbf{k}|$ and whose centre lies at the base of the \mathbf{k}_{in} and \mathbf{k}_{out} vectors.



$$\mathbf{Q} = 2|\mathbf{k}| \sin \theta = \frac{4\pi}{\lambda} \sin \theta \qquad |\mathbf{Q}| = \frac{2\pi}{d_{hkl}}$$

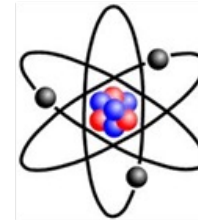
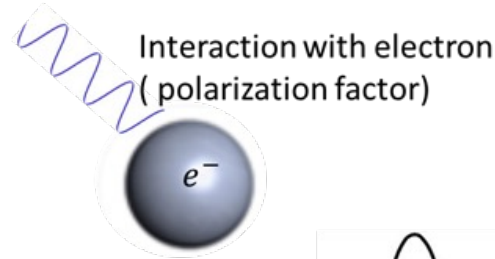
Structure factor - X-rays



Elastic scattering of X-rays is due to the interaction with electrons in an atom.

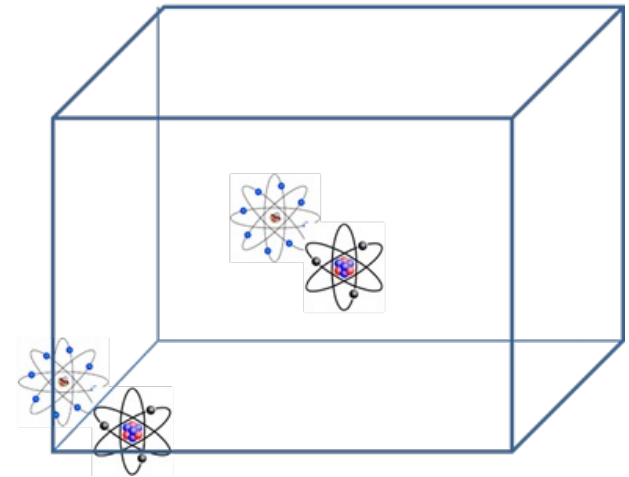
To know what the scattering power is of a crystal:

- ⇒ scattering from an electron,
- ⇒ scattering from an atom
- ⇒ scattering from the unit cell,



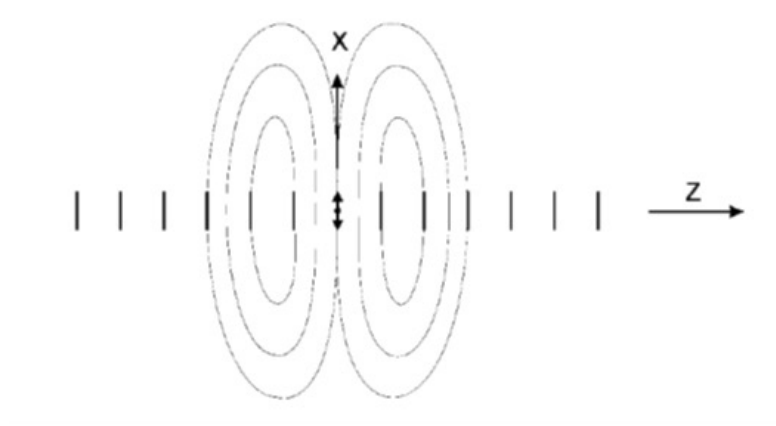
Scattering at an atom
(atomic form factor f)

Scattering from unit cell
(Structure factor F)



Interaction with electron

- Elastic scattering of an electromagnetic wave by electrons of the outer shell of an atom \Rightarrow Thompson scattering
- Same wavelength as the incoming wave and there will be a defined phase relationship, i.e. the radiation is coherent.
- Simple case: a planar wave traveling in the z direction, linear polarized in the direction x \Rightarrow This wave will cause the electron oscillate in the x direction and create a dipolar field. The electromagnetic radiation emitted by the oscillating electron will then not be spherical.



Intensity scattered wave

$$\left(\frac{e^2}{c^2 m_e}\right)^2 (1 + \cos^2 2\vartheta)$$

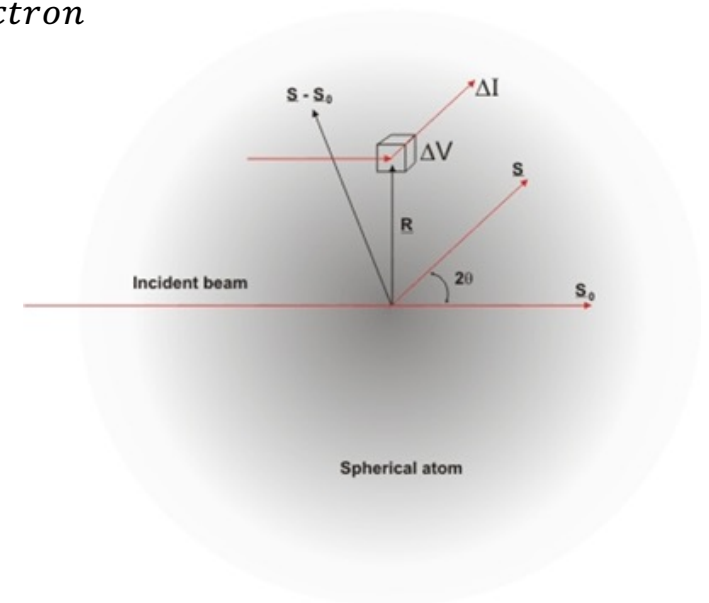
Interaction with an atom

The orbital electrons in an atom move very fast (of the order of 10^{-18} sec for one orbital) and therefore an impinging wave sees only an average electron cloud which is characterized by an electron density of charge $\rho(r')$.

Atomic scattering factor

$$f = \frac{\text{amplitude scattered by one atom}}{\text{amplitude scattered by a single electron}}$$

$$f(k) = 4\pi \int_0^\infty r^2 \rho(r) \frac{\sin(\mathbf{k}-\mathbf{k}_0) \cdot \mathbf{r}}{(\mathbf{k}-\mathbf{k}_0) \cdot \mathbf{r}} \quad \text{where } \mathbf{k}-\mathbf{k}_0 = (\mathbf{s}-\mathbf{s}_0)/\lambda$$



Interaction with an atom

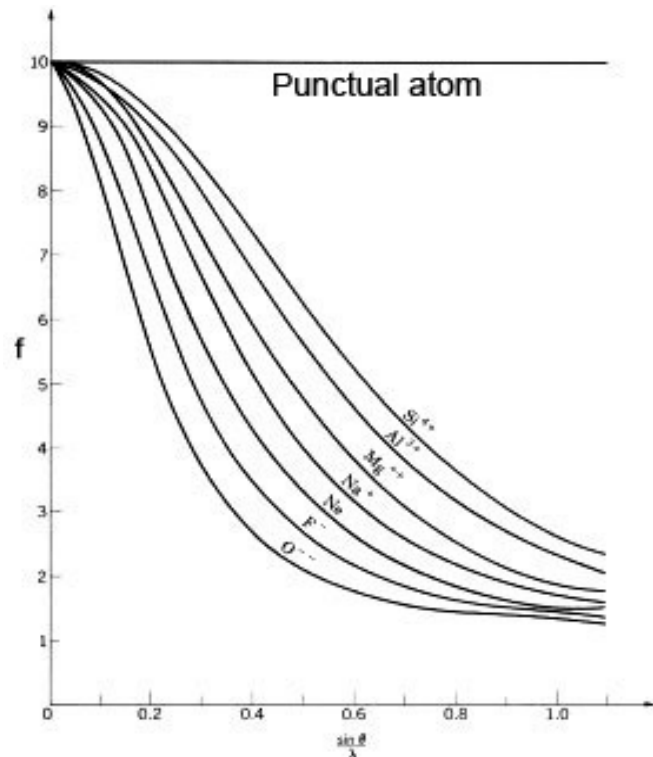
$$f(\mathbf{k}) = 4\pi \int_0^\infty r^2 \rho(r) \frac{\sin(\mathbf{k}-\mathbf{k}_0) \cdot \mathbf{r}}{(\mathbf{k}-\mathbf{k}_0) \cdot \mathbf{r}} \quad \text{where } \mathbf{k}-\mathbf{k}_0 = (\mathbf{s}-\mathbf{s}_0)/\lambda$$

$4\pi \int r^2 \rho(r) dr = Z$ i.e. # electrons in atom.

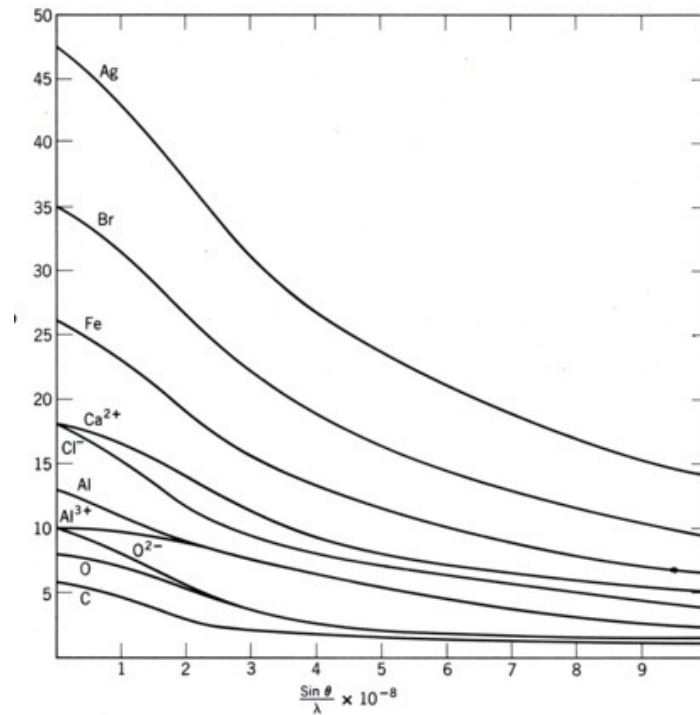
$\Rightarrow f = Z$ when $\theta=0$ (forward direction),

$\Rightarrow F < Z$ for all other angles of scattering. **The form factor depends via $(\mathbf{s}-\mathbf{s}_0)$ on $\sin\vartheta/\lambda$.**

Interaction with an atom



Atomic scattering factors for several ions with the same number of electrons. One can observe that the O^{2-} has a more diffuse electronic cloud than Si^{4+} and shows a faster decay.



Atomic scattering factors calculated for atoms and ions with different numbers of electrons. Hydrogen (only one electron) scatters very little as compared with other elements.

Neutron scattering length

- When a neutron interacts with an atom, it doesn't "see" the electron cloud (as X-rays do); it interacts mainly with the nucleus via the strong nuclear force.
- That interaction is so short-ranged that, to the neutron wave, the atom acts like a tiny point scatterer — almost like a small obstacle that sends part of the wave off in different directions.
- Because it's impossible to resolve the details of that nuclear potential, we describe the effect with one simple number:

The scattering length, b

- This is a measure of how strongly and with what phase the neutron wave is scattered by a nucleus.

Neutron scattering length

- It has dimensions of length (typically femtometres, 10^{-15} m).
- It can be positive or negative \rightarrow meaning the scattered wave can be in or out of phase with the incoming wave.
- It depends on the nuclear isotope, not on the chemical state. That's why neutrons are powerful for isotope contrast — e.g. H vs D.
- It's tabulated for each isotope (e.g. $b_{\text{Fe}} = 9.45$ fm, $b_{\text{Cu}} = 7.7$ fm, etc.).

Neutron scattering length

Scattering length b :

- Describes how strongly a single nucleus scatters a neutron wave (like a “point mirror”).
- Can be positive or negative; depends on isotope.

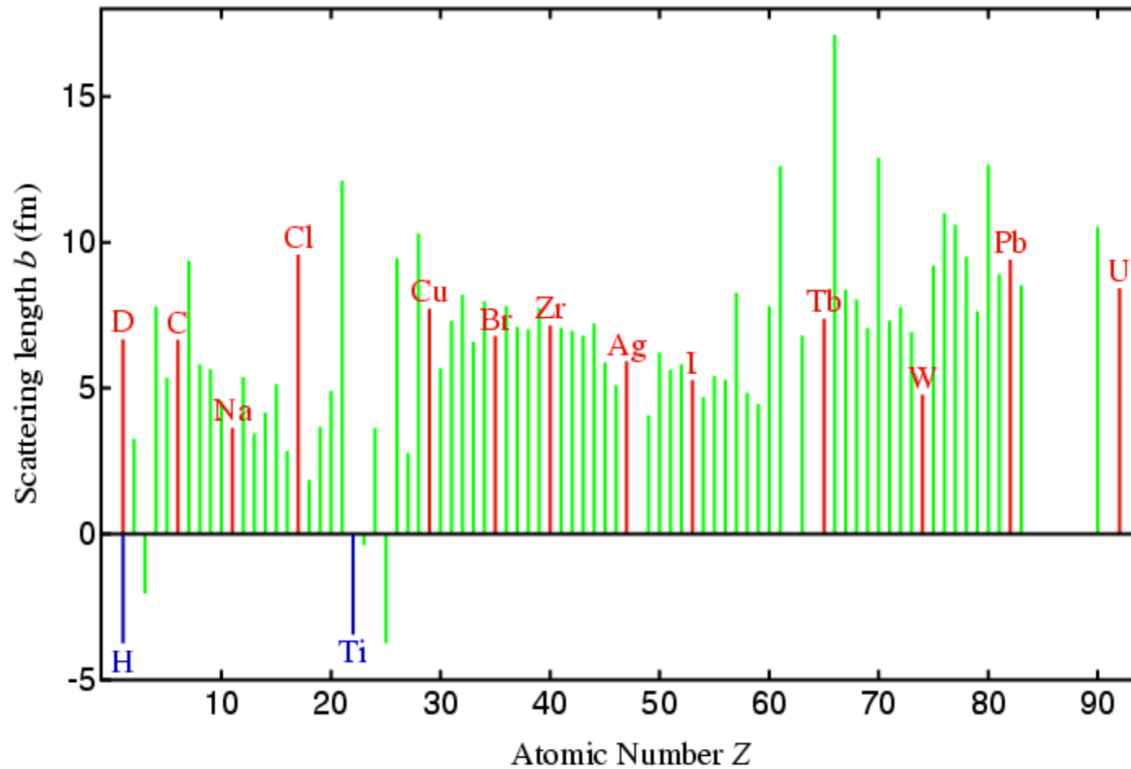
Scattering length density $\rho = N b$:

- Describes how strongly a bulk material scatters neutrons.
- Analogous to refractive index for light.
- Differences in ρ between regions create contrast in diffraction, SANS, or reflectometry.

X-rays vs neutrons

- The **scattering length density** (\AA^{-2}) plays the same conceptual role for neutrons that **electron density** ($e / \text{\AA}^3$) does for X-rays — both describe how the wave accumulates phase and interferes inside the material.
- The unit difference comes from the fact that:
 - For X-rays, the scattering amplitude is **dimensionless** per atom but multiplied by electron density (per volume).
 - For neutrons, the amplitude **already has dimensions of length**, so when multiplied by number density (per volume), it gives an **area density** (\AA^{-2}).

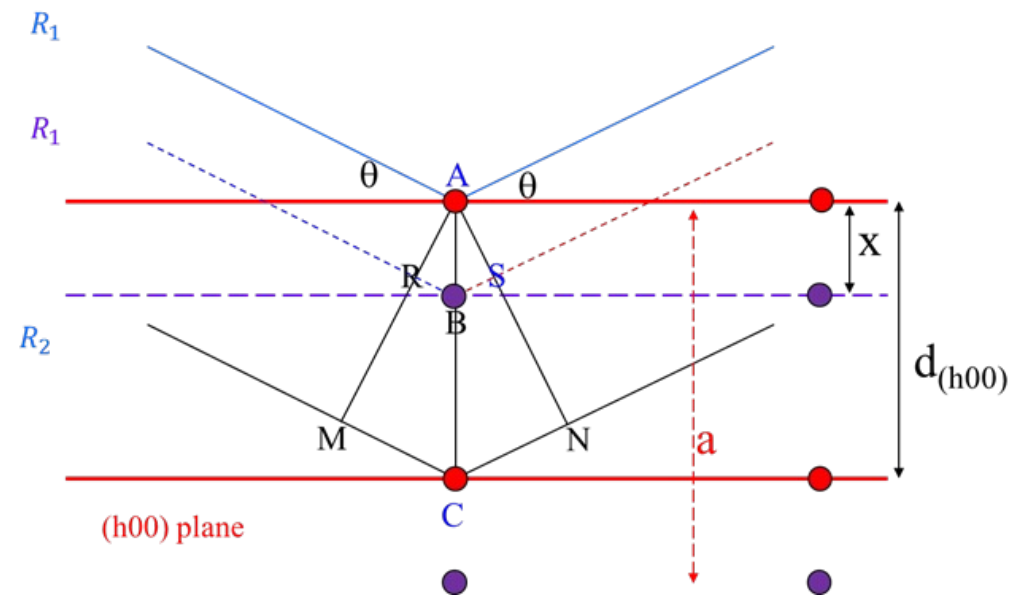
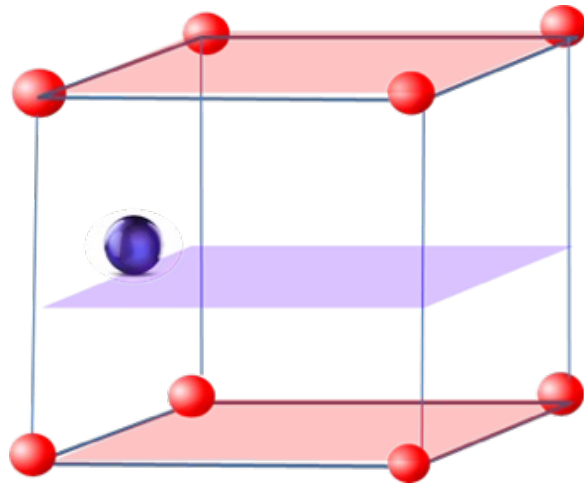
X-rays vs neutrons



- X-rays scatter in proportion to Z , so **heavy elements dominate**.
- Neutrons scatter from nuclei with no systematic dependence on Z , giving **unique sensitivity to light atoms** and isotopes.
- To a neutron with typical thermal or cold energies (meV scale), the nucleus looks like a point scatterer.
- That means the scattering amplitude (the scattering length b) is **independent of Q** or energy — at least over a wide range.

Interaction with a unit cell

Let's consider a simple cubic unit cell with a motif with one (red) atom at a lattice point and one (blue) atom in one of the faces at a position x from the top face. The atoms are different chemical species. The red planes are those that fulfill the Bragg equation. The purple plane is parallel to the Bragg planes but does not fulfill the Bragg equation.



Interaction with a unit cell

The path difference between the rays (R1 and R2) impinging on the (h00) planes (Bragg fulfilled)

$$MCN = 2AC \sin\theta = 2 d_{h00} \sin\theta = \lambda$$

The path difference between R1 and R3

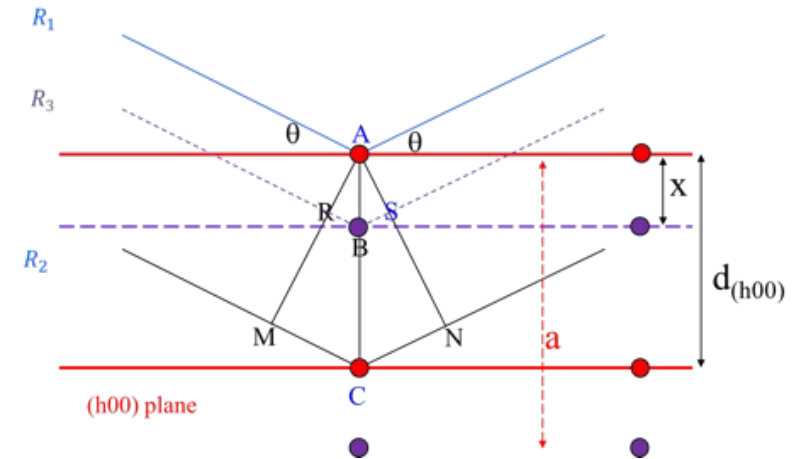
$$RBS = 2AB \sin\theta = AB \lambda / d_{h00}$$

AC is the distance between the lattice planes (h00)

$$AC = d_{h00} = a/h \text{ and } \frac{AB}{AC} = \frac{x}{a/h}$$

$$RBS = \frac{x}{a} \lambda \text{ or a path difference } RBS = h \frac{x}{a} \lambda$$

For an atom sitting halfway (x/a=1/2) there will be maximal reduction in intensity



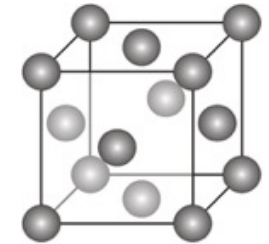
Interaction with a unit cell

Structure factor:

$$F_{hkl} = \sum_j f_j \exp[-i2\pi(hx_j + ky_j + kz_j)]$$

where f_j is the atomic form factor of the j^{th} atom, (x_j, y_j, z_j) is its position in the unit cell expressed in fractions of the unit-cell lattice vectors, and the summation is over the j atoms within the unit cell. The scattered intensity I_{hkl} is the absolute square of F_{hkl} .

Interaction with a unit cell



FCC lattice, atoms on lattice points

Positions of equivalent atoms: $(0,0,0)$, $(\frac{1}{2}, \frac{1}{2}, 0)$, $(\frac{1}{2}, 0, \frac{1}{2})$, $(0, \frac{1}{2}, \frac{1}{2})$

$$F = f \left[e^{i[2\pi(0)]} + e^{i[2\pi(\frac{h+k}{2})]} + e^{i[2\pi(\frac{k+l}{2})]} + e^{i[2\pi(\frac{l+h}{2})]} \right]$$

$$= f [1 + e^{i\pi(h+k)} + e^{i\pi(k+l)} + e^{i\pi(l+h)}]$$

$e^{i\pi n} = 1$ when n is even
 $= -1$ when n is odd

hkl all even or odd: $F=4f$

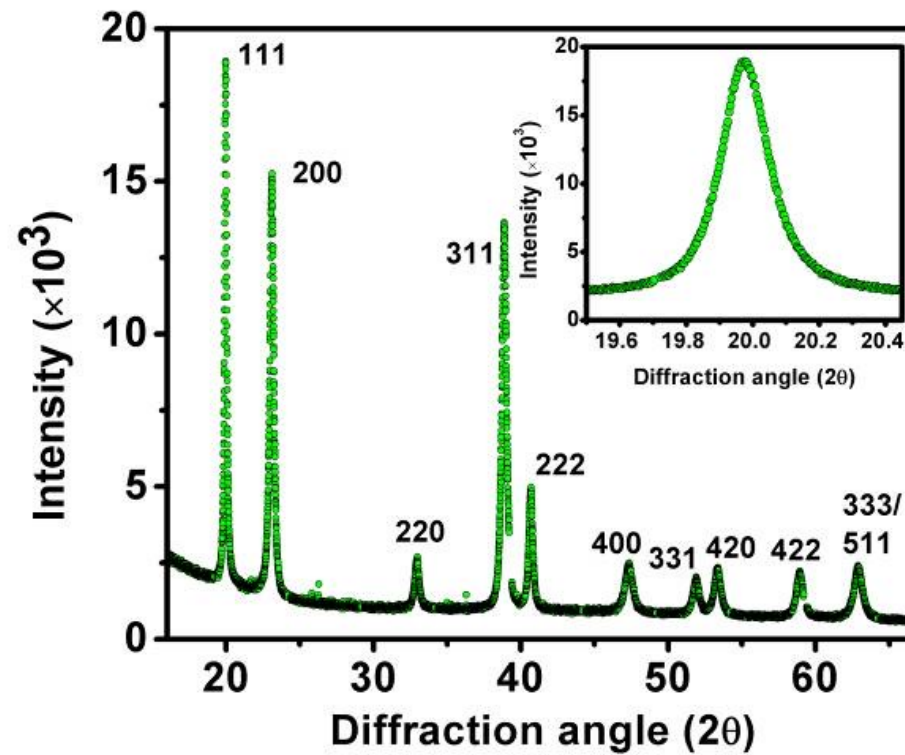
e.g. $111, 200, 220, 333, 420$

hkl mixed: $F=0$

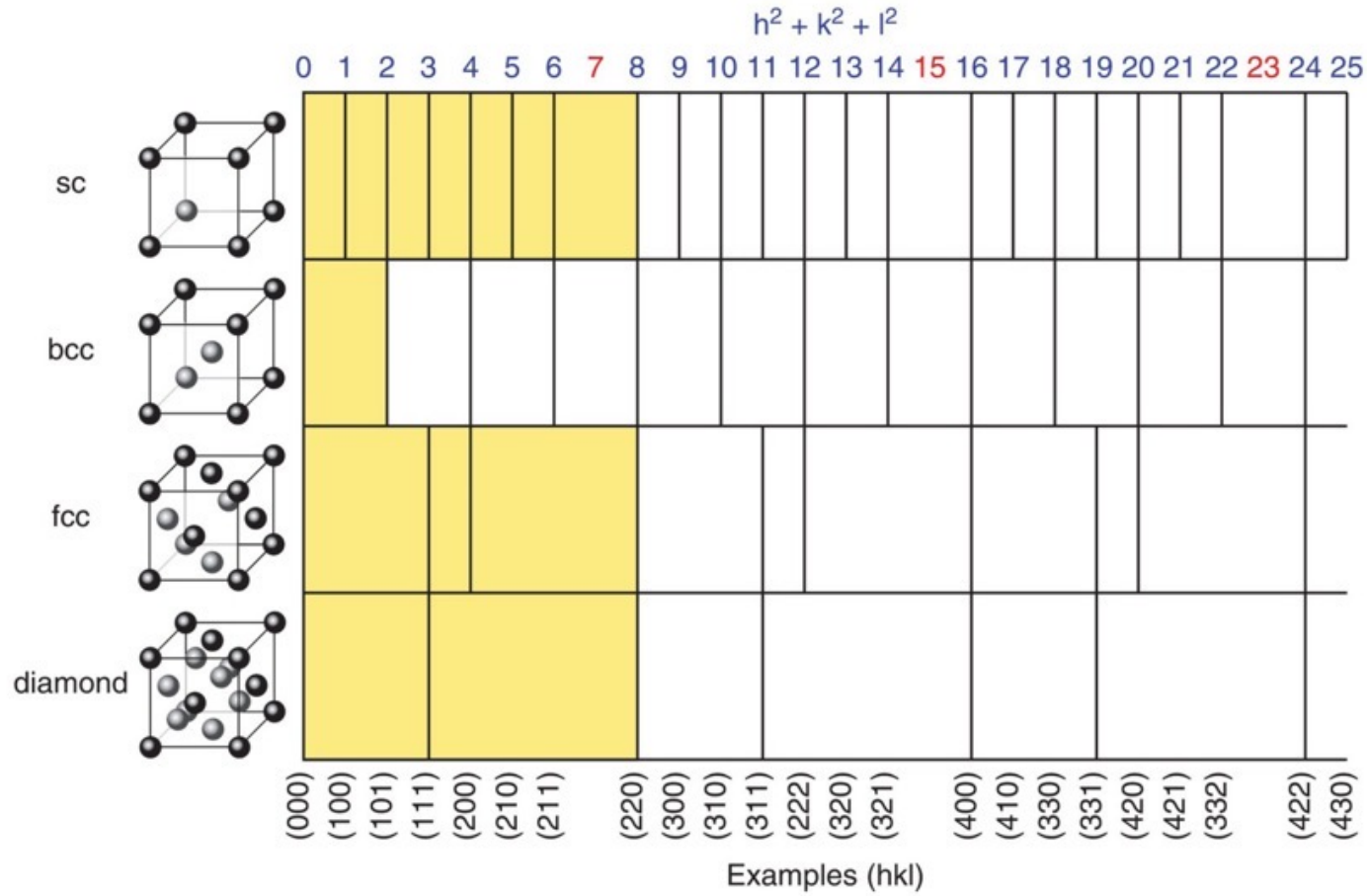
e.g. $100, 211; 210, 032, 033$

Interaction with a unit cell

- Example: nanocrystalline Ni



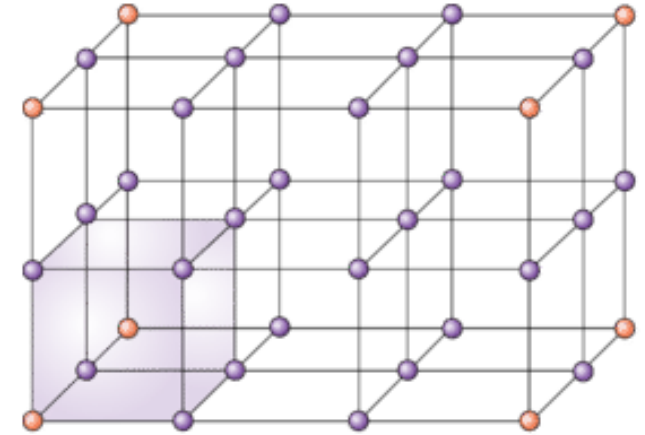
Interaction with a unit cell



Chemical ordering

- Two kinds of atoms on α and β -sites.
- Atomic fractions: x_A and x_B .
- y_α and y_β fractions of α and β -sites
- Define following parameters:
 - r_α : fraction of α -sites occupied by the right atom
 - w_α : fraction of α -sites occupied by the wrong atom
 - r_β : fraction of β -sites occupied by the right atom
 - w_β : fraction of β -sites occupied by the wrong atom

The long-range order parameters can be defined as: $S = (r_\alpha - x_A)/y_\beta = (r_\beta - x_B)/y_\alpha$



Chemical ordering: CuAu

$$\beta = 000, \frac{1}{2} \frac{1}{2} 0; \alpha = \frac{1}{2} 0 \frac{1}{2}; 0 \frac{1}{2} \frac{1}{2}; y_\alpha = \frac{1}{2}; y_\beta = \frac{1}{2};$$

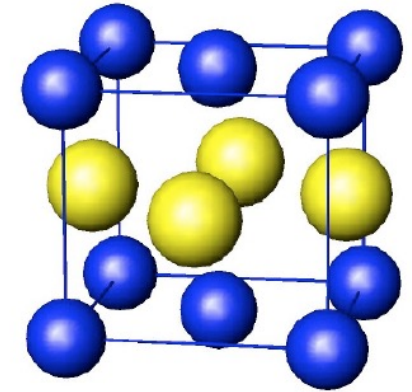
$$F = (r_\alpha f_A + w_\alpha f_B)[e^{\pi i(h+l)} + e^{\pi i(k+l)}] + (r_\beta f_B + w_\beta f_A)[1 + e^{\pi i(h+k)}], \quad (12.7)$$

hkl unmixed;

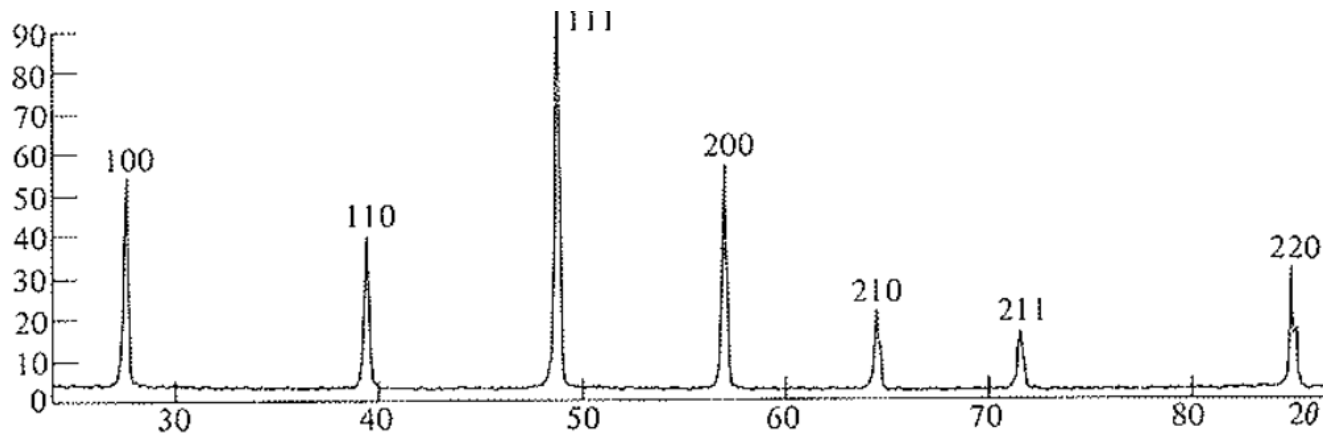
$$F = 2[(r_\alpha f_A + w_\alpha f_B) + (r_\beta f_B + w_\beta f_A)] = 4(x_B f_B + x_A f_A) \text{ Fundamental,}$$

$h + k = \text{even}, k + l = \text{odd};$

$$F = 2[(r_\beta f_B + w_\beta f_A) - (r_\alpha f_A + w_\alpha f_B)] = 2S(f_B - f_A) \text{ Superstructure.}$$



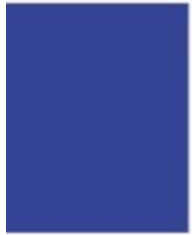
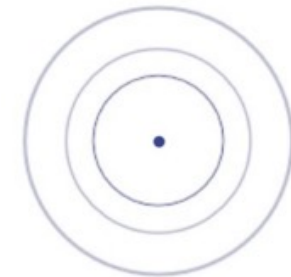
AuCu



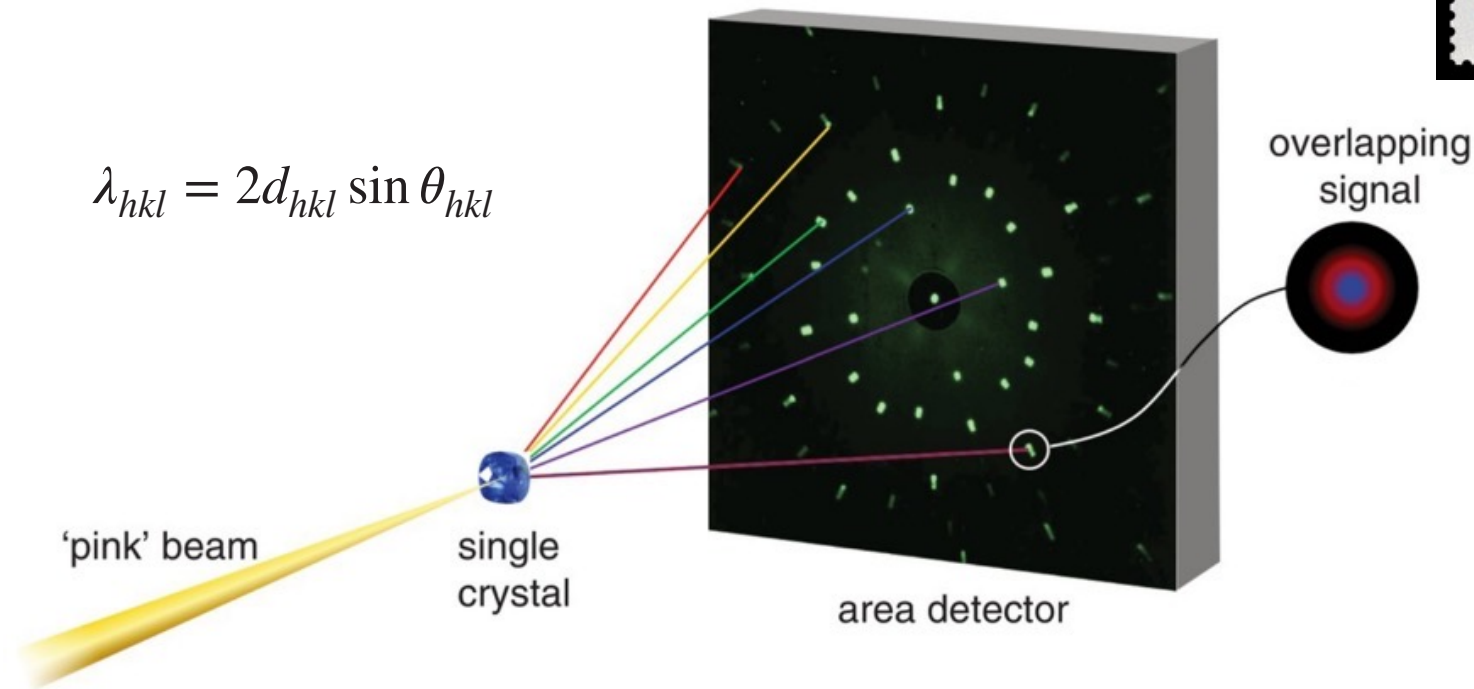
Diffraction methods

Method	Wavelength	Sample angle	Detector angle	Measured
Laue	Variable	Fixed	Fixed	Intensity vs. angle
Rotating crystal	Fixed	Variable	Fixed	Intensity vs. angle
Powder	Fixed	Variable/fixed	Variable	Intensity vs. angle
Energy dispersive	Variable	Fixed	Fixed	Intensity vs. energy
Neutron time-of-flight	Variable	Fixed	Fixed	Intensity vs. time
Bragg coherent diffraction imaging	Fixed	Variable	Fixed	Intensity vs. angle

Sample types

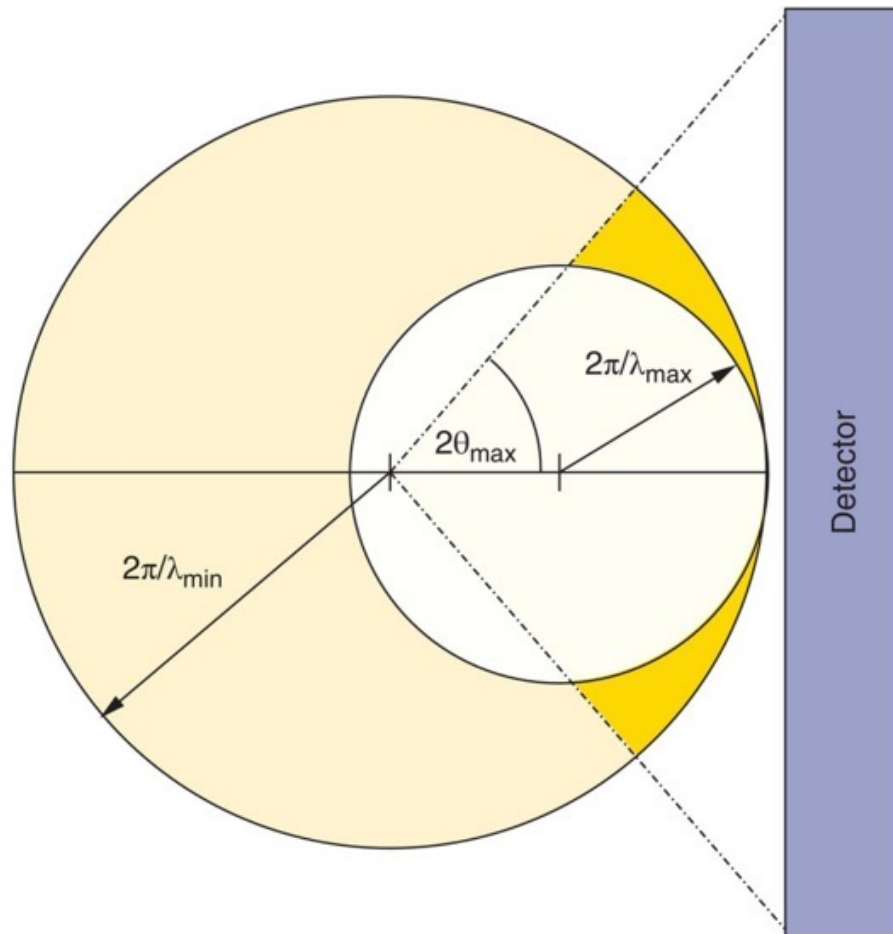
single
crystaltwinned
crystalcrystal with
mosaic spreadtextured
samplepowder
samplenanocrystalline
powder

Single crystal diffraction - Laue



- Pink beam: many wavelengths
- Bragg equation fulfilled for multiple combinations of d and θ

Single crystal diffraction - Laue



Laue diffraction provides a lot of structural information in a very short time. However, it is not as well-suited as monochromatic scattering for determining the full atomic structure of a crystal, due on the one hand to the often complex and unknown intensity distribution of the 'pink' incident x-ray beam .

In addition, families of lattice planes that are parallel to one another, for example the (111), (222), (333) ... planes, have Laue diffraction maxima overlapping at the same position, resulting in a loss of information. This is called the 'energy overlapping problem'.

Application: stress in thin films

- Position spots related to both orientation AND shape of the crystal unit cell
- Any rotation or distortion of the shape of the unit cell will result in offset peak positions
- Positions Laue spots \Rightarrow crystal orientation + deviatoric strain (stress) tensor
- In praxis: the positions of the reflections \mathbf{q}_{hkl} with respect to the laboratory reference frame are calculated by:

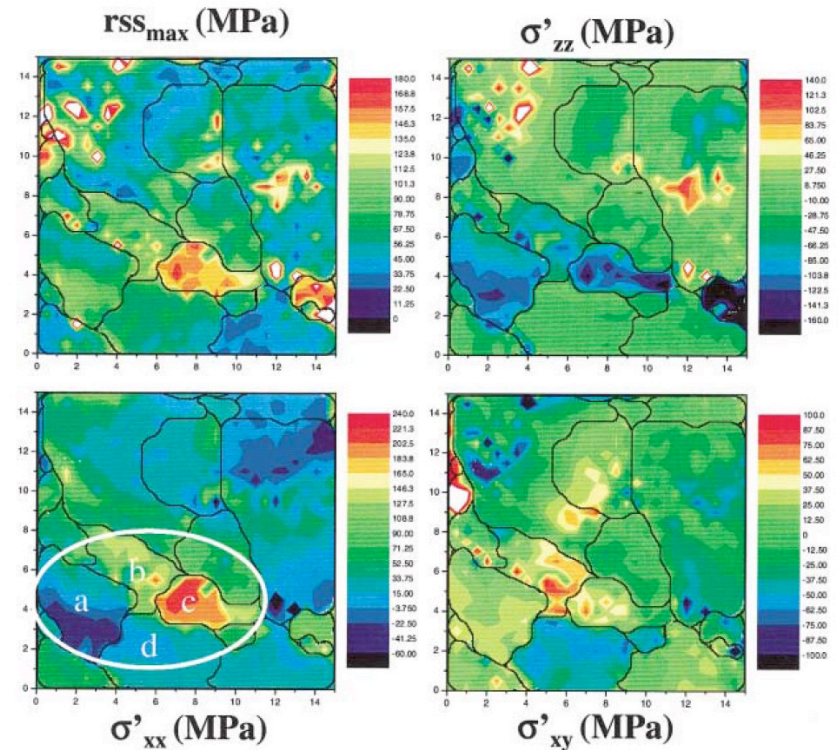
$$\mathbf{q}_{hkl} = \mathbf{U} \mathbf{B} \mathbf{G}_{hkl}$$

where \mathbf{G}_{hkl} is the reciprocal-lattice vector for the hkl reflection, \mathbf{B} depends on elastic strain and \mathbf{U} is the rotation matrix between laboratory and crystal frame.

$$\begin{pmatrix} \boldsymbol{\varepsilon}_{11} & \boldsymbol{\varepsilon}_{12} & \boldsymbol{\varepsilon}_{13} \\ \boldsymbol{\varepsilon}_{12} & \boldsymbol{\varepsilon}_{22} & \boldsymbol{\varepsilon}_{23} \\ \boldsymbol{\varepsilon}_{13} & \boldsymbol{\varepsilon}_{23} & \boldsymbol{\varepsilon}_{33} \end{pmatrix} = \begin{pmatrix} \boldsymbol{\varepsilon}_{11} - \frac{\Delta}{3} & \boldsymbol{\varepsilon}_{12} & \boldsymbol{\varepsilon}_{13} \\ \boldsymbol{\varepsilon}_{12} & \boldsymbol{\varepsilon}_{22} - \frac{\Delta}{3} & \boldsymbol{\varepsilon}_{23} \\ \boldsymbol{\varepsilon}_{13} & \boldsymbol{\varepsilon}_{23} & \boldsymbol{\varepsilon}_{33} - \frac{\Delta}{3} \end{pmatrix} + \begin{pmatrix} \frac{\Delta}{3} & 0 & 0 \\ 0 & \frac{\Delta}{3} & 0 \\ 0 & 0 & \frac{\Delta}{3} \end{pmatrix}$$

Application: stress in thin films

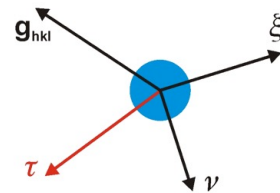
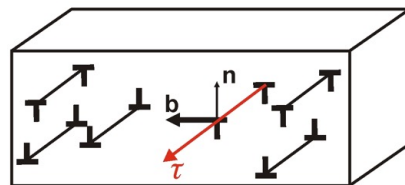
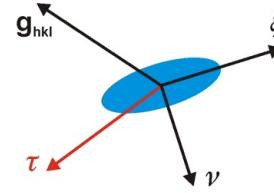
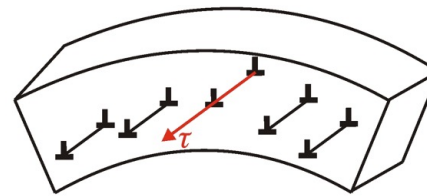
- Crystal orientation and deviatoric strain tensor can be refined simultaneously when sufficient spots are present. The hydrostatic component can be determined by an energy scan of at least one spot.
- Example: Al 0.5 wt % Cu thin film with thickness of $0.5\mu\text{m}$ deposited at 400C on a SiN membrane on a Si frame. During cooling stresses arise in individual grains. X-ray beam spot size: $0.8\mu\text{m}$.



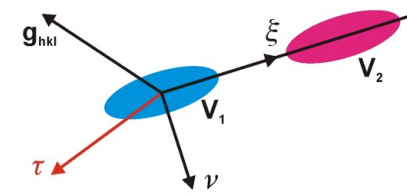
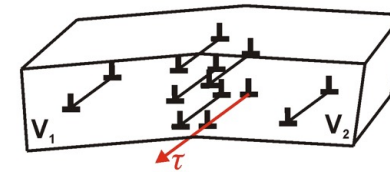
Spolenak *et al*, Phys. Rev. Lett **90**, 096102 (2003)

Application: microcompression of single crystals

- Microstructural variations within the illuminated volume can lead to change in shape of spots

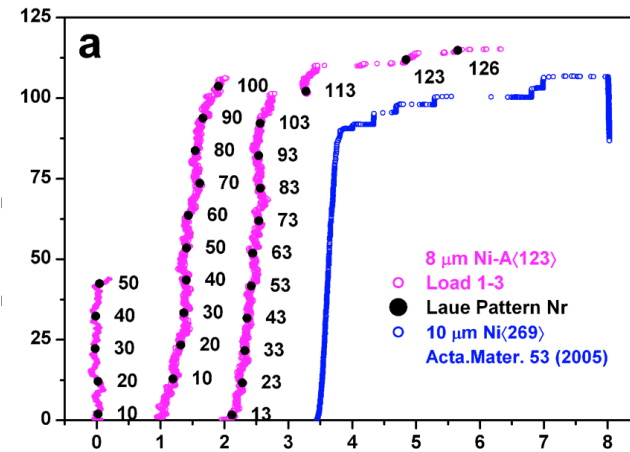
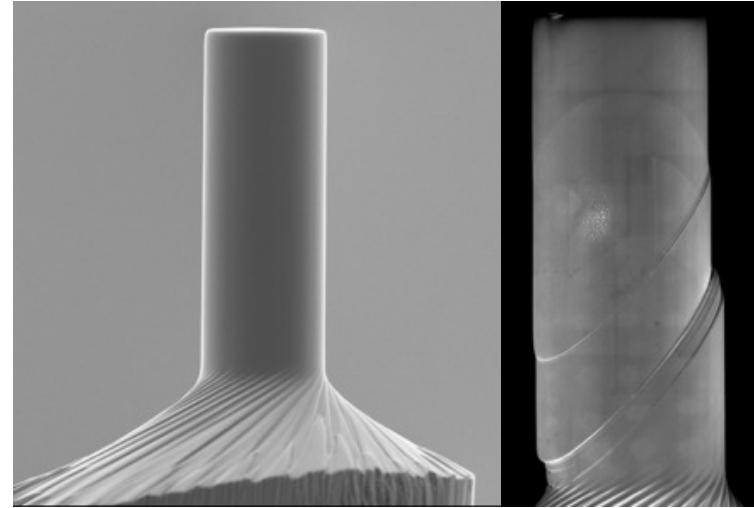
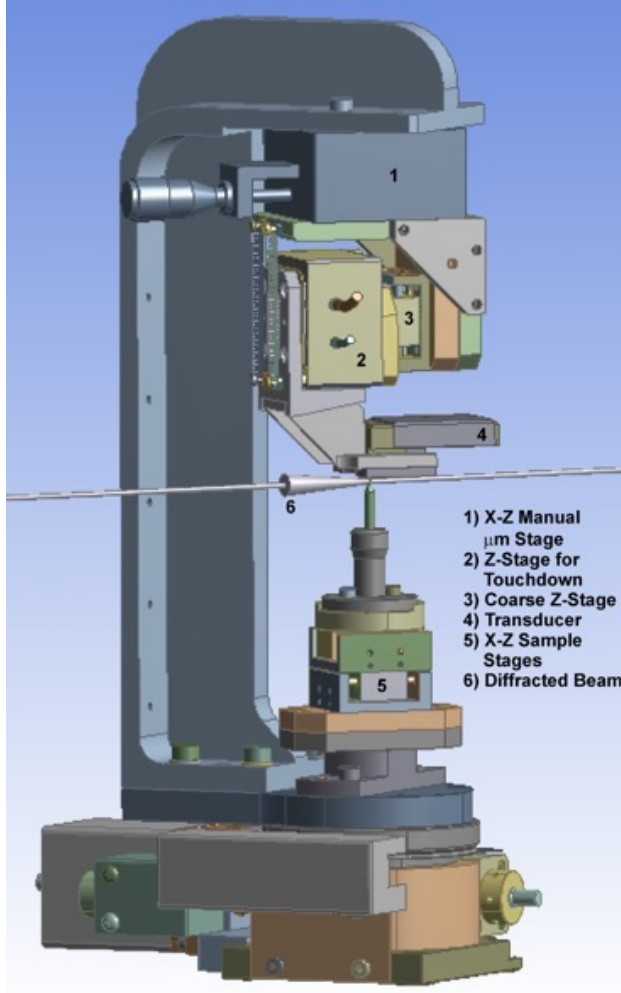
Statistically stored
dislocations

Curvature

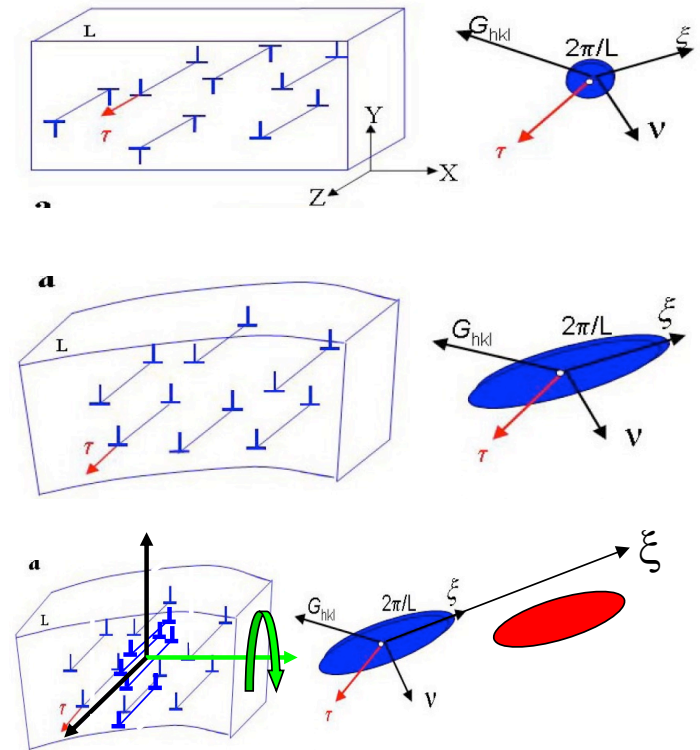
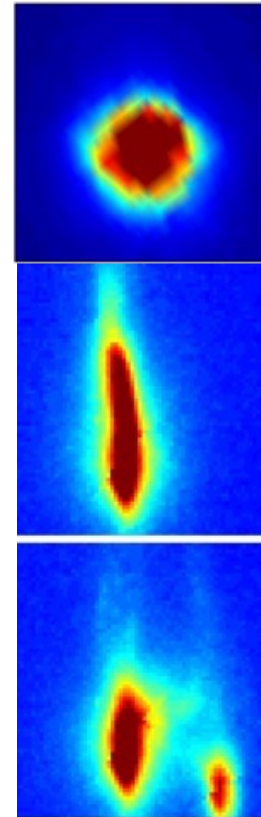
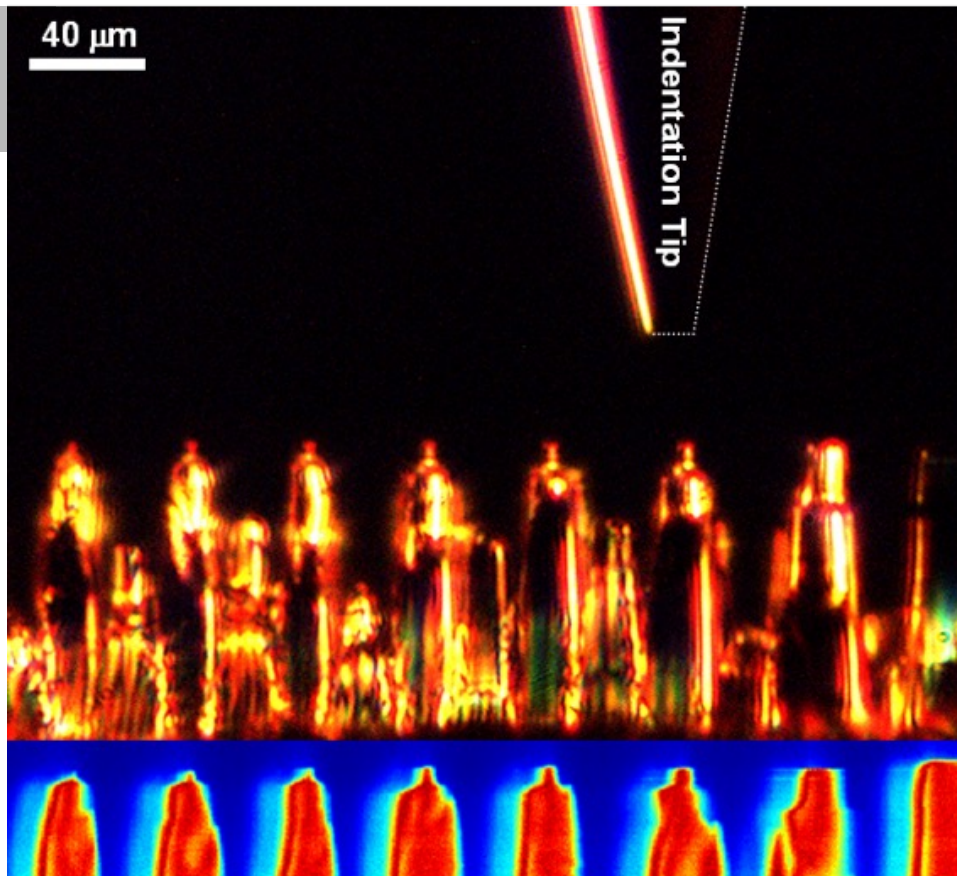


Small-angle boundary

Application: microcompression of single crystals



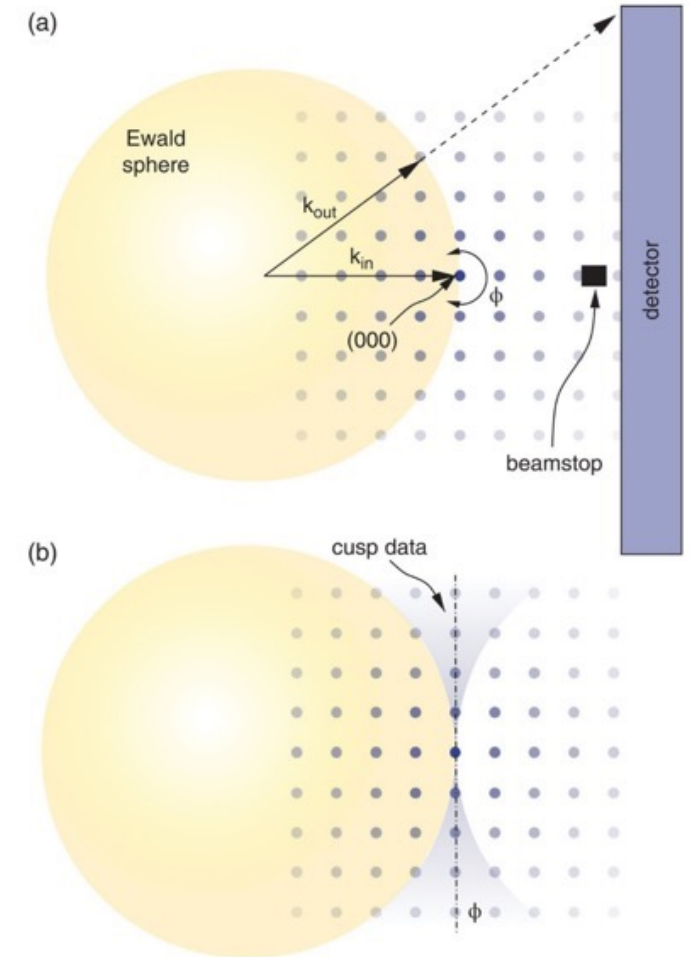
Application: microcompression of single crystals



Time-resolved laue diffraction of deforming micropillars, Physical Review Letters **99**, 145505 (2007)

Single crystal diffraction – rotation method

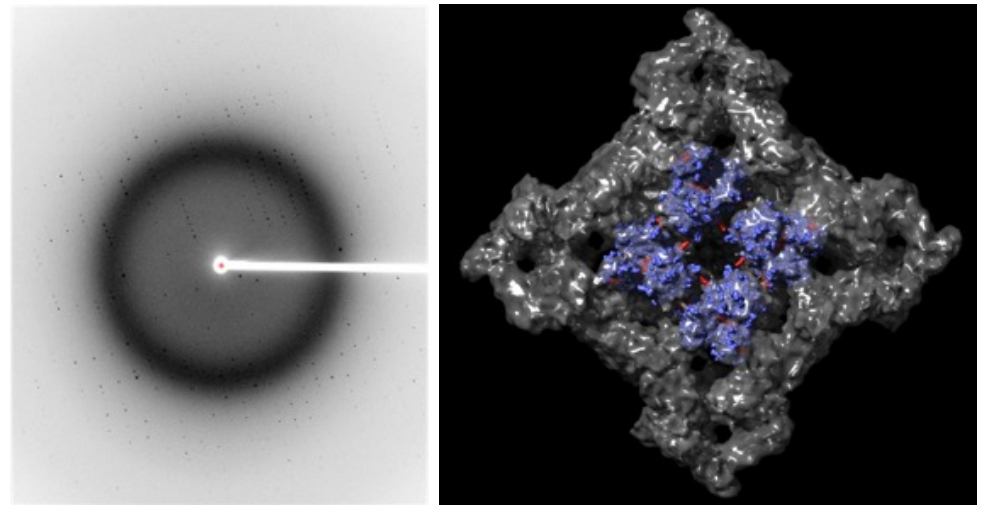
- In the large majority of single-crystal diffraction experiments, monochromatic radiation is used and the so-called ‘rotation’ or ‘oscillation’ method is applied.
- By rotating the crystal around an axis perpendicular to the incident beam (ϕ), diffraction maxima pass through the surface of the Ewald sphere and are registered on a 2D x-ray detector
- When viewed from above the plane containing the ϕ -axis, one sees that for a given crystal orientation relative to the axis, some data cannot be accessed (known as ‘cusp’ data and shaded blue here). However, by reorienting the crystal axis (typically by 90°), this data can also be recorded.



Application: protein crystallography

- Goal: to study the three-dimensional structure of biological macromolecules.
- Unfortunately, it is only possible to measure the amplitude of the diffraction pattern spots by experimental means; the phase information is missing
- Without phase information it is difficult to reconstruct the electron density in the unit cell. There exist various methods to circumvent this:
(<https://www.ruppweb.org/Xray/101index.html>)

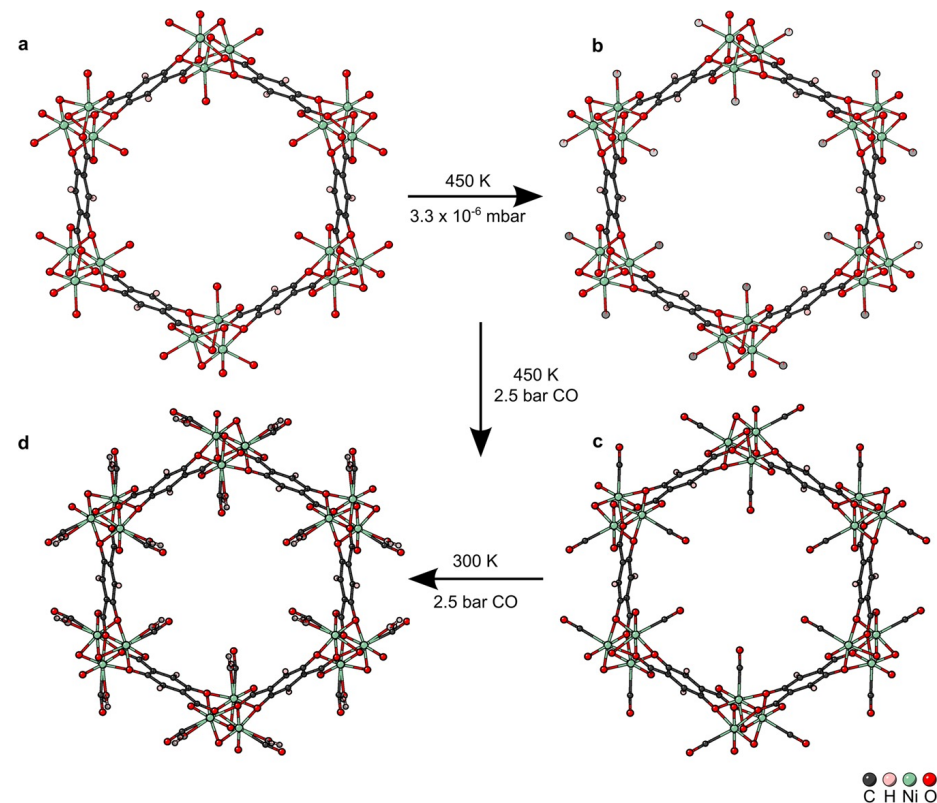
Data collection: wavelength = 0.097nm, Canadian Light Source - 1 second per frame, total of ~360 frames, step size 0.5 degrees



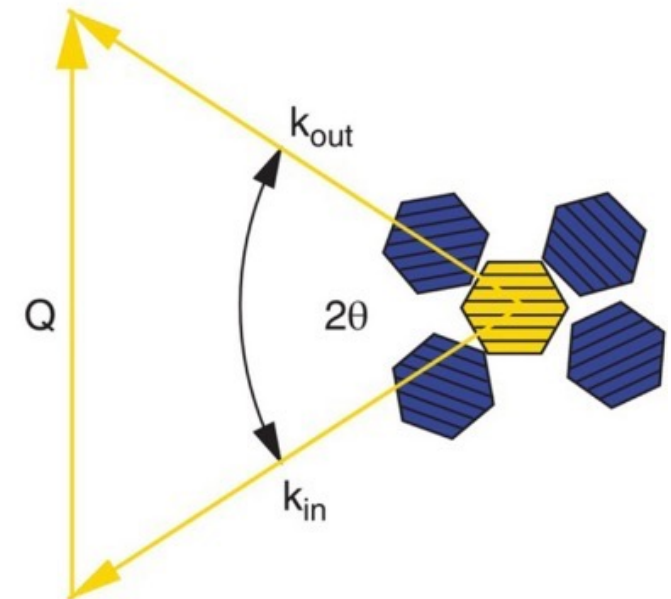
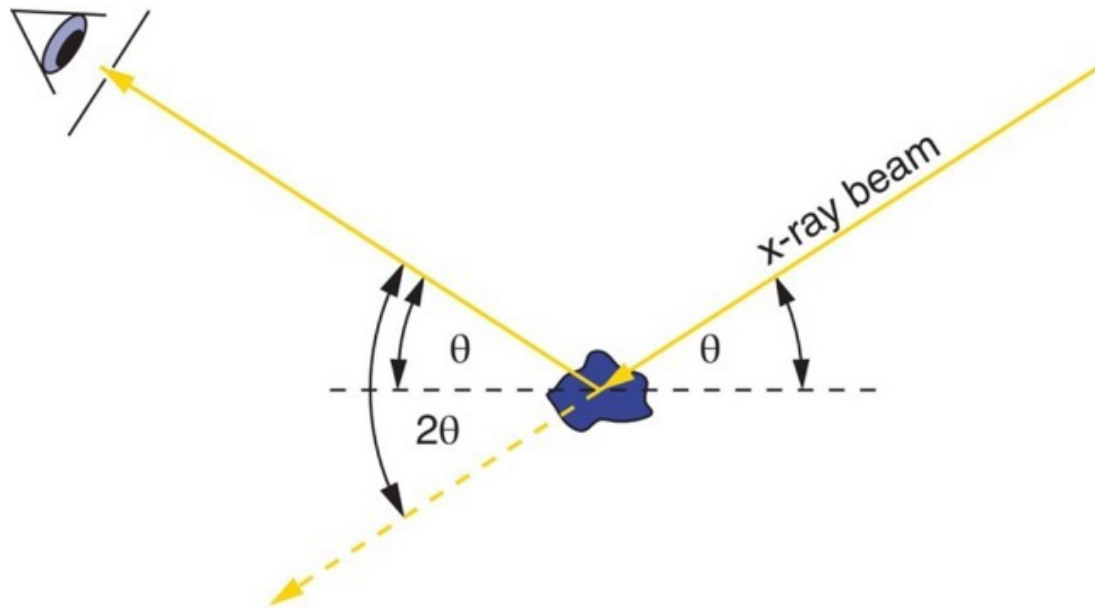
Courtesy: F. Van Petegem, UBC, Canada

In situ single-crystal synchrotron X-ray diffraction studies of metal-organic frameworks (2023)

- Study performed on single crystals of metal-organic frameworks (MOFs) under gas adsorption conditions via synchrotron single-crystal X-ray diffraction.
- 340 degrees phi sweep (1700 images, 0.2 deg/image).
- Allows the observation of the binding mechanism of CO and NO in Ni-CPO-27

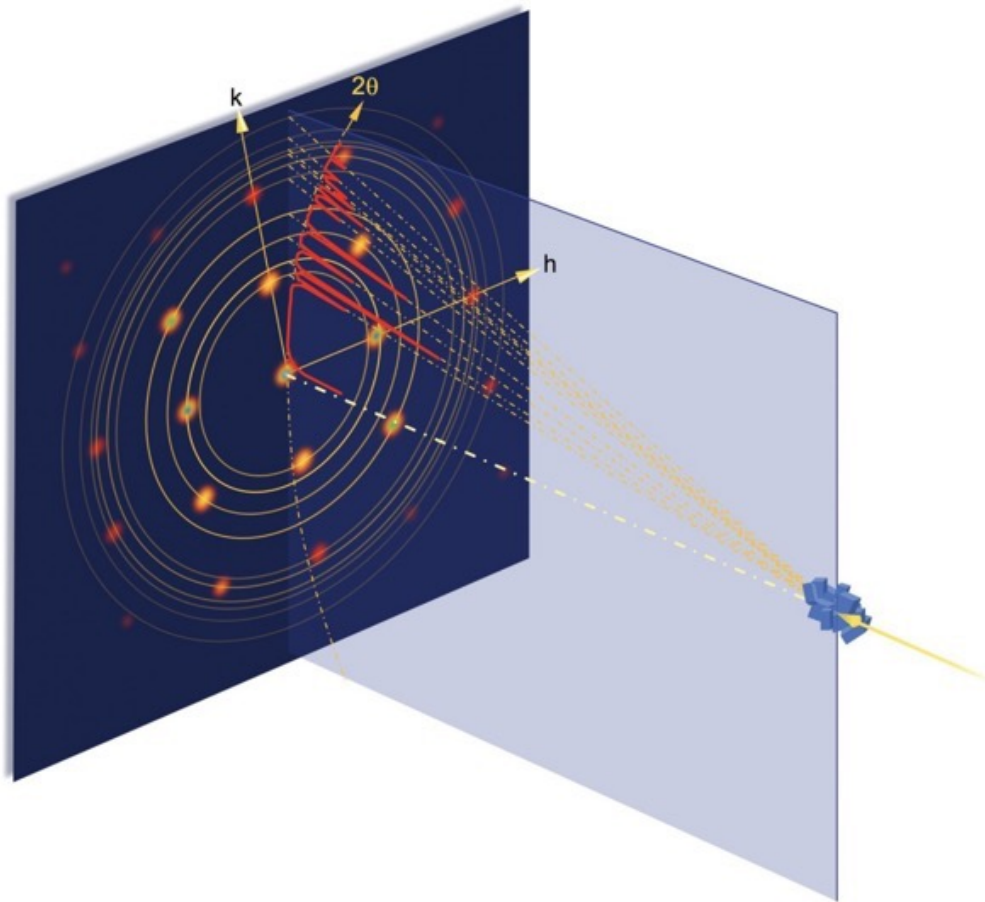


Powder diffraction

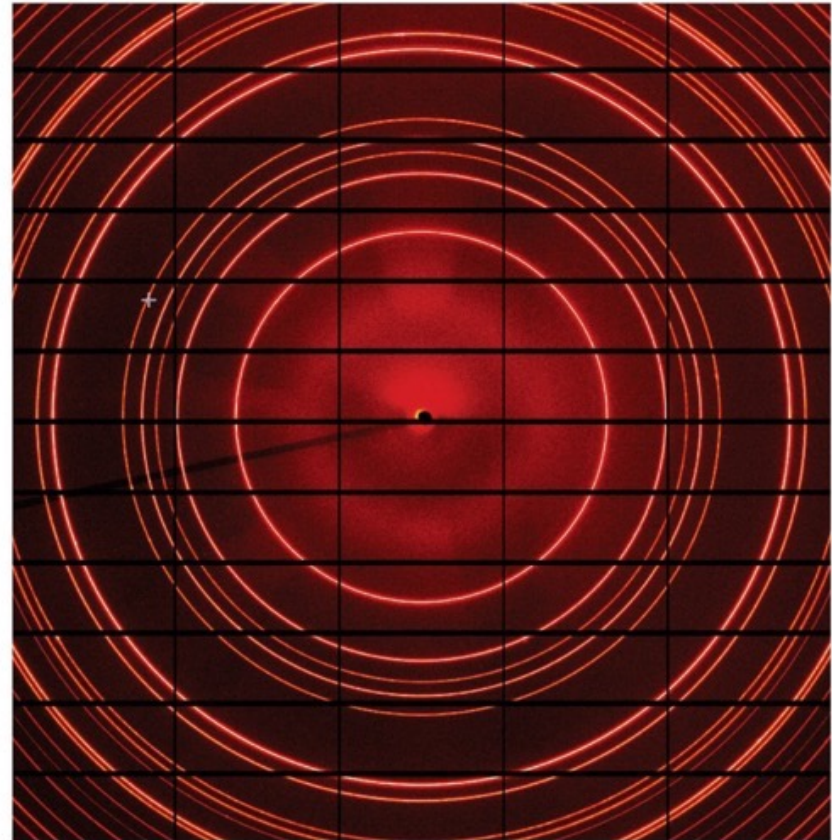
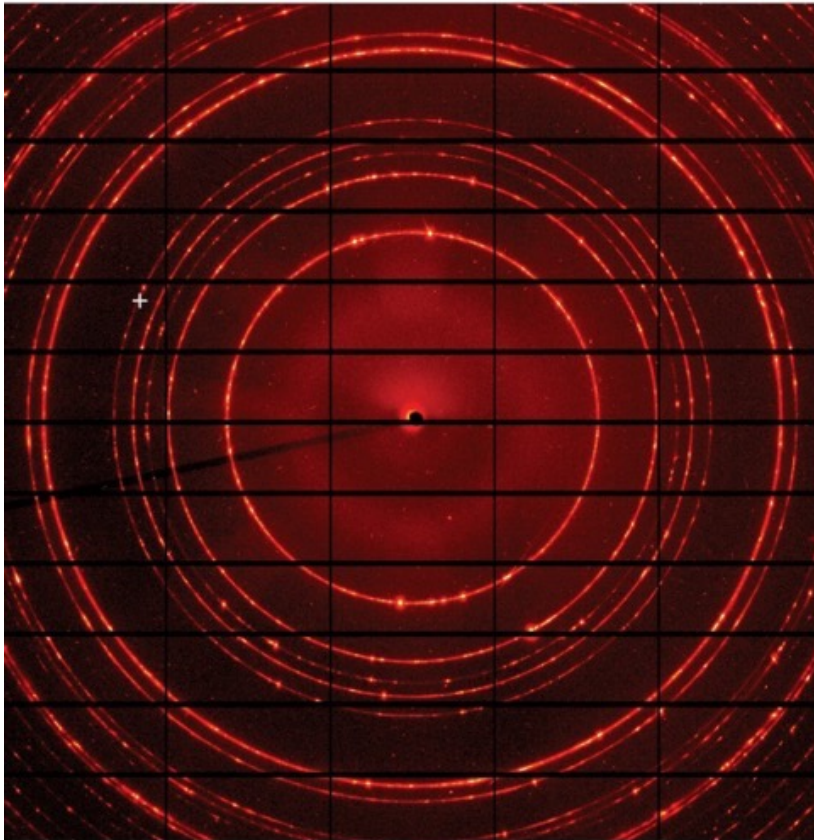


Conditions for diffraction in a powder sample. A detector will only see a diffracted signal if the d_{hkl} spacing, the orientation of the crystallite, and the angle of the detector 2θ to the incident x-ray beam leads to the diffraction condition being satisfied. This is fulfilled by the yellow-highlighted crystallite.

Powder diffraction



A schematic of a powder diffraction experiment. Those crystallites with crystal planes (hkl) at an angle θ given by the Bragg law to the incoming beam will diffract. The cylindrical symmetry of the experimental setup about the incident beam axis means cones of diffracted signal are produced. A diffraction pattern is obtained by scanning radially out from the beam axis with a detector in a plane that contains that axis.



The effect of spinning or shaking a powder sample during data acquisition

Rietveld refinement

- The collapse of three-dimensional reciprocal space onto one-dimensional data sets leads to a severe reduction of information, caused by an accidental and systematic peak overlap. This is known as the grave powder problem
- In 1969, Hugo Rietveld published the seminal article on what has become known as the Rietveld refinement method (cited over 22'000 times).
- The underlying idea relies on modeling a calculated powder diffraction pattern, described by a set of parameters.
- All of these parameters can be simultaneously refined by the least-squares method, until the calculated pattern matches the experimentally collected data.
- Since then, many 'whole powder pattern fitting' methods have been developed.

The intensity $I(2\theta)$ at the angle 2θ can be written as:

$$I(2\theta) = \sum_{i=1}^m F_i^2 \chi_i(2\theta_i - 2\theta) C_i$$

F_i is the structure factor for the i^{th} reflection

χ_i the peak shape function

C_i geometric factor including multiplicity and Lorentz factor

Refinement parameters may include lattice parameters, atomic positions, thermal parameters, site occupancy, peak asymmetry, Lorentz and polarization correction, axial divergence, background coefficients, strain and size broadening, ...

Lorentz factor

- Polarization correction: accounts for polarization state of incident beam (in most powder x-ray diffractometers, unpolarized)

$$P = 1 - \cos^2(2\theta)$$

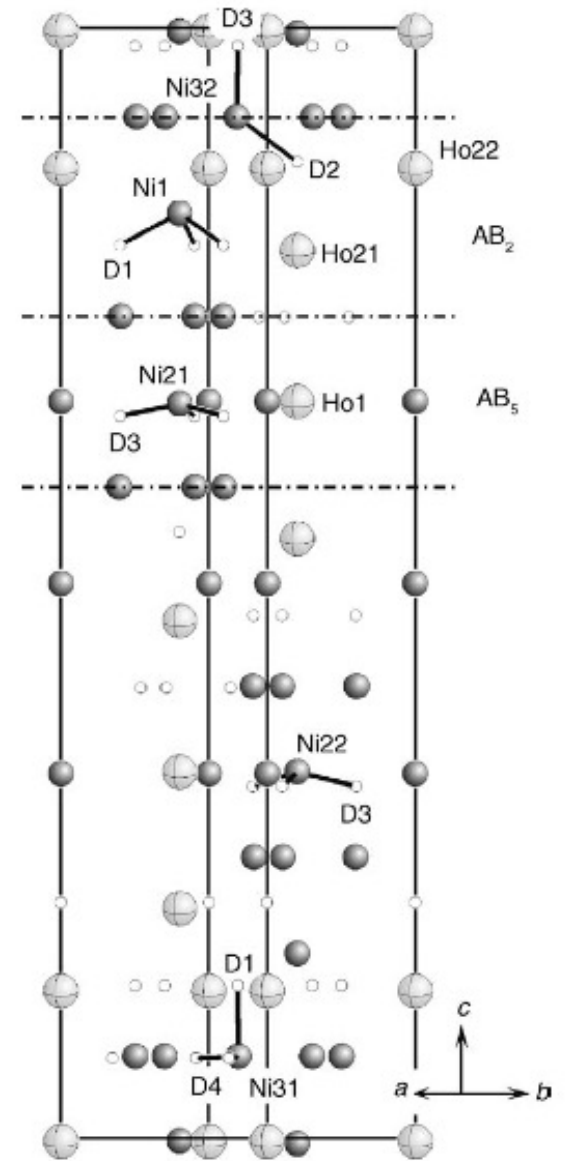
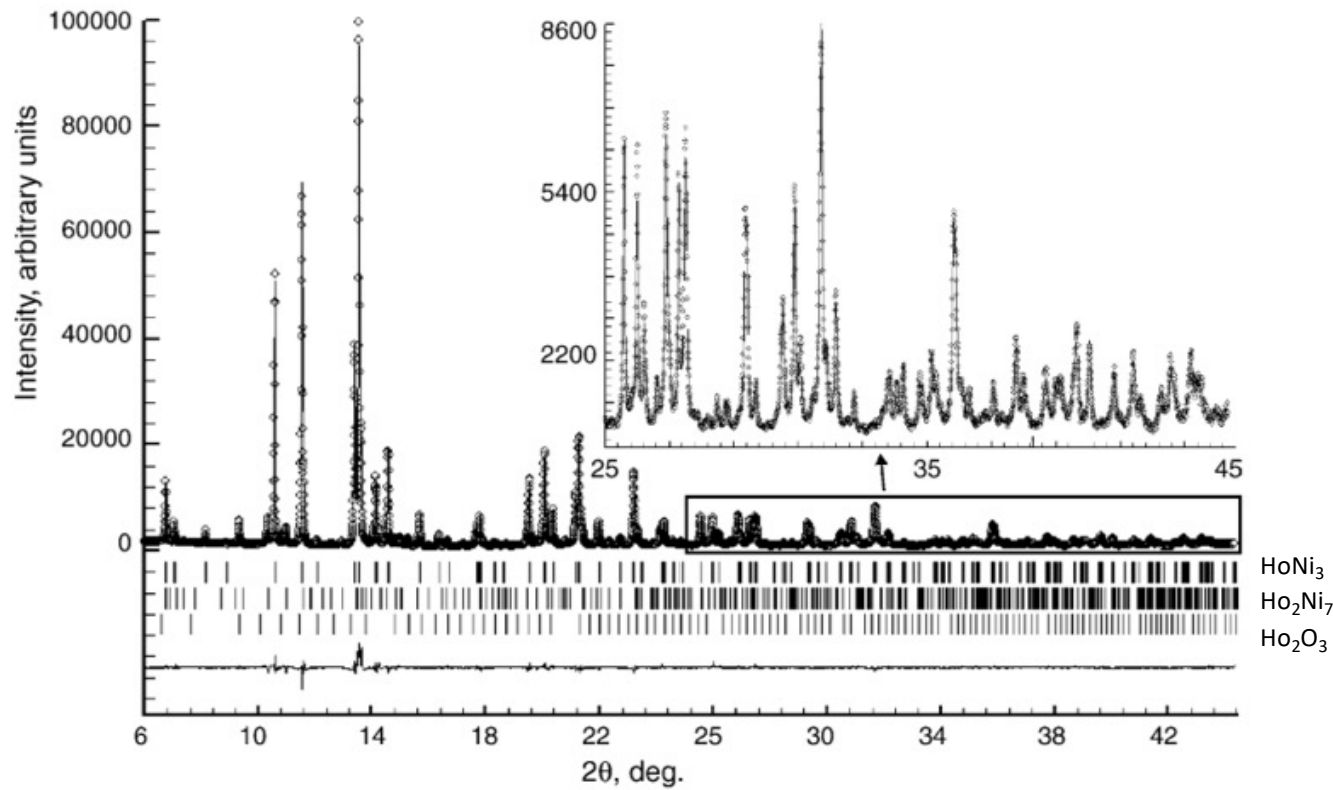
- Lorentz correction: takes into account change in scattering volume size & scan rate as a function of angle for a particular diffraction geometry

$$L = 1/(\sin^2 \theta \cos \theta)$$

- Lorentz–polarization factor

$$LP = (1 - \cos^2(2\theta)) / (\sin^2 \theta \cos \theta)$$

Rietveld refinement



There exist many data analysis routines that include Rietveld refinement, such as

Fullprof: <http://www.ill.eu/sites/fullprof>

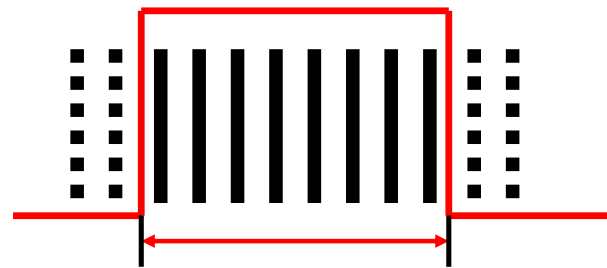
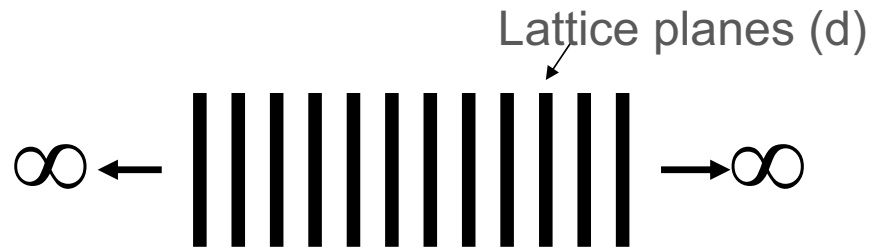
GSAS: <http://www.ncnr.nist.gov/xtal/software/gsas.html>

MAUD: <http://maud.radiographema.com>

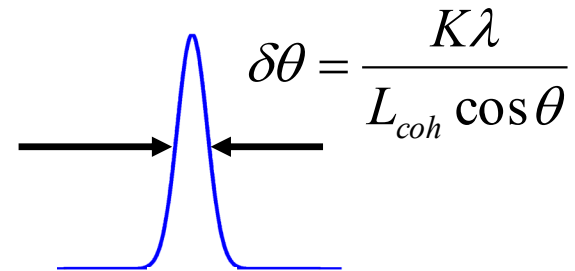
The International Centre for Diffraction Data: <http://www.icdd.com>

- Peak profiles are determined by many factors. The most important ones include:
 - Resolution function
 - Coherent scattering length
 - Grain size
 - Anti-phase boundaries
 - Faulting
 - Microstrain
 - Inhomogeneous elastic strain
 - Dislocations
 - Grain surface relaxation
 - Solid solution inhomogeneity
 - Temperature factors
- Peak profile is a convolution of the profiles from all of these contributions

Grain size analysis



Coherent scattering length L_{coh}




Size broadening due to incomplete 'canceling'
of small deviations from the Bragg angle

Grain size analysis

- Scherrer formula:
$$B(2\theta) = \frac{K\lambda}{L \cos \theta}$$
- - the most common values for K are:
 - 0.94 for FWHM of spherical crystals with cubic symmetry
 - 0.89 for integral breadth of spherical crystals with cubic symmetry
 - 1, because 0.94 and 0.89 both round up to 1
- K actually varies from 0.62 to 2.08
- For an excellent discussion on K, refer to J.I. Langford and A.J.C. Wilson, *J. Appl. Cryst.* **11** (1978) p102

Grain size analysis – examples



Crystallite size L	Peak FWHM (Cu K α , 2 θ \approx 40°)
1 μ m	\sim 0.001° (instrument-limited)
100 nm	\sim 0.01°
10 nm	\sim 0.1°
3 nm	\sim 0.3°

Dislocation density

Elastic strain variations



distribution of lattice distances

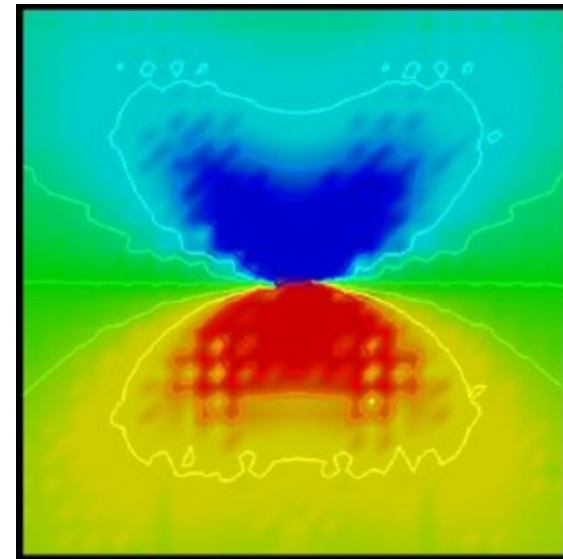
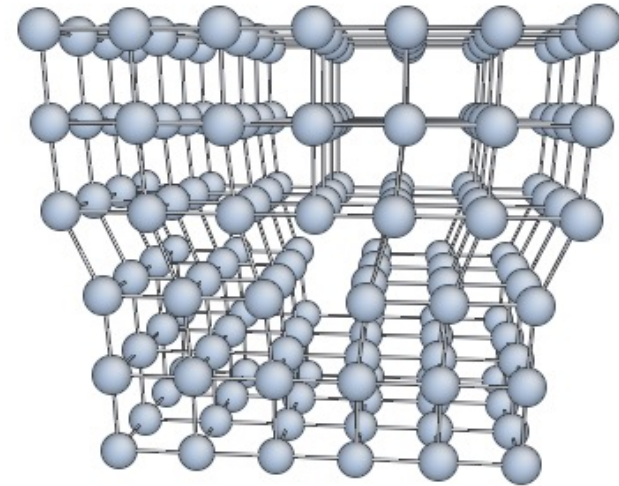


peak broadening

Dislocations: anisotropic strain distribution



Dislocation contrast factor C



Dislocation density

- Modified Williamson-Hall method
 - T. Ungar et al. *Appl. Phys. Lett.* 69, 3173 (1996)

- Fourier analysis

$$A_{hkl}^D = \exp \left[-\frac{1}{2} \pi b^2 \bar{C}_{hkl} \rho d_{hkl}^* L^2 f^* \left(\frac{L}{R_e} \right) \right],$$

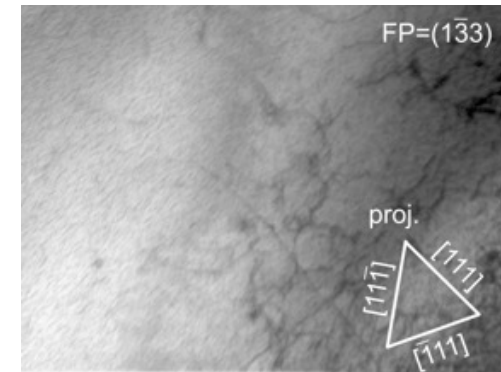
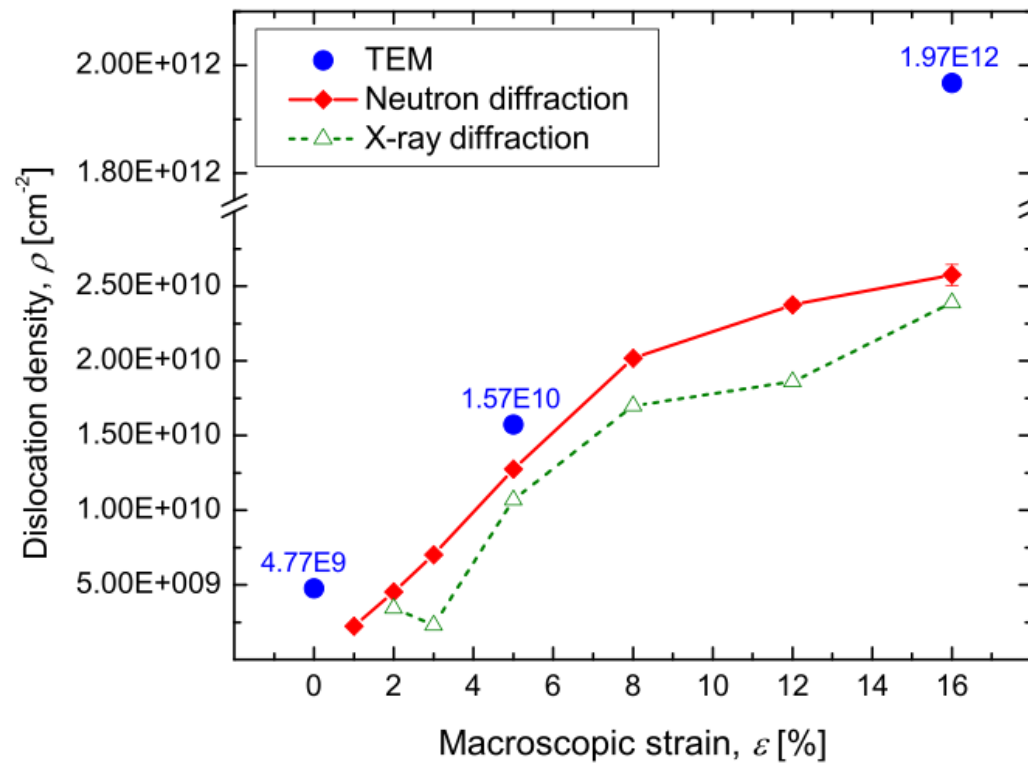
– *X-ray Diffraction*, B.E. Warren, Dover Publications, 1990

- Full pattern fitting (e.g. PM2K)
 - M. Leoni et al. *J. Appl. Crystall.* 40, 719 (2007)

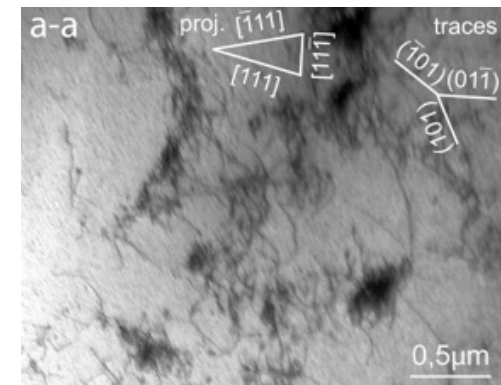
Parameters: dislocation density, cut-off radius and character

Dislocation density

- Example: deformation of a low carbon C10E steel.



↓ 5% deformation

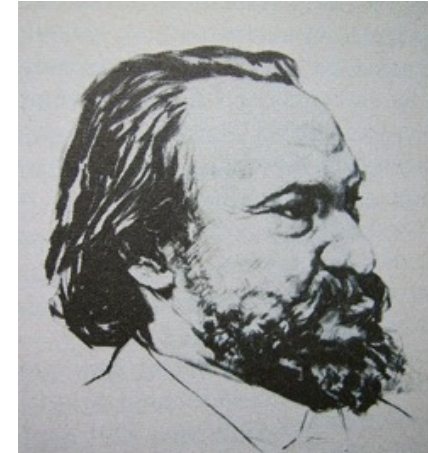
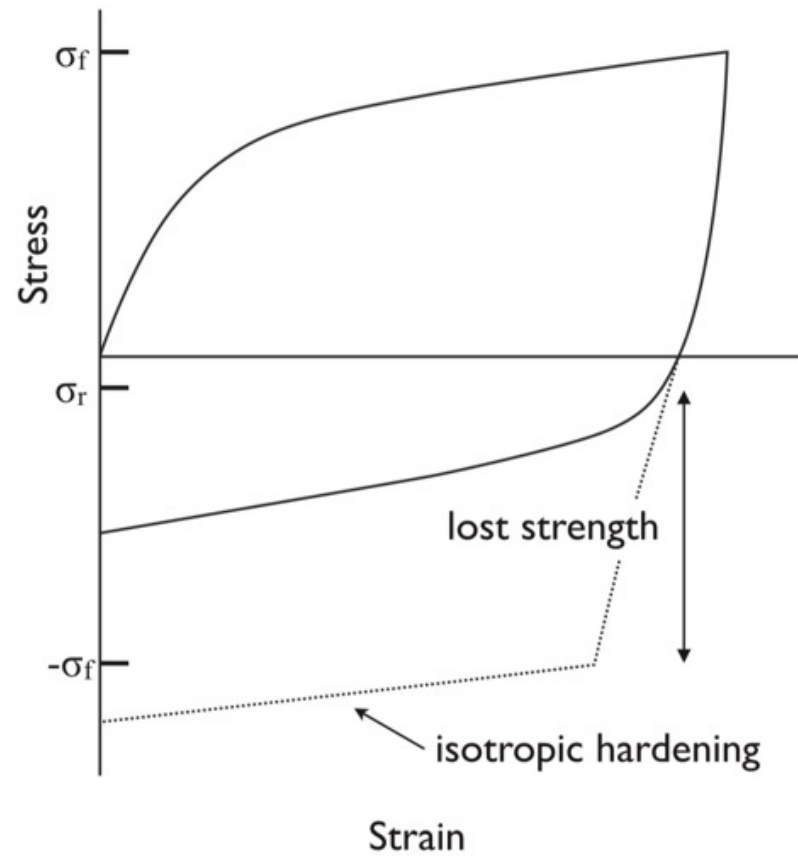




The story of copper

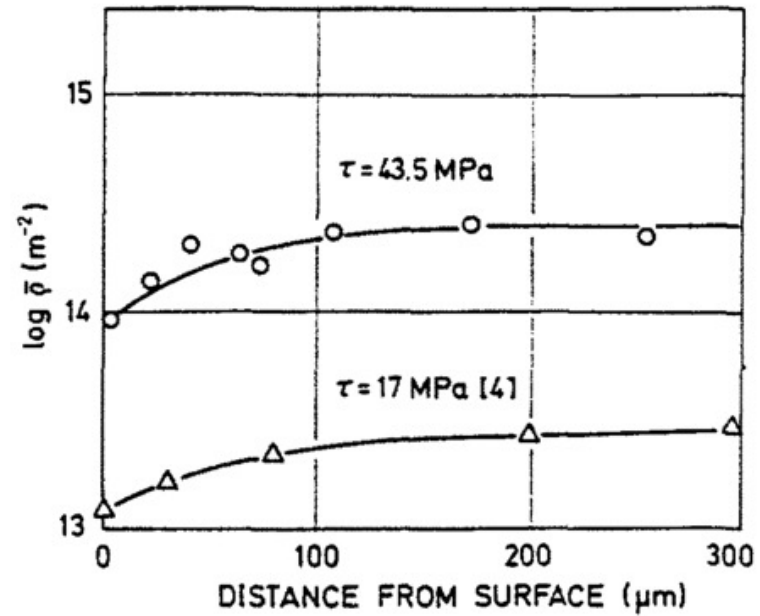
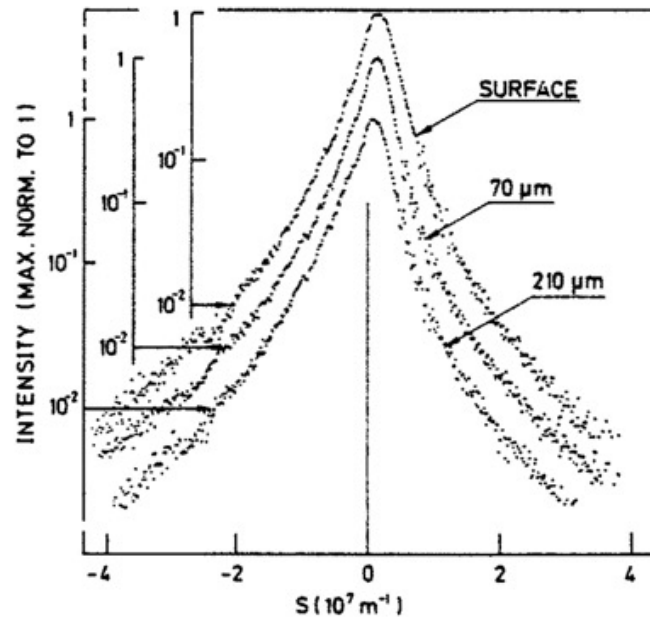
The story of copper

- Bauschinger effect (1881), *Civiling.N.F.*, 27, 289.



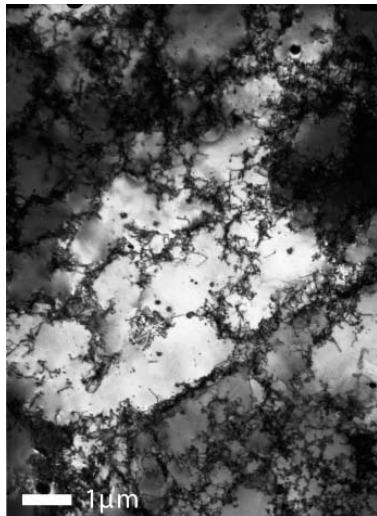
The story of copper

Ungar et al. (1982) Acta. Metall. 30, 1861

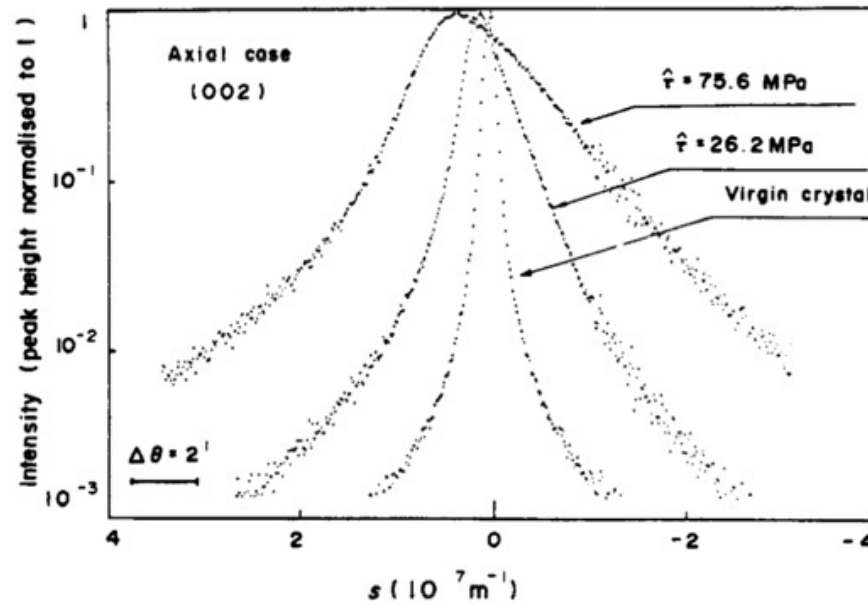


Dislocation density measurements based on approach Wilkens (physica status sol 2, 359 (1970)).

The story of copper



Plastically deformed Cu

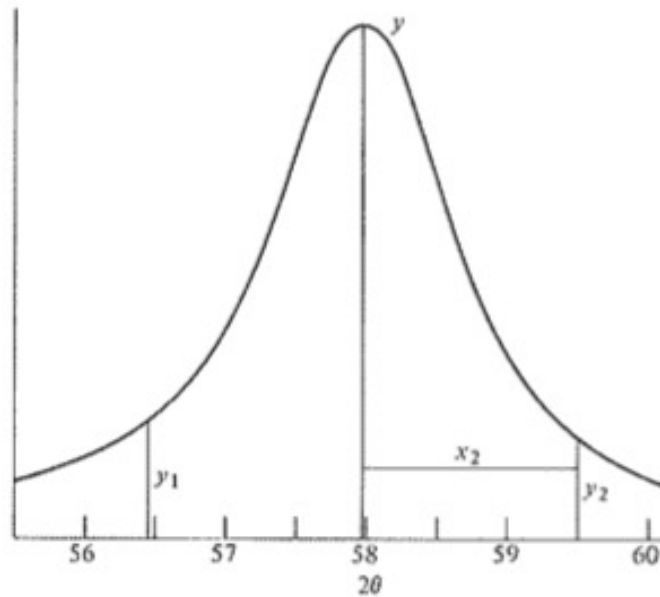


Origin of strong peak asymmetry?

H. Mughrabi, Acta Metall. 31 (1983) 1367

The story of copper

Faulting?

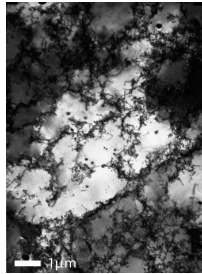


Sample	Line	D_e [10 ² Å]	β_c [10 ⁻⁴ Å ⁻¹]		M^*	ρ^* [10 ¹⁰ cm ⁻²]
			β_c	β_g		
70% rolled	400		0	44.1	12.6	22.0
	200	4.7	0	22.0	12.6	5.5
	222		23.2	16.4	1.26	16.1
	111	11.7	5.8	6.2	2.51	2.3
20% rolled	400		6.2	40.9	12.6	18.9
	200	6.8	1.6	20.4	12.6	4.7
	222		28.0	0	< 0.5	-
	111	8.4	7.0	0	< 0.5	-
Fatigued	400		0	41.6	12.6	19.6
	200	2.7	0	20.8	12.6	4.9
	222		0	28.9	12.6	9.5
	111	3.3	0	14.5	12.6	2.4
After tension	400		28.9	0	< 0.5	-
	200	2.9	7.2	0	< 0.5	-
	222		3.7	7.2	3.02	1.5
	111	4.4	0.9	3.6	5.01	0.3

$$\beta = \frac{\sqrt{3} \pi x_2 (y_1 - y_2)}{2A} \left\{ 1 + \left[\frac{\lambda}{4\pi D(\text{eff. } 200)(\sin \theta_2 - \sin \theta_0)} \right]^2 \right\}. \quad (13.76)$$

B.E. Warren X-ray diffraction (1969)

The story of copper



Composite model

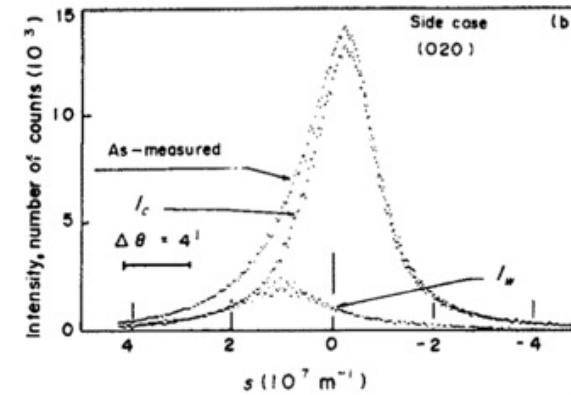
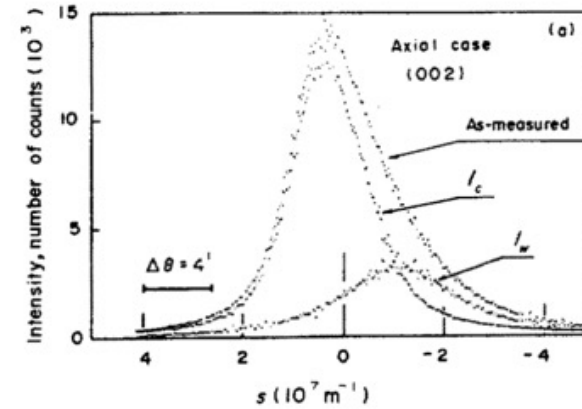
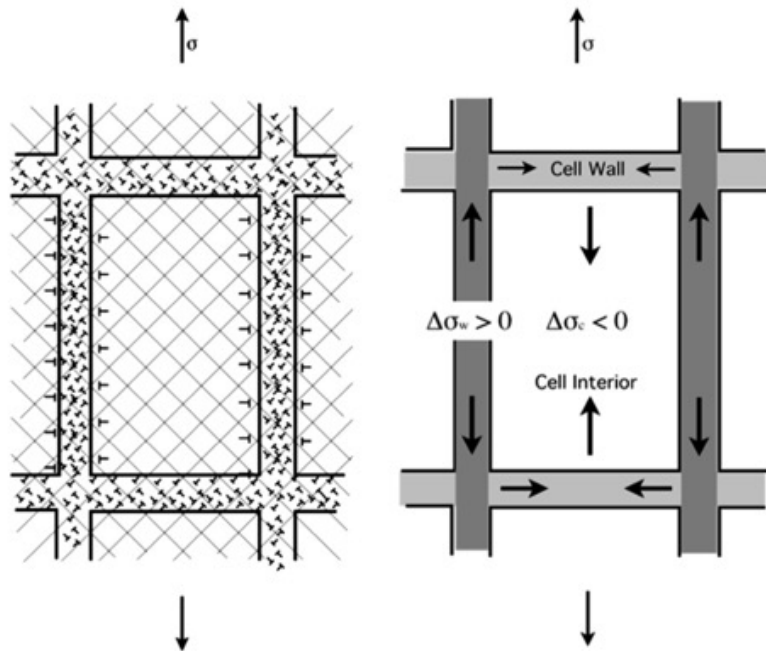


Fig. 4. Decomposed line profiles, $\hat{\tau} = 75.6$ MPa. (a) Axial case, $g = (002)$, (b) side case, $g = (020)$.

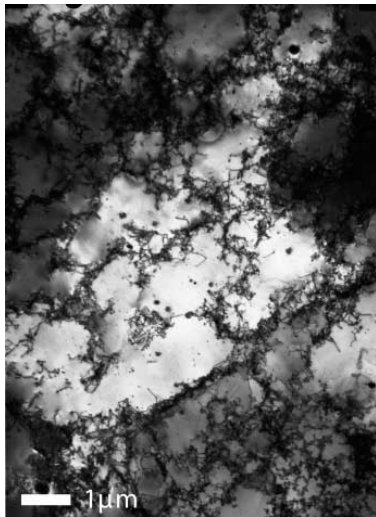
H. Mughrabi, Acta Metall. 31 (1983) 1367

Advantage or disadvantage?

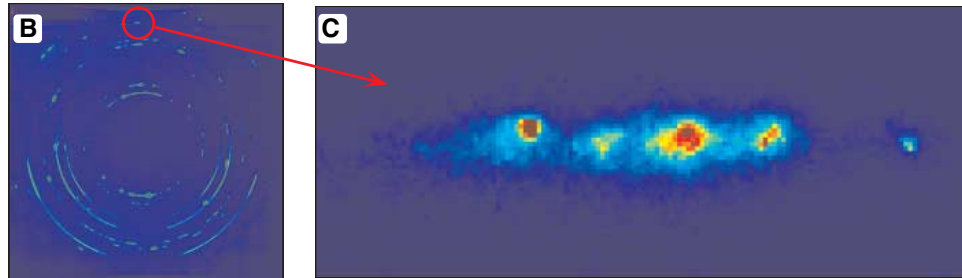
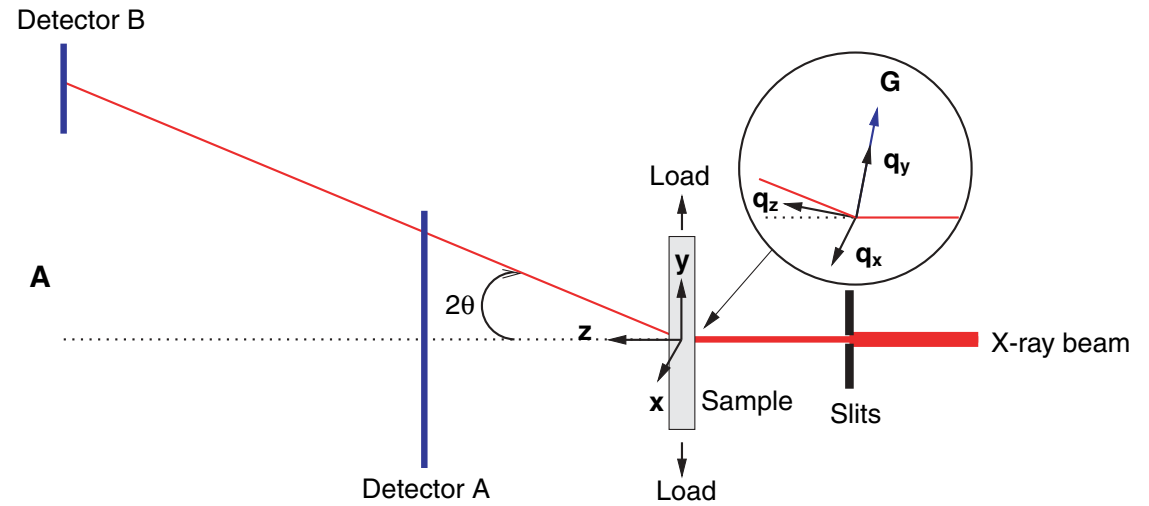
- One of the big advantages of x-ray powder diffraction: provides statistical relevant information (compared to, for instance, electron microscopy)
- One of the big disadvantages of x-ray powder diffraction: provides only averaged information, sometimes obscuring the source of changes in peak shape.
- Solution: move away from conventional powder diffraction and use local x-ray probes



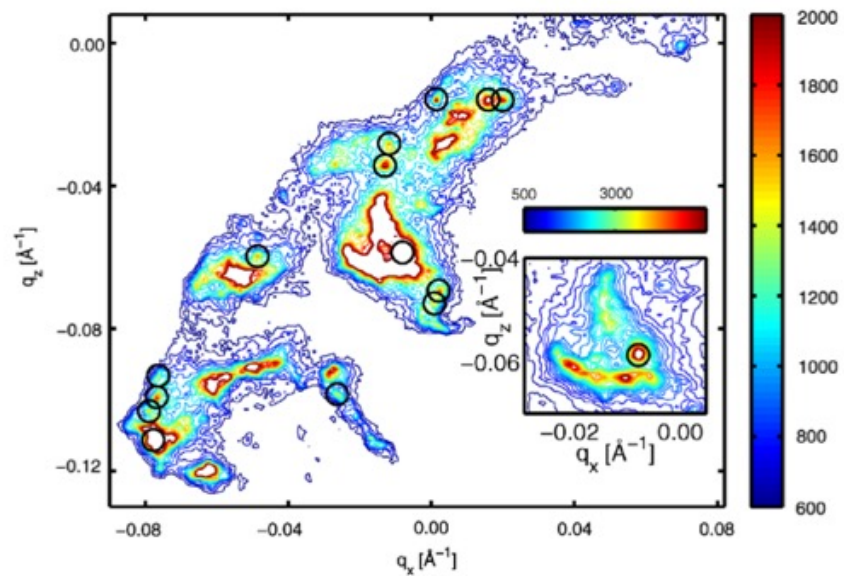
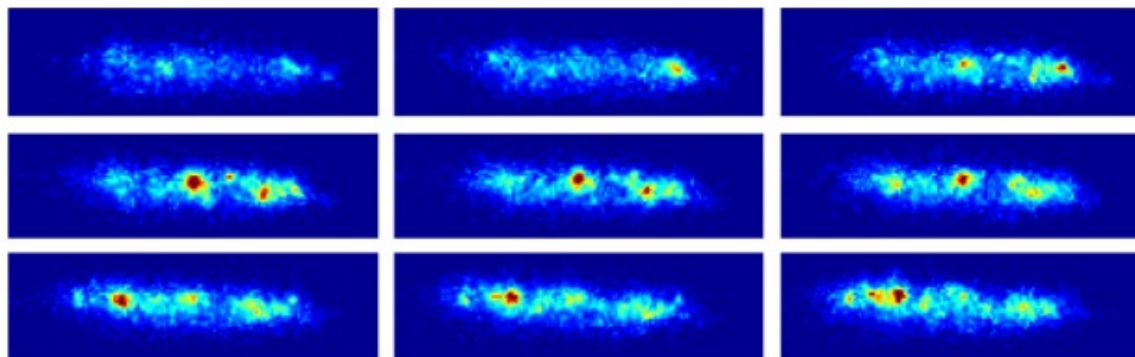
New insights into the old Cu problem



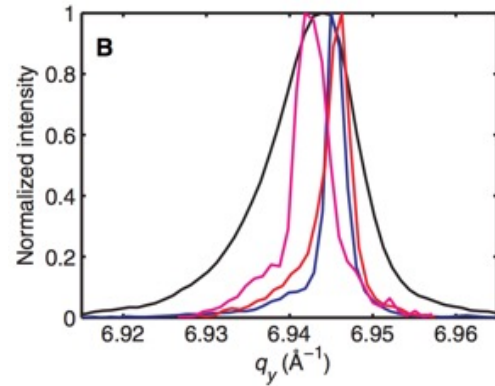
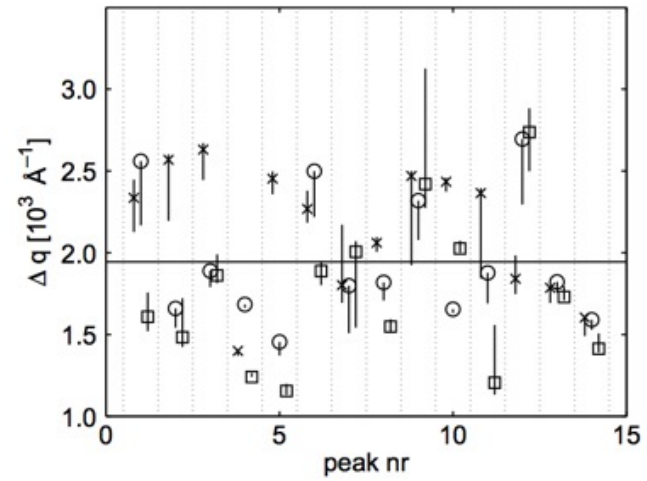
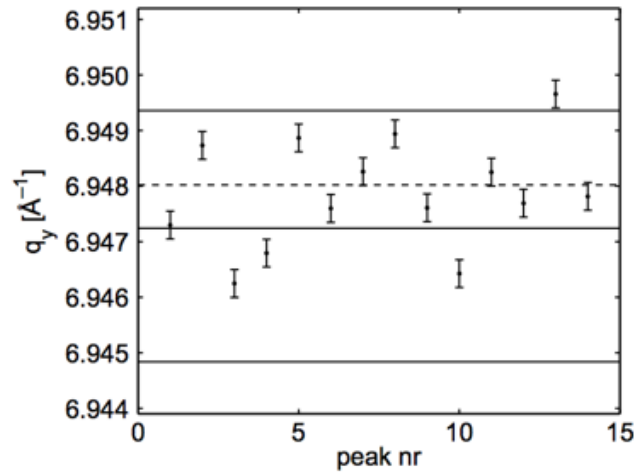
Plastically deformed Cu



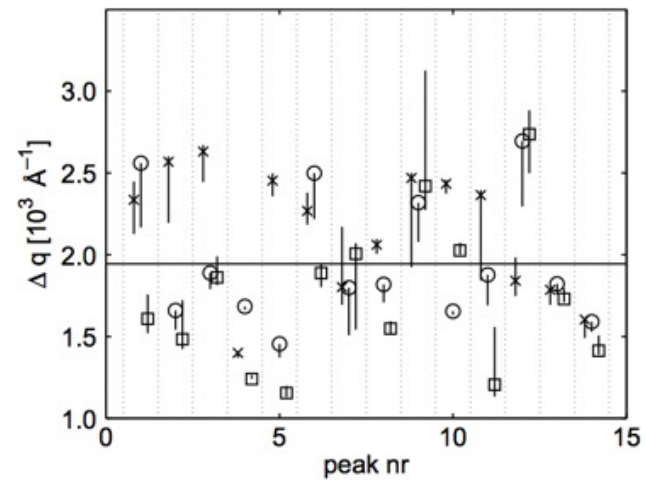
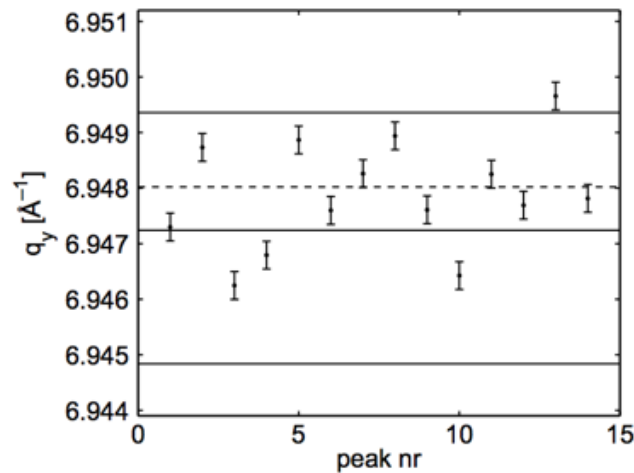
New insights into the old Cu problem



New insights into the old Cu problem



New insights into the old Cu problem



Sub-grains are dislocation-poor ($<10^{13} \text{ m}^{-2}$)

,Bulk' diffraction peaks are composed of diffuse background (dislocation walls) + sum of sharp peaks from the sub-grains, each with a different stress level, leading to broad diffraction peaks



Take home messages

Critically assess all possible causes for peak broadening

Each method will give you a number

Use multiple analysis techniques

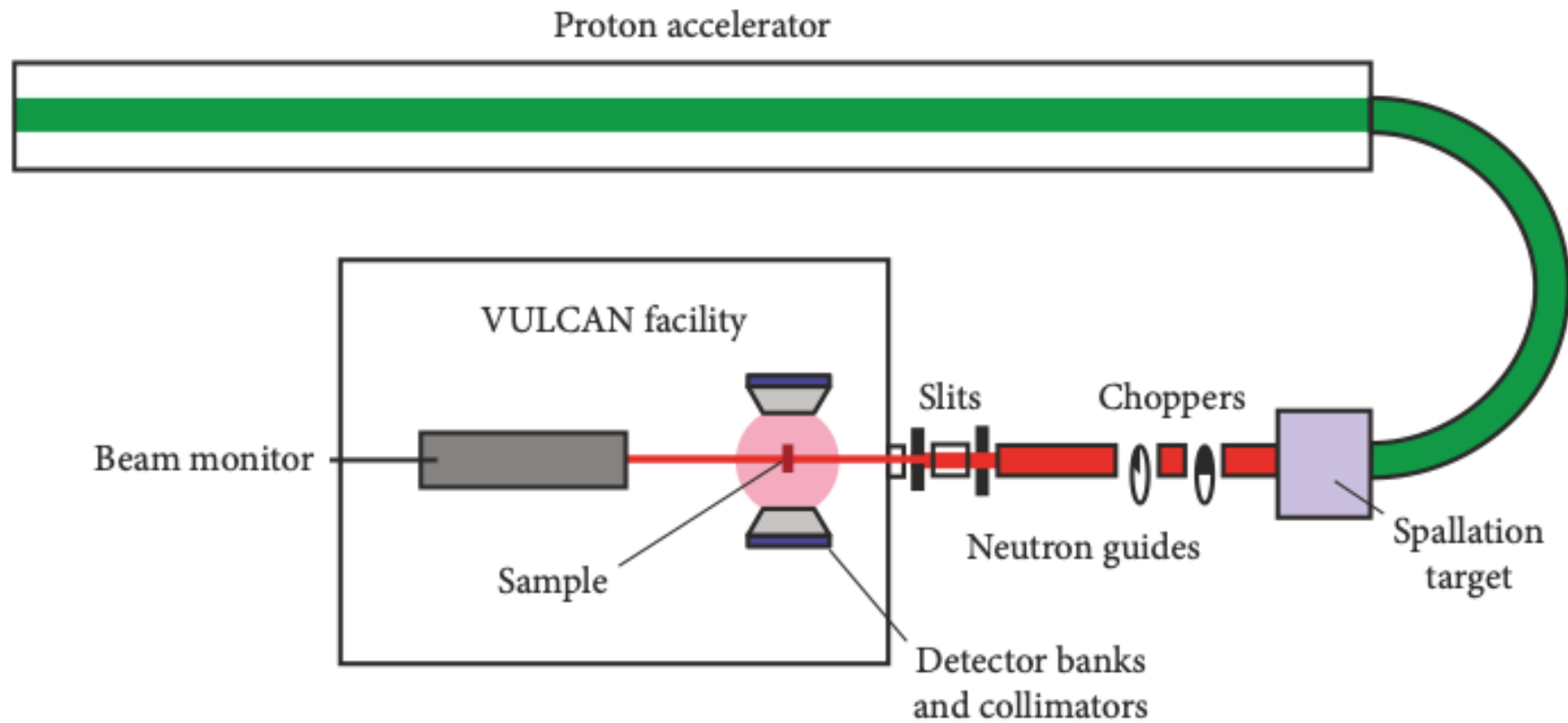
Neutron time-of-flight

- Velocity of cold and thermal neutrons with wavelength λ is low enough to reliably measure the time t needed to fly distances L (of the order of metres):

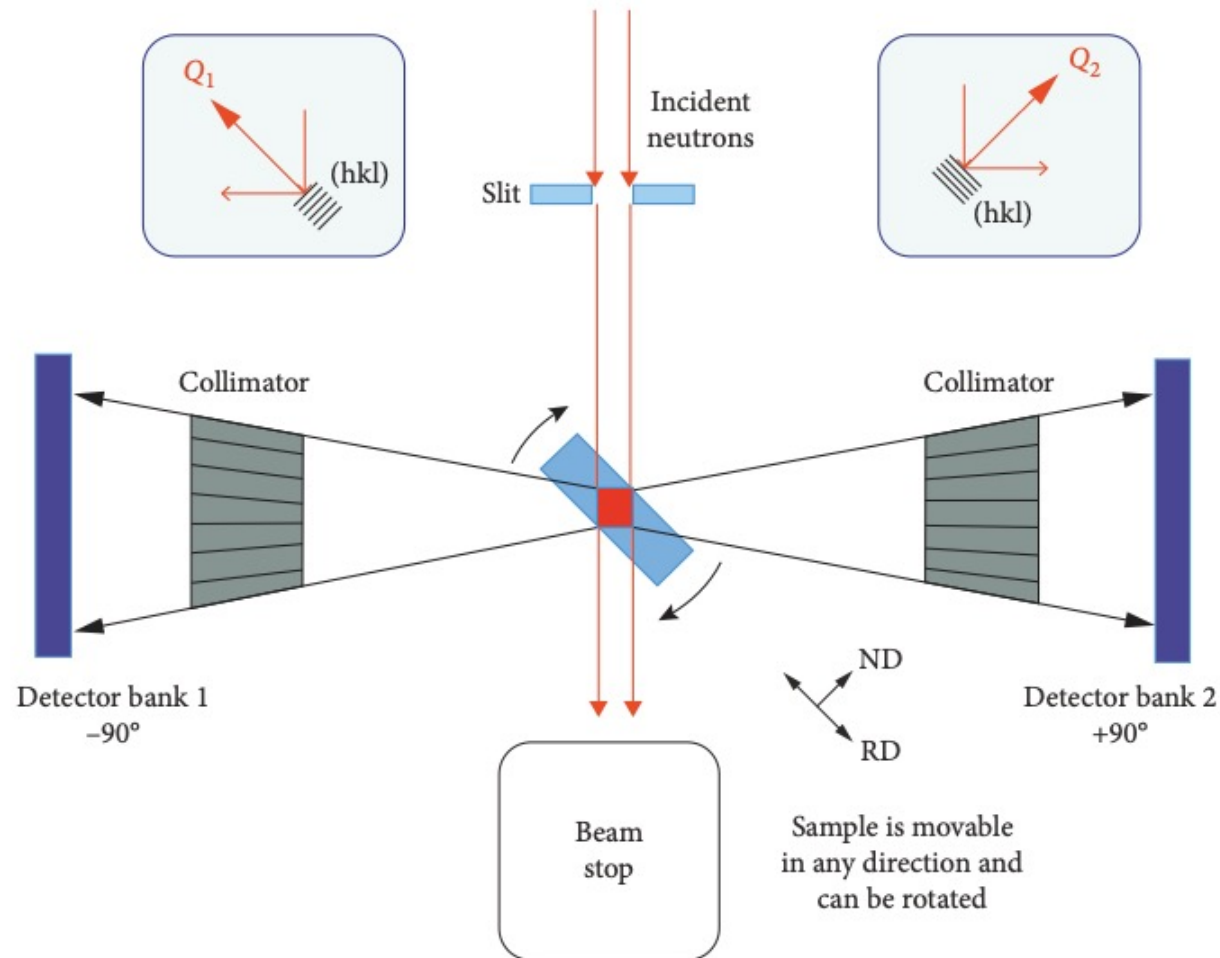
$$t = \frac{\lambda m_n}{2\pi\hbar} L$$

- Start signal is provided by:
 - Timing signal of the pulsed source
 - Signal from a chopper
- Stop signal is provided by the neutron detector
- ToF allows to
 - determine the wavelength of a detected neutron
 - work with a pink neutron beam
 - work at fixed diffraction angles

Neutron time-of-flight



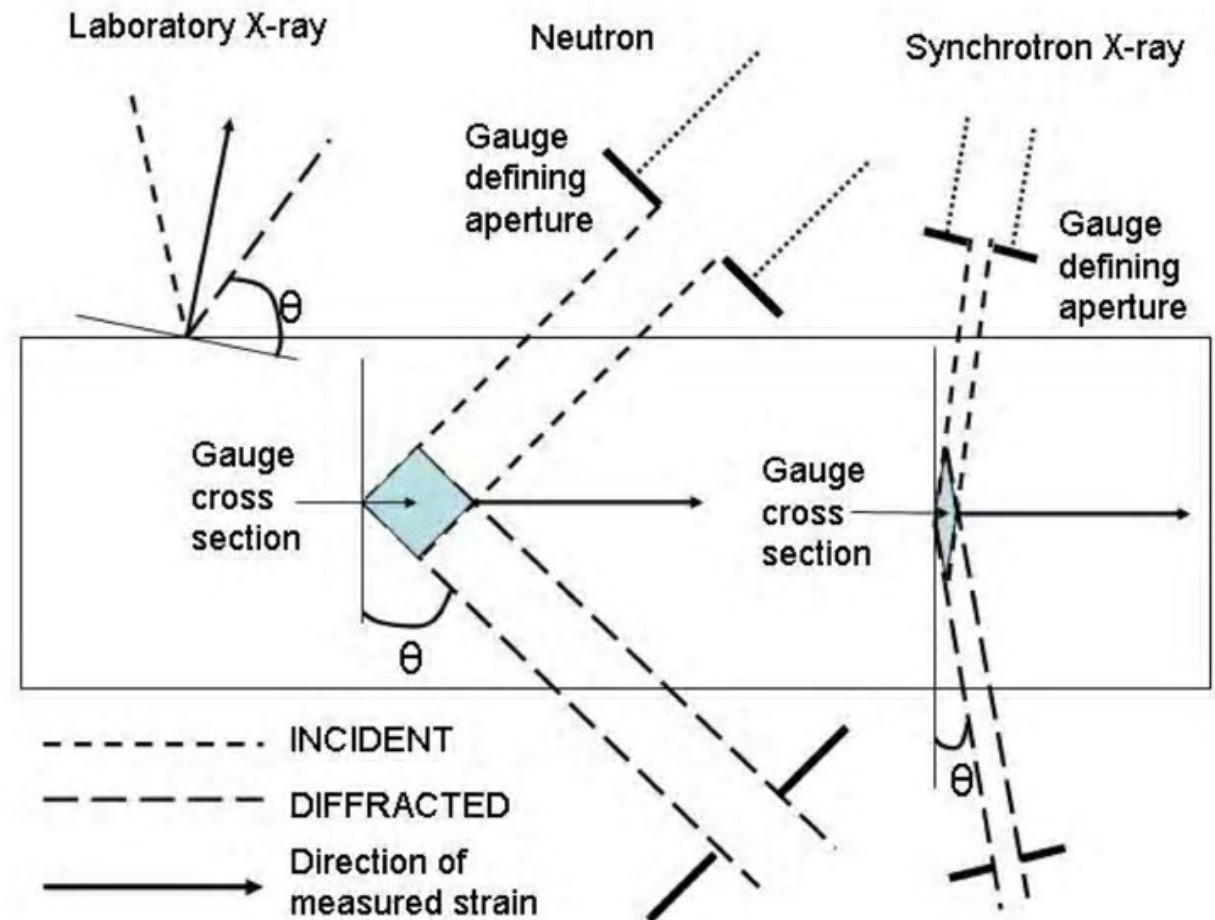
Neutron time-of-flight



X-ray versus neutrons

Factors to consider:

- Penetration depth
- Flux
- Activation
- Sample environment
- Grain statistics
- Gauge volume
- ...



A square gauge volume has important advantages for residual stress measurements. Elastic strain is defined as the relative change of the lattice spacing d_{hkl} from the stress-free lattice spacing d_{hkl}^0

$$\varepsilon_{hkl} = \frac{d_{hkl} - d_{0,hkl}}{d_{0,hkl}} = \frac{\Delta d_{hkl}}{d_{0,hkl}} = \frac{\sin \theta_{0,hkl}}{\sin \theta_{hkl}} - 1$$

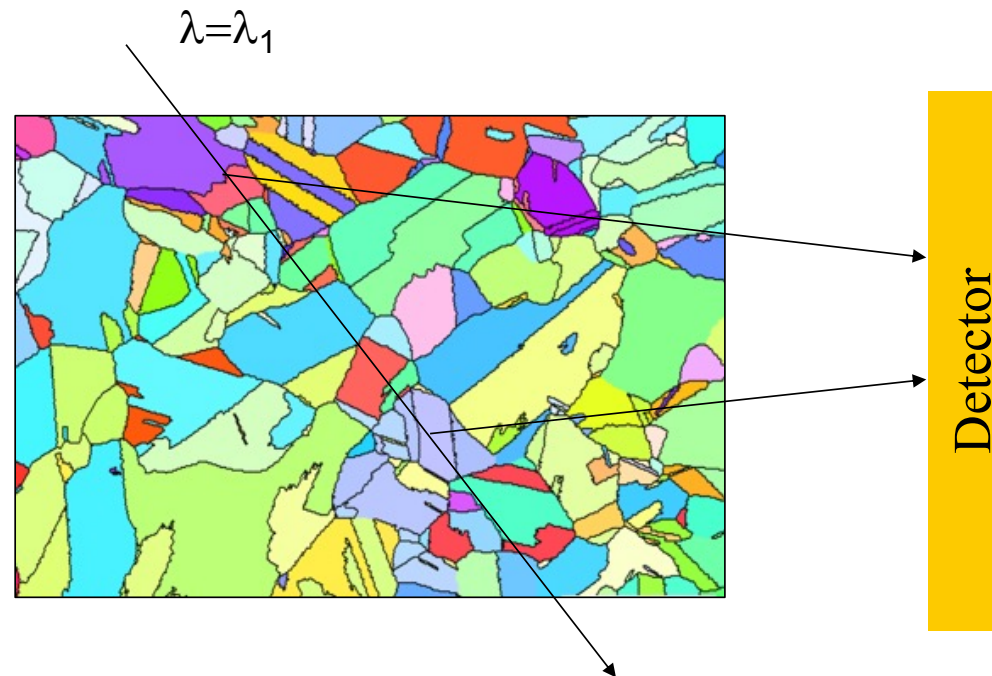
Stress σ_{ij} and elastic strain ε_{kl} are second rank tensors and are related through elastic constants C_{ijkl} :

$$\sigma_{ij} = \underline{C}_{ijkl} \varepsilon_{kl}$$

Full determination of the strain tensor requires measurements of the elastic strain in at least six independent directions. If the principal strain directions within the specimen are known, measurements along these three directions are sufficient.

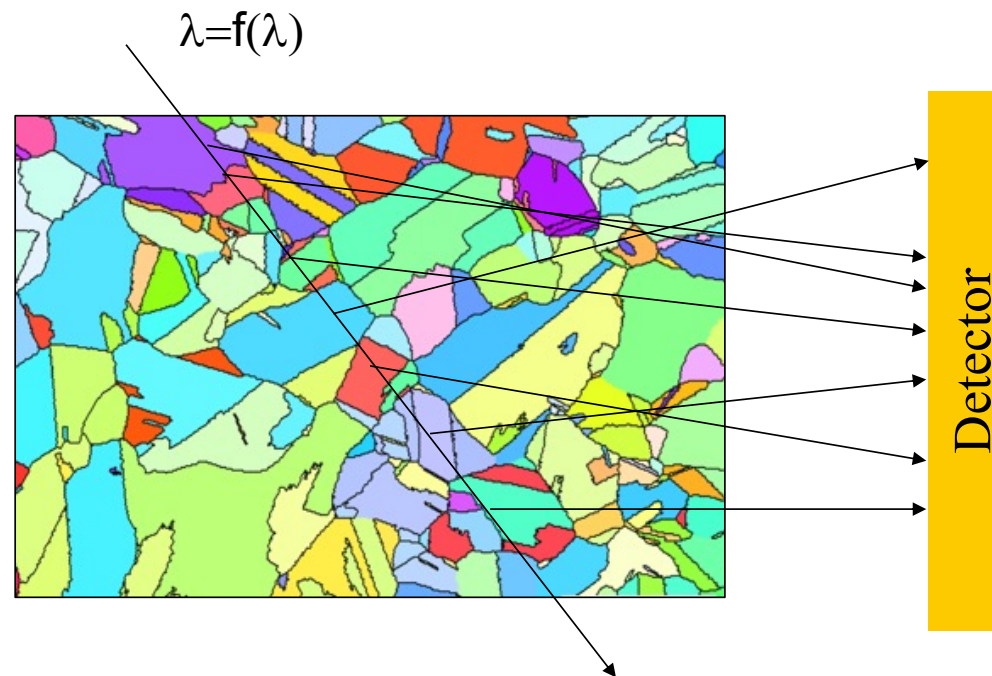
X-ray versus neutrons

- In order to obtain statistical relevant information, sufficient grains need to be in the gauge volume. In ToF, a pink beam is combined with a large neutron detector.



X-ray versus neutrons

- In order to obtain statistical relevant information, sufficient grains need to be in the gauge volume. In ToF, a pink beam is combined with a large neutron detector.



Application: residual stress measurements

- AA7449: Al-Zn-Mg-Cu
- Complex processing route with thermal treatments
- Residual stresses in large components because of different cooling rates during quenching

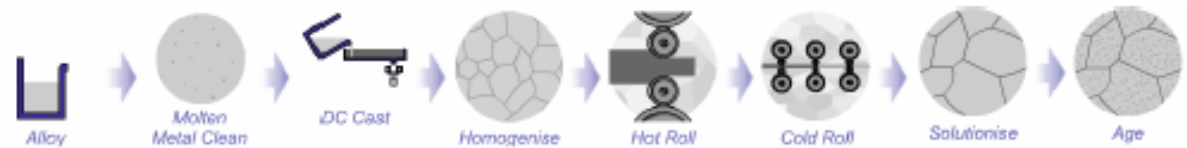
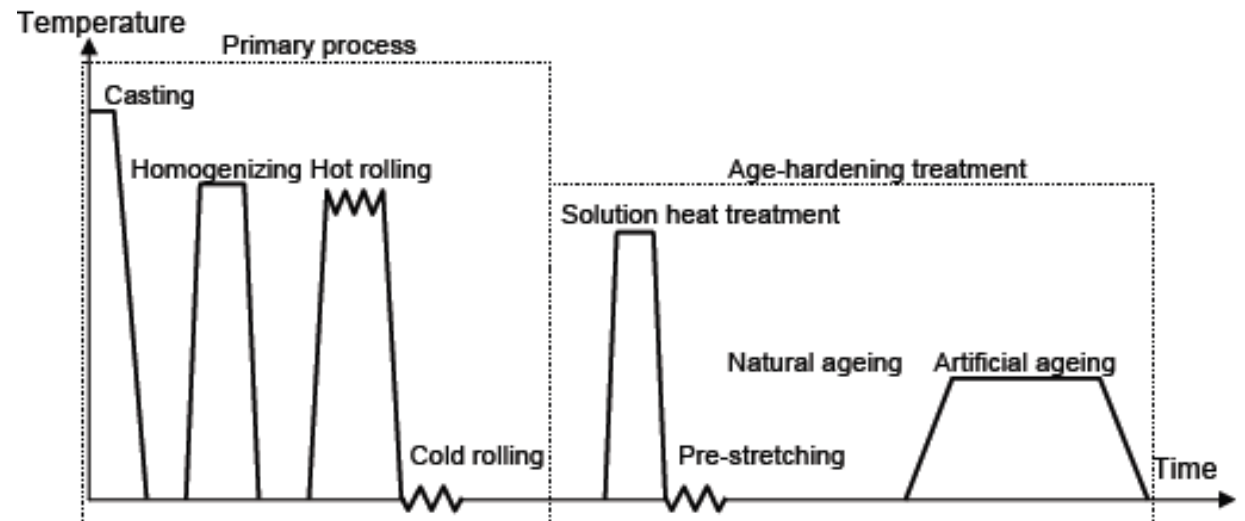


Fig. I-6. Schematics of the processing steps for AA7xxx



Understanding quenching:

<https://www.youtube.com/watch?v=gNrT-G2Zo9w>

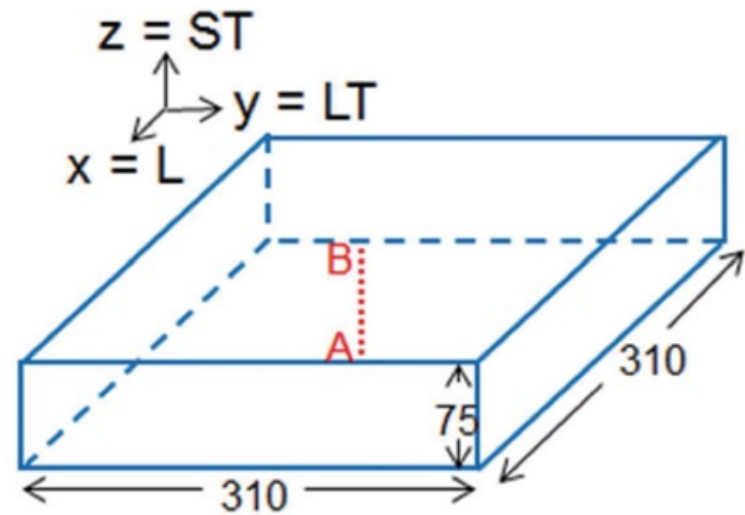
Prince Rupert's Drops:

<https://www.youtube.com/watch?v=6V2eCFsDkK0>

<https://www.youtube.com/watch?v=xe-f4gokRBs>

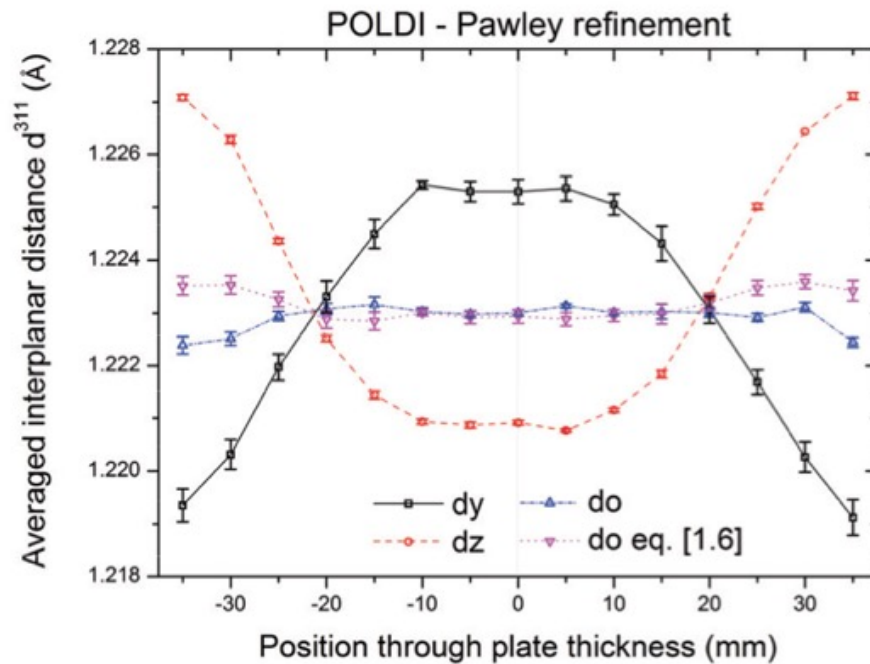
Application: residual stress measurements

- ToF neutron diffraction ideal:
 - Large penetration depth in aluminium
 - Large grain sizes
 - No need for high spatial resolution
- Residual stresses are measured along A-B



Application: residual stress measurement

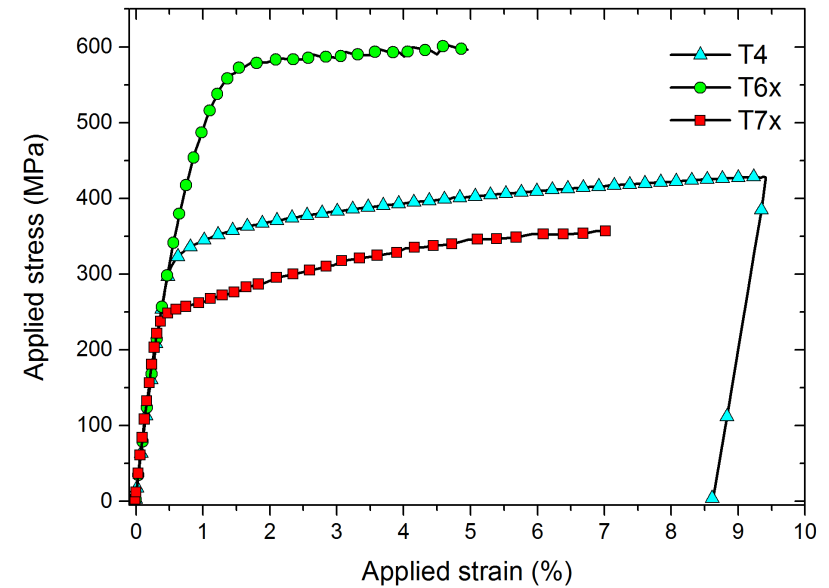
- Line profile through the plate thickness



→ In order to convert to stress we need the diffraction elastic constants. How to measure this?

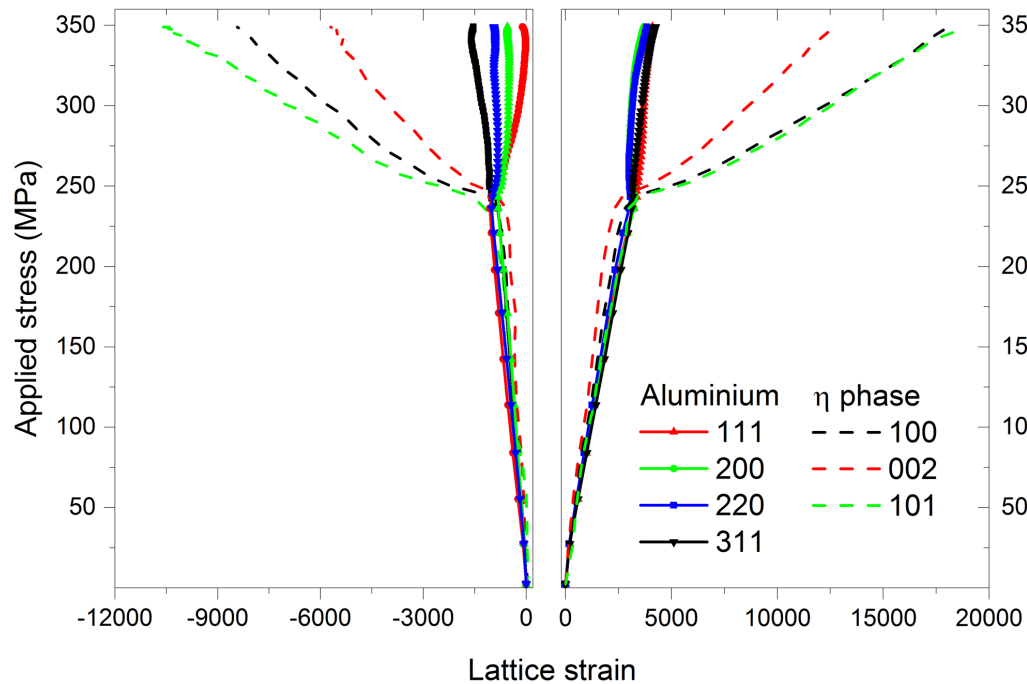
Application: residual stress measurements

- Cut dogbone samples out of thick block and perform tensile tests



Application: residual stress measurements

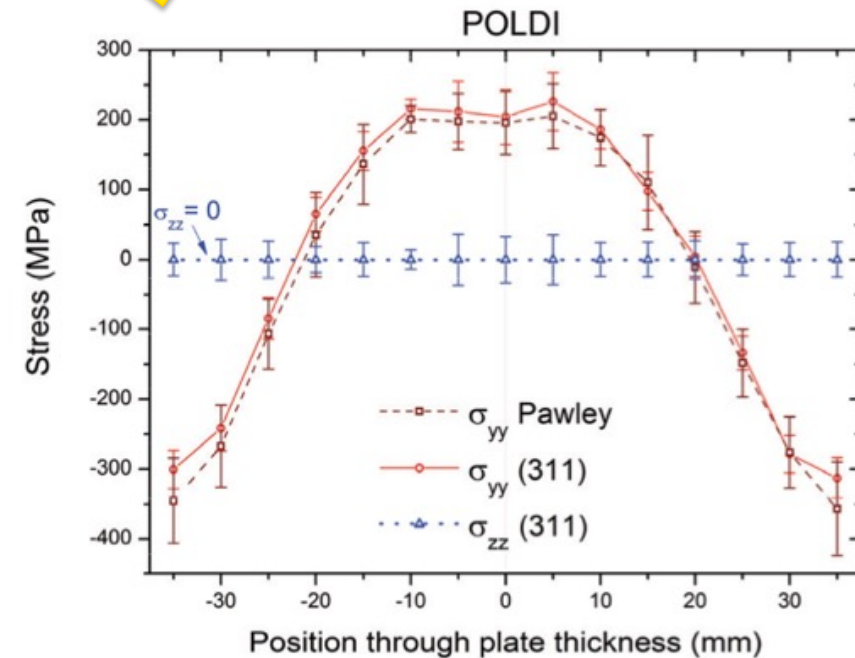
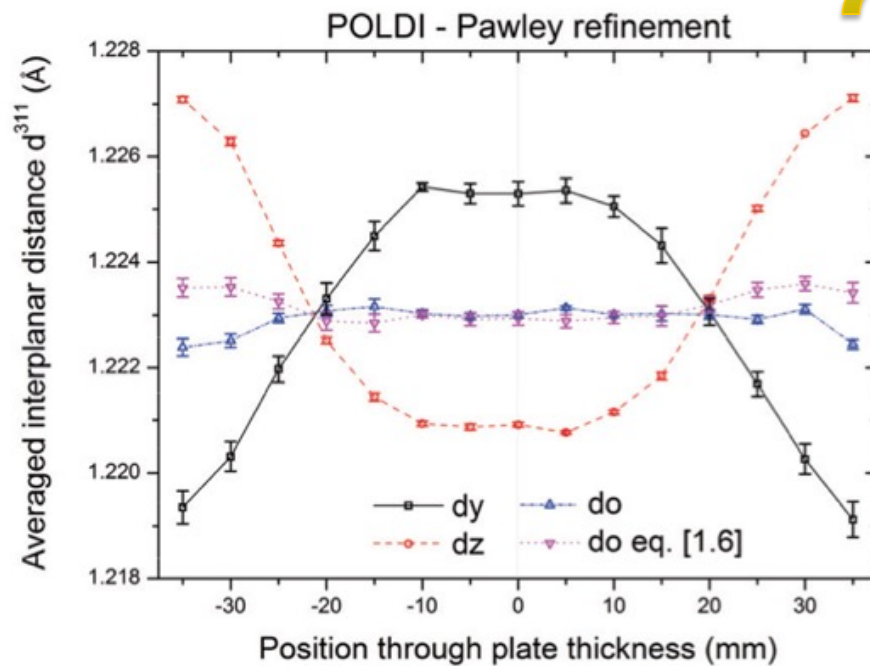
- Measure lattice strain as a function of applied stress.
- Slope in the elastic regime provides the diffraction elastic constants



Reflection	T4	T6x	T7x
Al {111}	73.8 ± 1.7	67.8 ± 2.6	69.8 ± 1.3
Al {200}	67.0 ± 3.2	69.3 ± 2.4	70.5 ± 1.2
Al {220}	72.5 ± 4.2	74.4 ± 3.6	73.3 ± 1.4
Al {311}	69.7 ± 3.1	70.7 ± 3.4	71.9 ± 1.2
η (100)			84.9 ± 1.5
η (002)			96.5 ± 2.4
η (101)			82.7 ± 2.6

Application: residual stress measurement

- Line profile through the plate thickness



What is Pawley refinement?

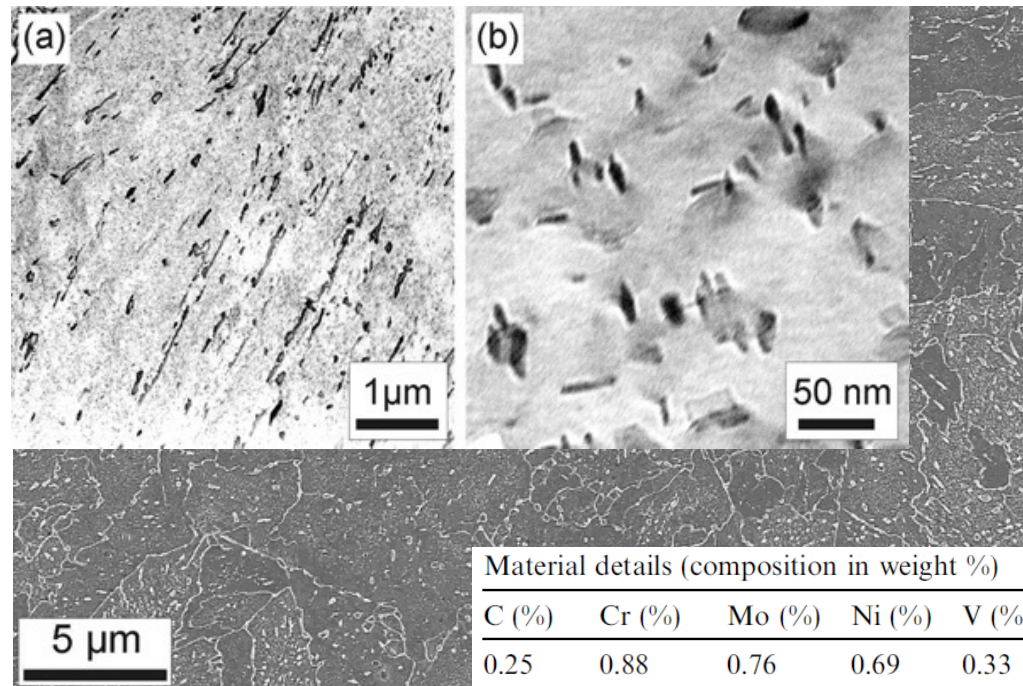
- Similar to Rietveld refinement
- Intensities are not calculated based on structure factor (bound to the structure) but are a fitting parameter
- Does not take into account texture
- Robust method for refinement of unit cell and less stringent than Rietveld
- Another alternative to Rietveld: Le Bai refinement
 - Can be used when there is no initial structural model.
 - Presume that all the integrated intensities are initially equal
 - After one iteration, isolated peaks will have an observed intensity equal to the observed area under the Bragg peak. For overlapping reflections, the procedure has to be tackled iteratively



The story of cementite

The story of cementite

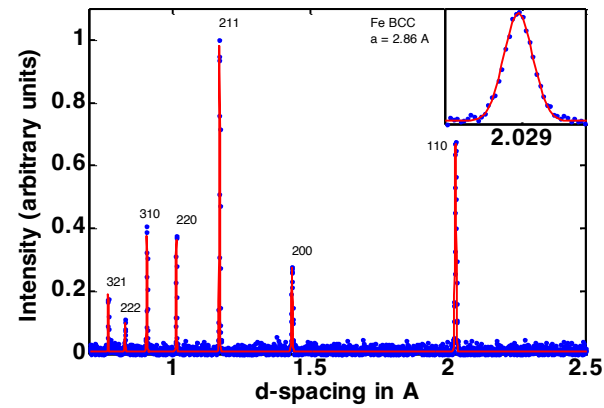
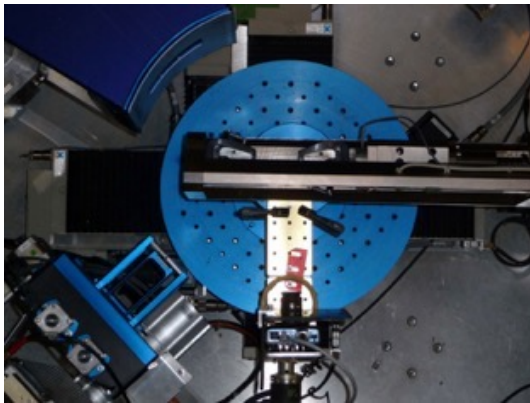
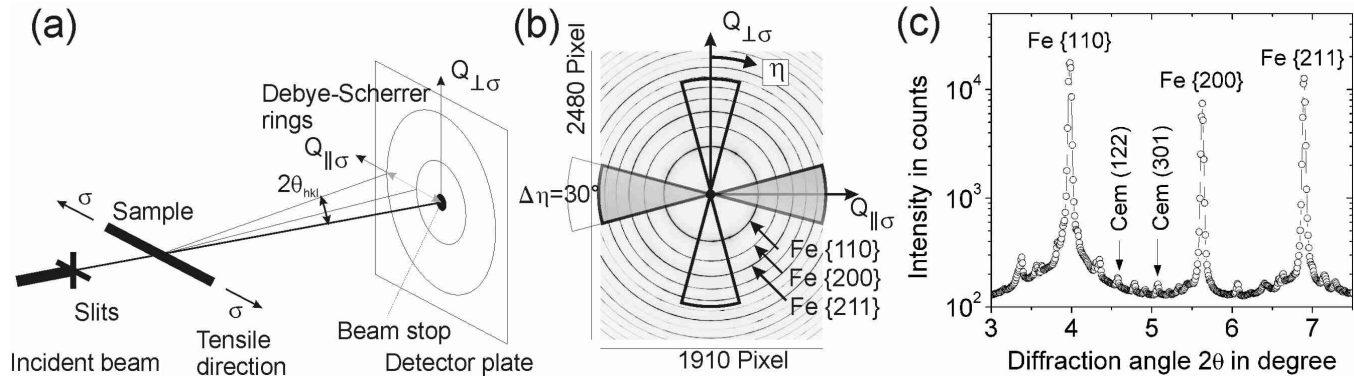
- Matrix – precipitates
- Ferrite – cementite (very heterogeneous)



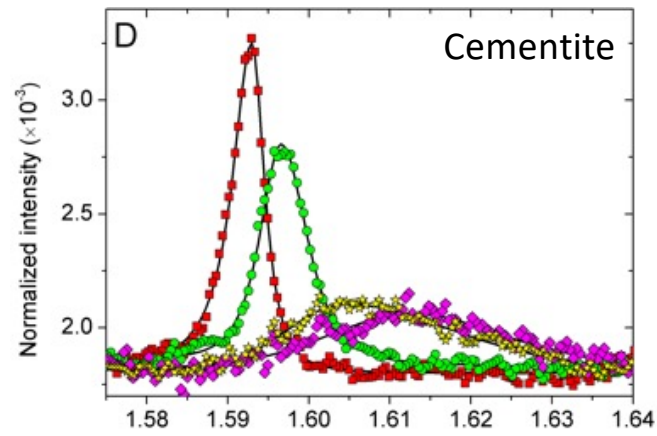
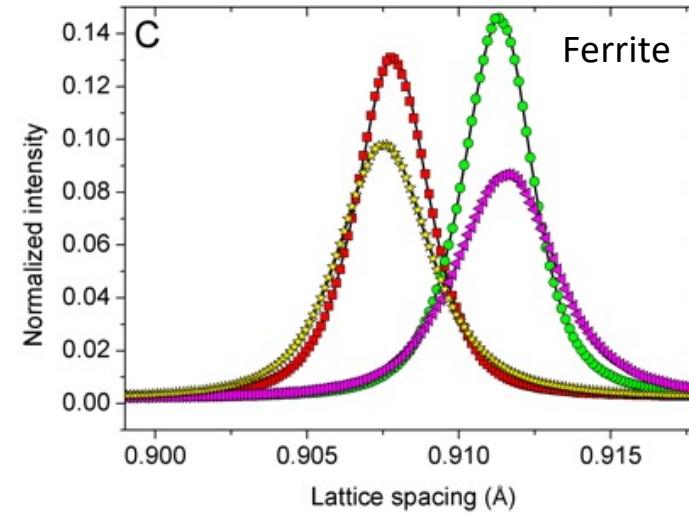
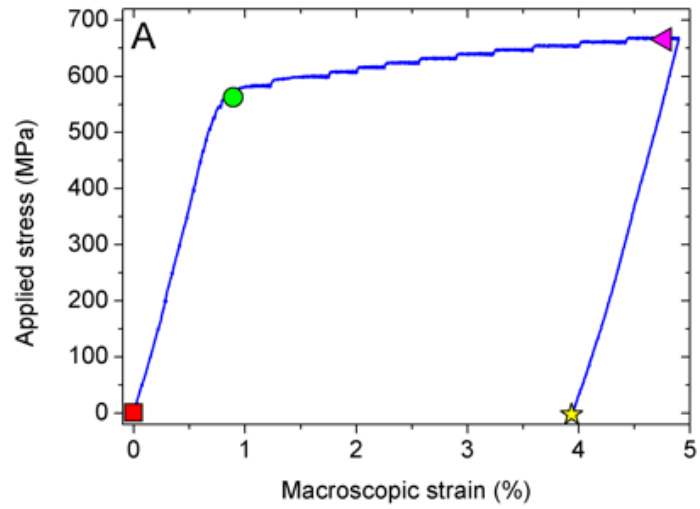
Issue with statistics

- When the sample cannot be rotated
 - Issue with large-grained materials
 - Issue with texture
- Solutions:
 - Small oscillations during acquisition of one spectrum
 - Time-of-Flight neutron diffraction
 - But, neutron diffraction doesn't pick up phases with low volume fraction

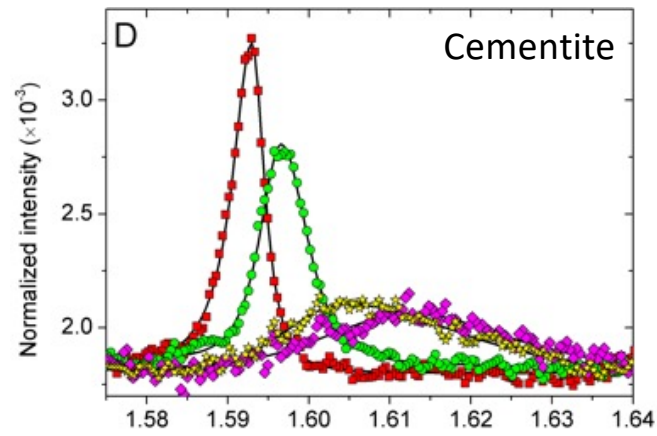
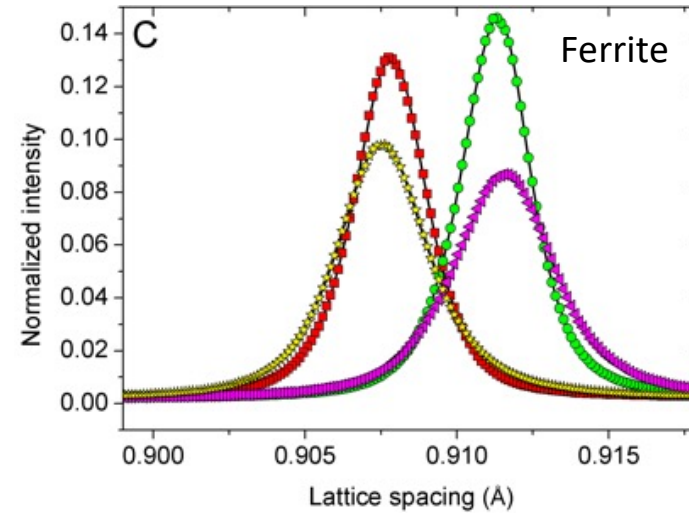
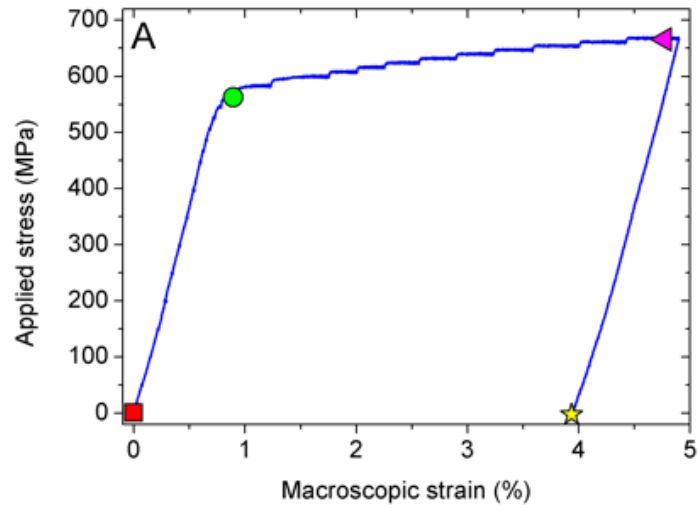
Combine X-Rays and Neutrons



Evolution peak profiles

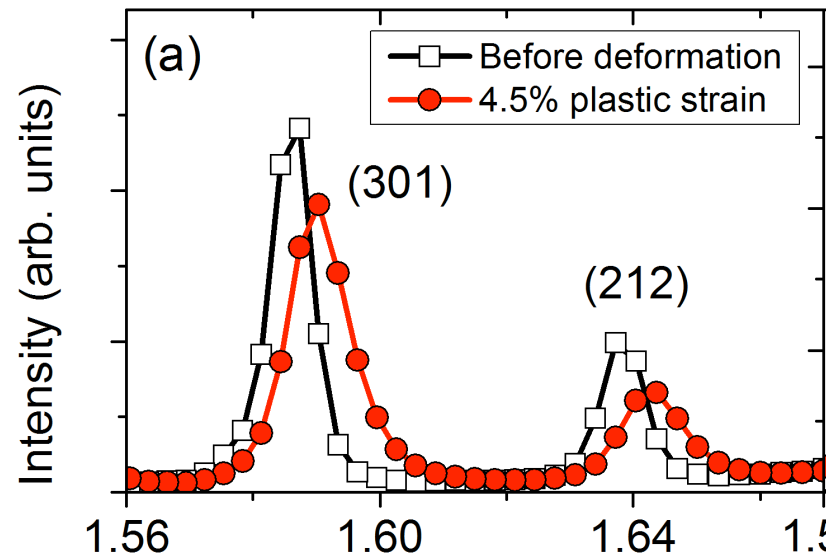
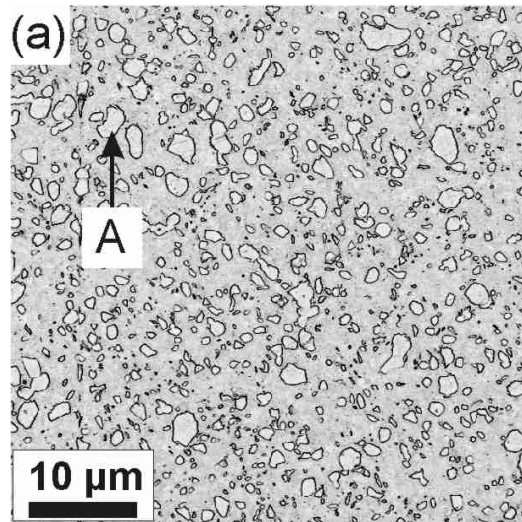


Evolution peak profiles



→ Cementite plastically deformed?

Homogeneous ferrite – cementite structure

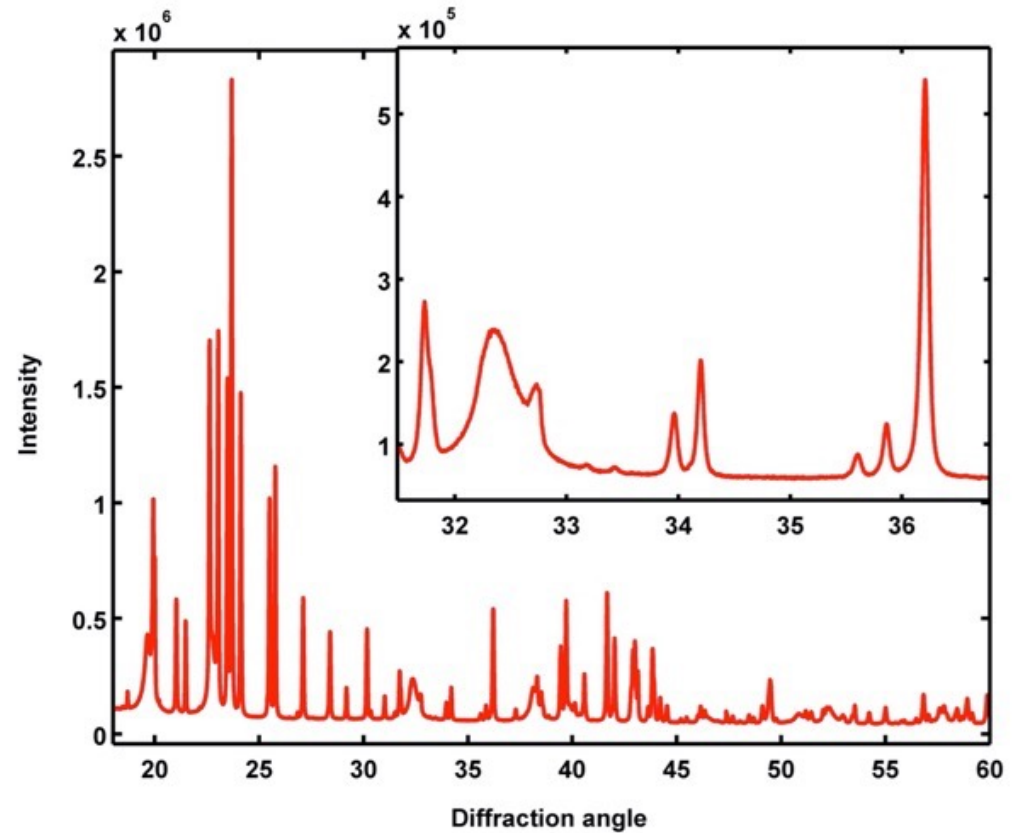


Much less cementite peak broadening in homogeneous structure ...

Broadening in cementite?



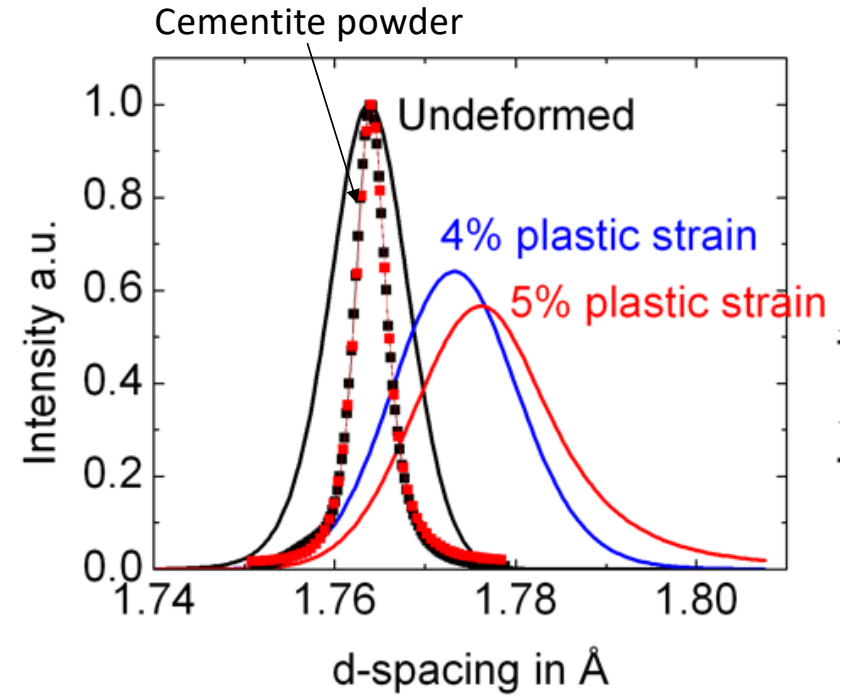
- Separate carbide powder from the matrix: ca. 3wt.%
- Record diffraction pattern (Cementite & Vanadium Carbide)
- Compare before and after deformation



Broadening in cementite?

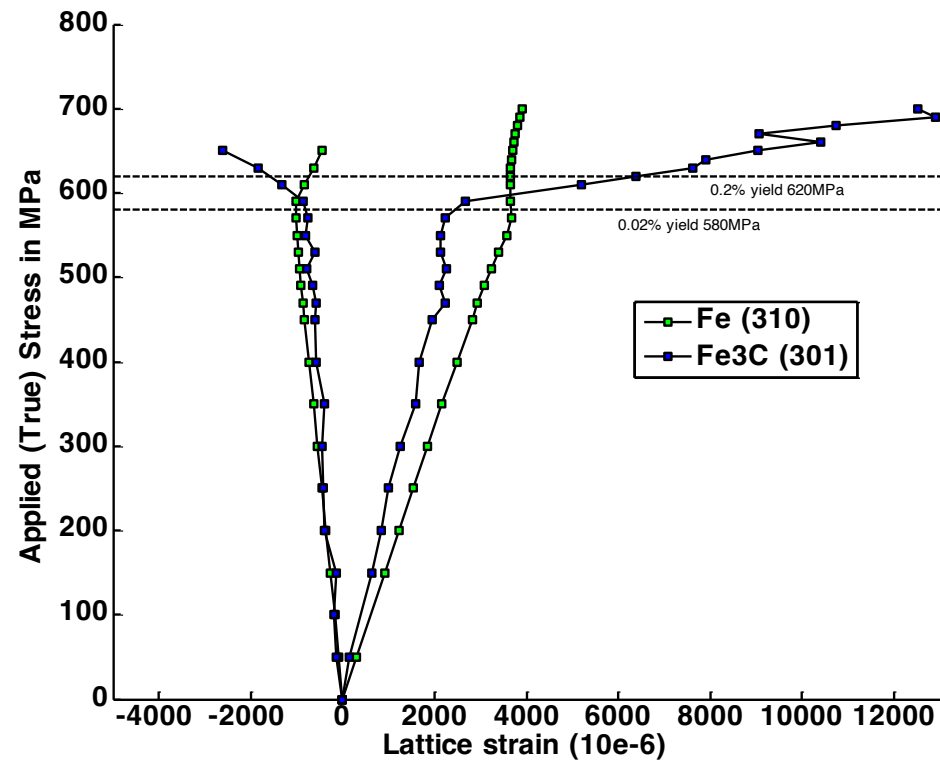


Not broadening because of size
Not broadening because of dislocations
So what is it?



Cementite broadening comes from ...

Different stress levels in the precipitates (diffraction peaks consist of many narrower peaks, slightly shifted compared to each other)

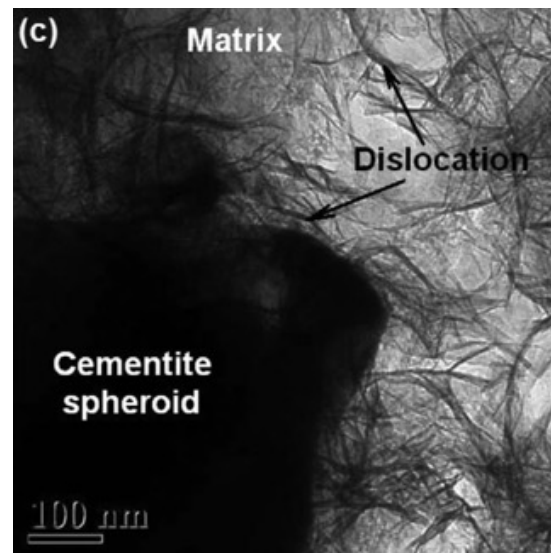


Cementite broadening comes from ...

Different stress levels in the precipitates (diffraction peaks consist of many narrower peaks, slightly shifted compared to each other)

or ...

Pile-up of dislocations at the precipitate – matrix interface causing strong strain gradients inside the precipitates





Take home messages:

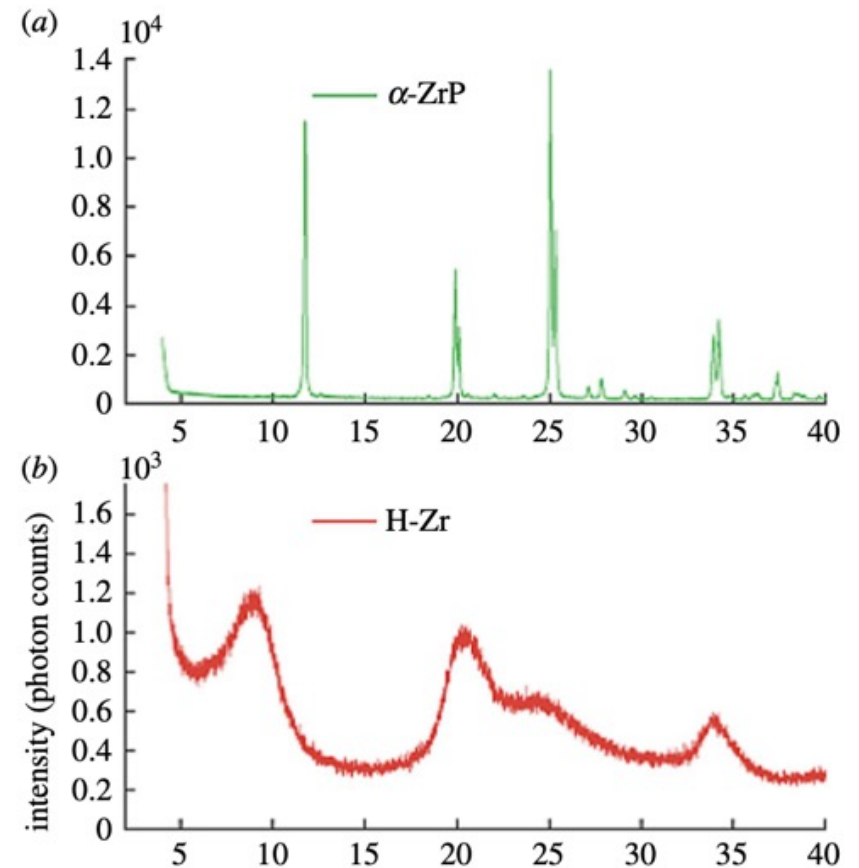
Heterogeneous microstructure can lead to significant peak broadening

Peak broadening not necessarily an indication for plasticity



Pair distribution function

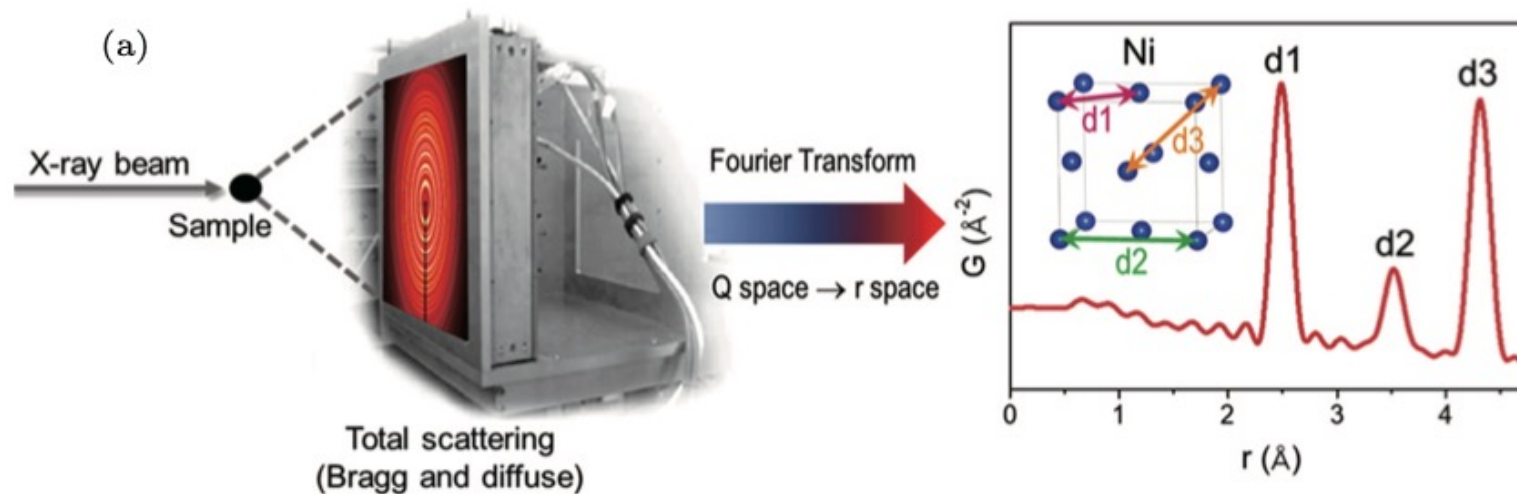
- X-ray powder diffraction ideal for materials with sufficiently large grain size
- For nanocrystalline materials with grain sizes in the range of a few nm or for amorphous materials, the diffraction peaks become very broad and diffuse.
- Peak profile analysis does not work, as several assumptions do not hold up at very small grain sizes.
- In the pair distribution function a wide range of reciprocal space is probed.



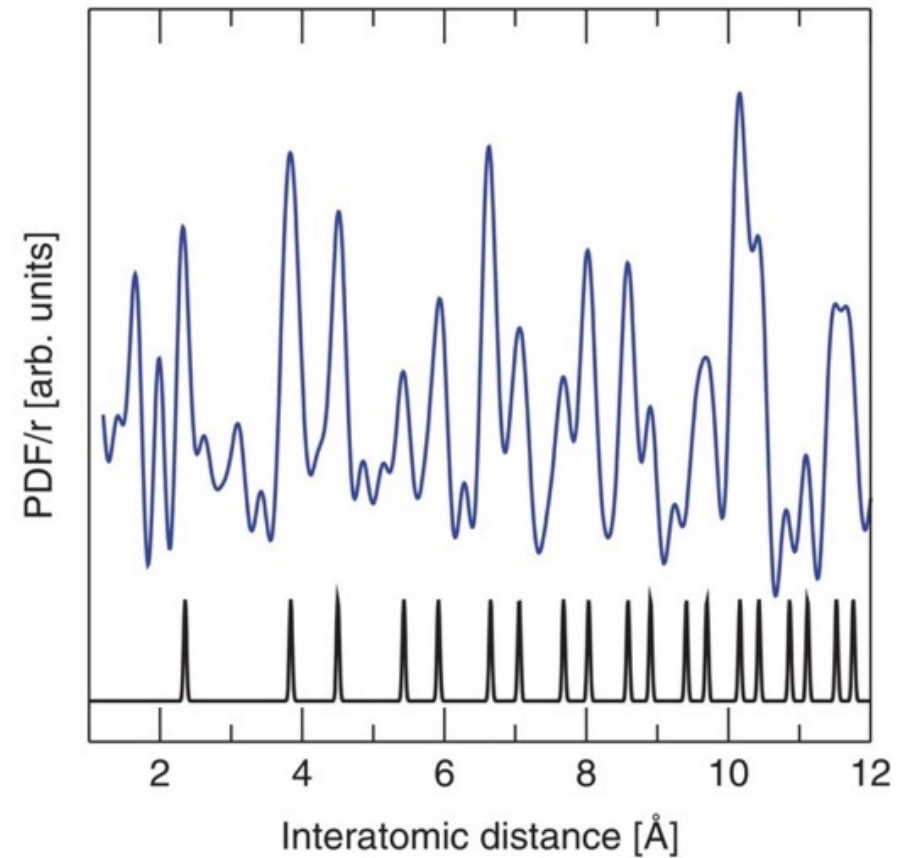
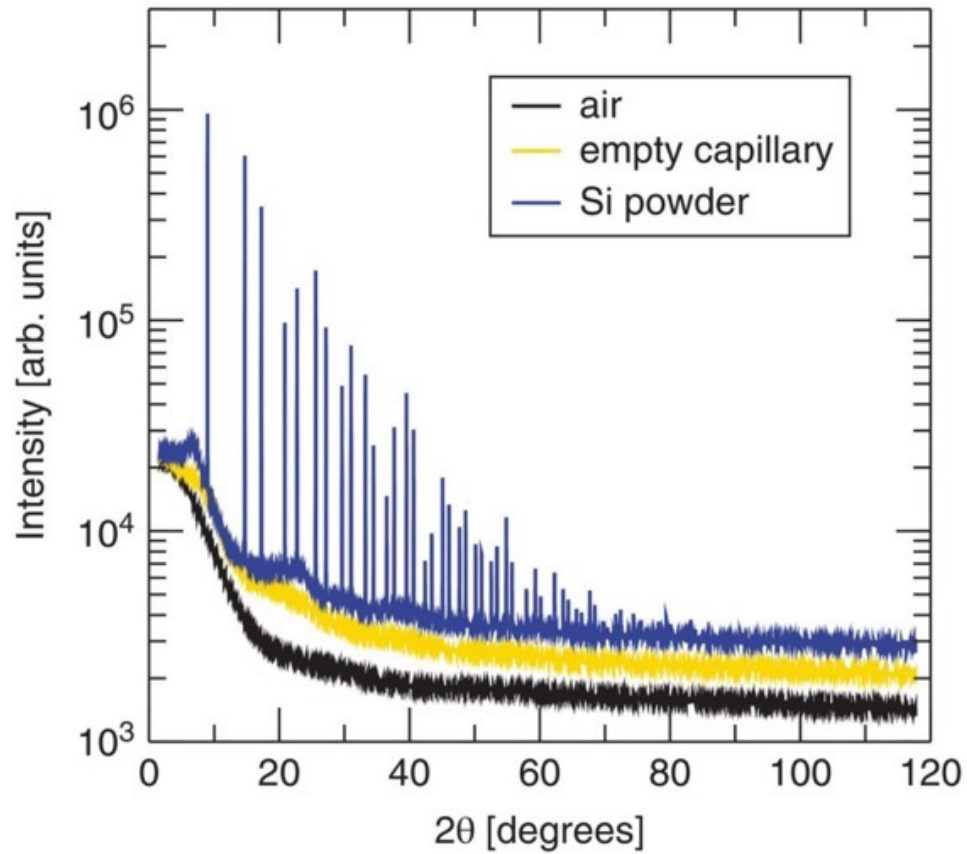
Pair distribution function

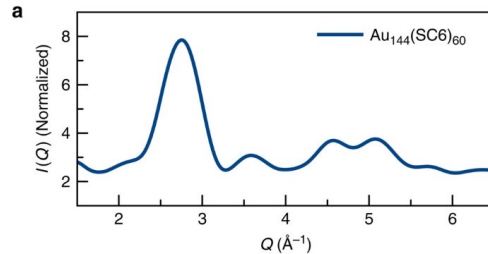
PDF:
$$g(r) = \frac{1}{4\pi\rho_0 r^2 N} \sum_i \sum_{j \neq i} \delta(r - r_{ij})$$

With ρ_0 the average number density of atoms, N the total number of atoms and r_{ij} the distance between atoms i and atom j . The PDF gives the scaled probability of finding two atoms in a material a distance r apart



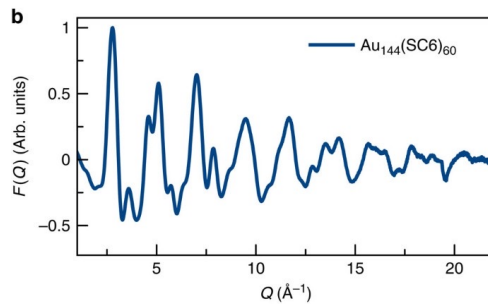
Pair distribution function





Material & question

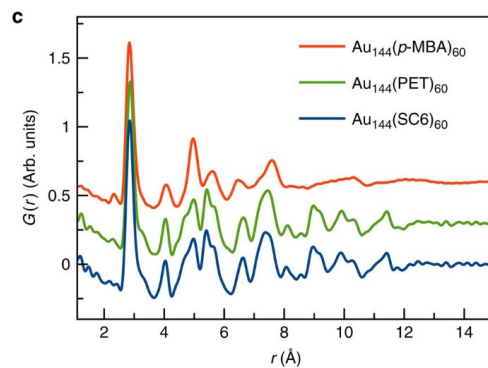
Ultra-small, *magic-sized* gold nanoclusters $\text{Au}_{144}(\text{SR})_{60}$. Can we determine their atomic structure when conventional Bragg diffraction is too sparse/broadened to solve it?



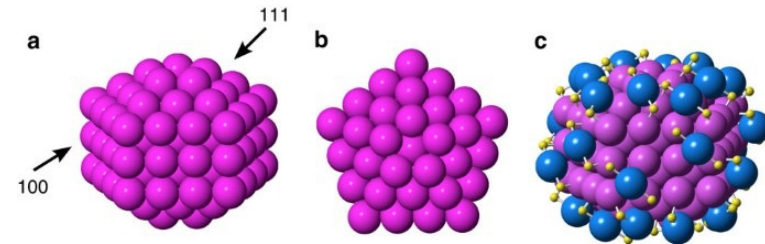
What they did

Collected **X-ray total scattering** from powders of $\text{Au}_{144}(\text{SR})_{60}$.

Performed **PDF analysis** (Fourier transform of total scattering) to obtain **$G(r)$** and fit structural models.



Resolved **structural polymorphism** (distinct 3D atomic arrangements) that ordinary powder XRD could not uniquely reveal





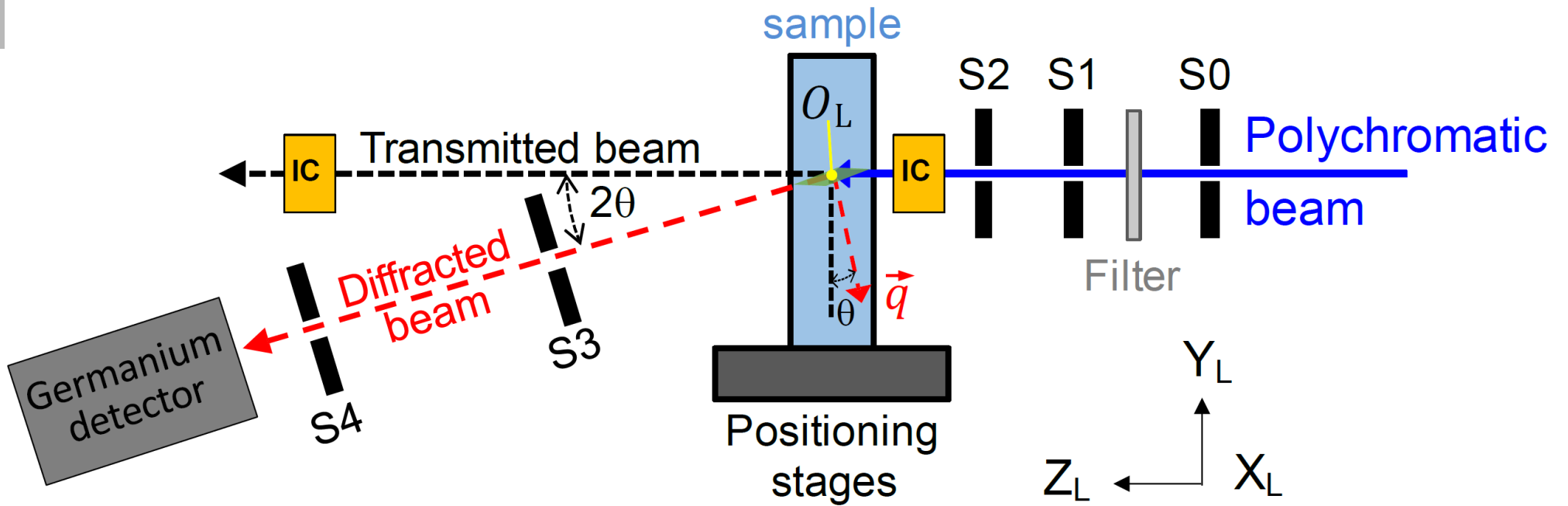
Energy dispersive X-ray diffraction

- In EDXRD the diffraction angle θ is kept constant and the lattice spacing d is obtained experimentally by determining the energy E of the diffracted beams of the originally polychromatic beam:

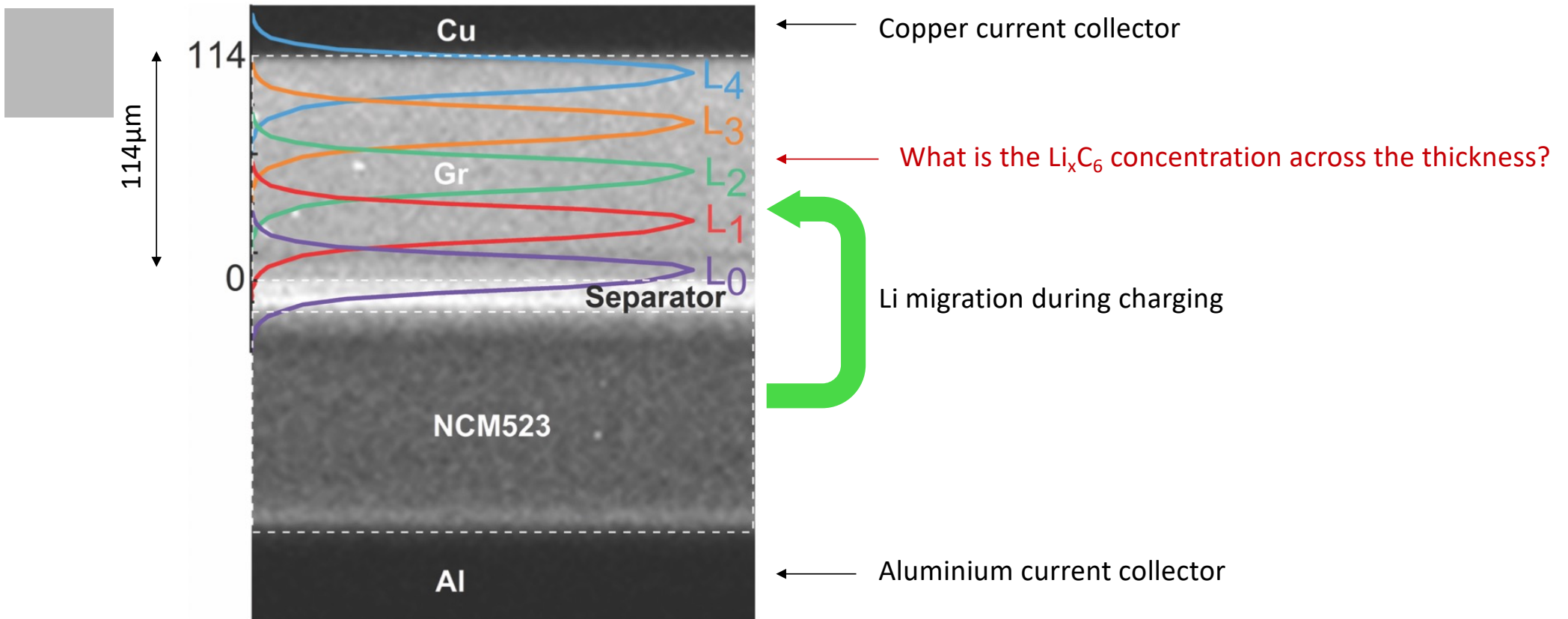
$$d = \frac{hc}{2E \sin \theta}$$

- Usually used in combination with high X-ray energies to allow for large penetration depths.
- No need for a goniometer, can even be made portable.
- When using a wide energy range, depth-dependent measurements are possible.

Energy dispersive X-ray diffraction



Application – Battery research



Quantifying lithium concentration gradients in the graphite electrode of Li-ion cells using operando energy dispersive X-ray diffraction.

Koffi P. C. Yao et al, Energy & Environmental Science 12 (2019) 656

Experiment:

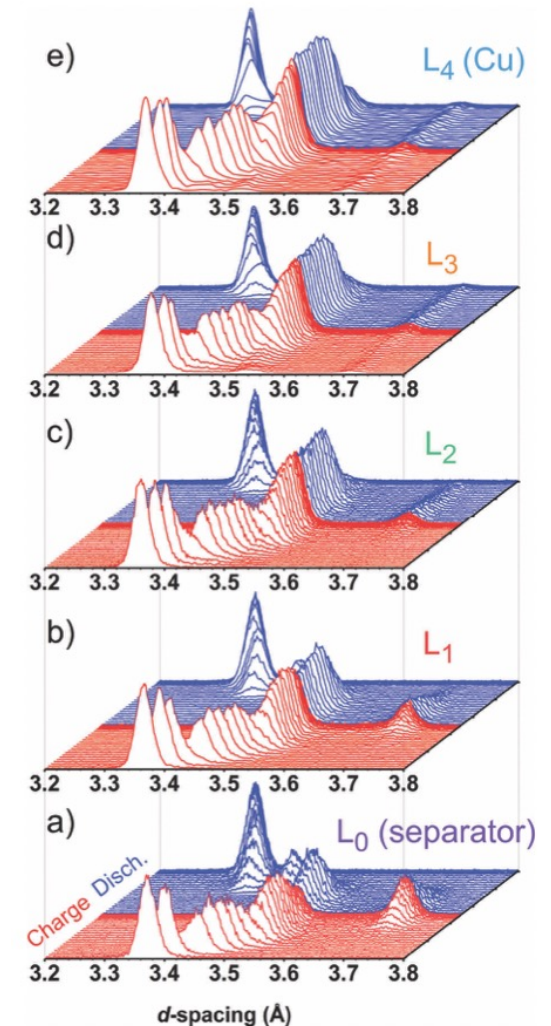
- X-ray photons with energies between 5 and 250 keV
- Ge detector placed at a fixed angle $\theta \approx 3^\circ$
- X-ray beam was $18.3 \mu\text{m} \times 1045 \mu\text{m}$
- 1 min per acquisition for a total period of 3 h per charge/ discharge cycle

Analysis

- The Li–Gr intercalation system exhibits several phases (commonly referred to as stages)
- The Li content x is found by:

$$x = \sum_i x_i = \sum_i \Gamma_i / \sum_j f_j^{-1} \Gamma_j \quad \Gamma_j = I_j^{hkl} / (m_j^{hkl} |F_j^{hkl}|^2)$$

with f_j is the fractional Li content of the corresponding Li_xC_6 phase j , I^{hkl} is the relative integrated flux of scattered X-ray photons from phase j , m_{hkl} is the multiplicity of the Bragg reflection with the Miller indices (hkl) originating from phase j in the peak region of interest, and F_{hkl} is the corresponding scattering factor



Species	Strongest Bragg peak, (hkl)	Multiplicity m_{hkl}	Estimated F_{hkl}	Value of f_i
graphite	(002)	2	16.8	0
LiC ₃₀	(004)	2	49.72	1/5
LiC ₁₈	(004)	2	33.85	1/3
LiC ₁₂	(002)	2	50.2	1/2
LiC ₆	(001)	2	25.3	1

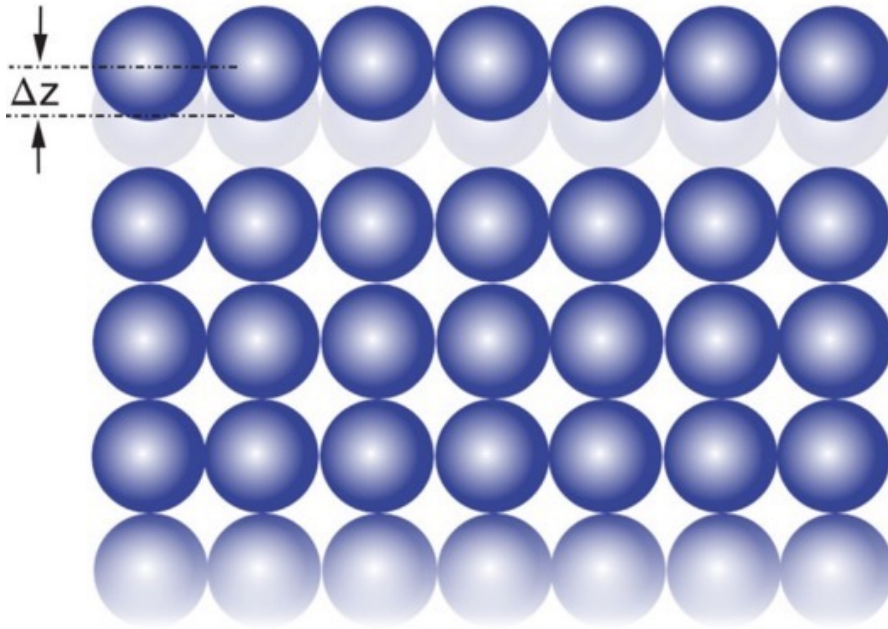
Quantifying lithium concentration gradients in the graphite electrode of Li-ion cells using operando energy dispersive X-ray diffraction.

Koffi P. C. Yao et al, Energy & Environmental Science 12 (2019) 656

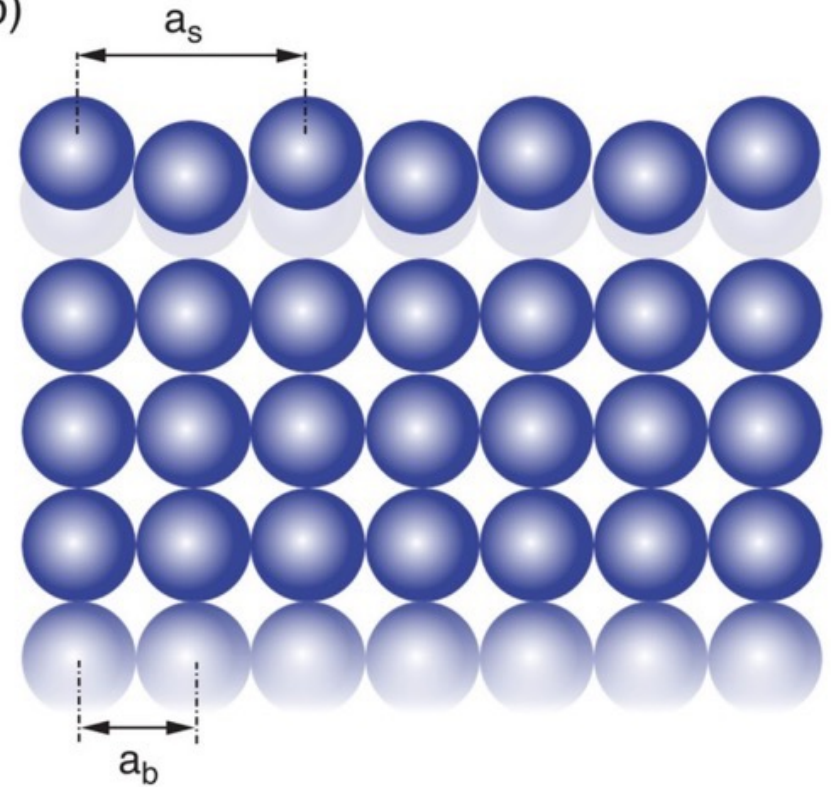


Surface X-ray diffraction

(a)



(b)



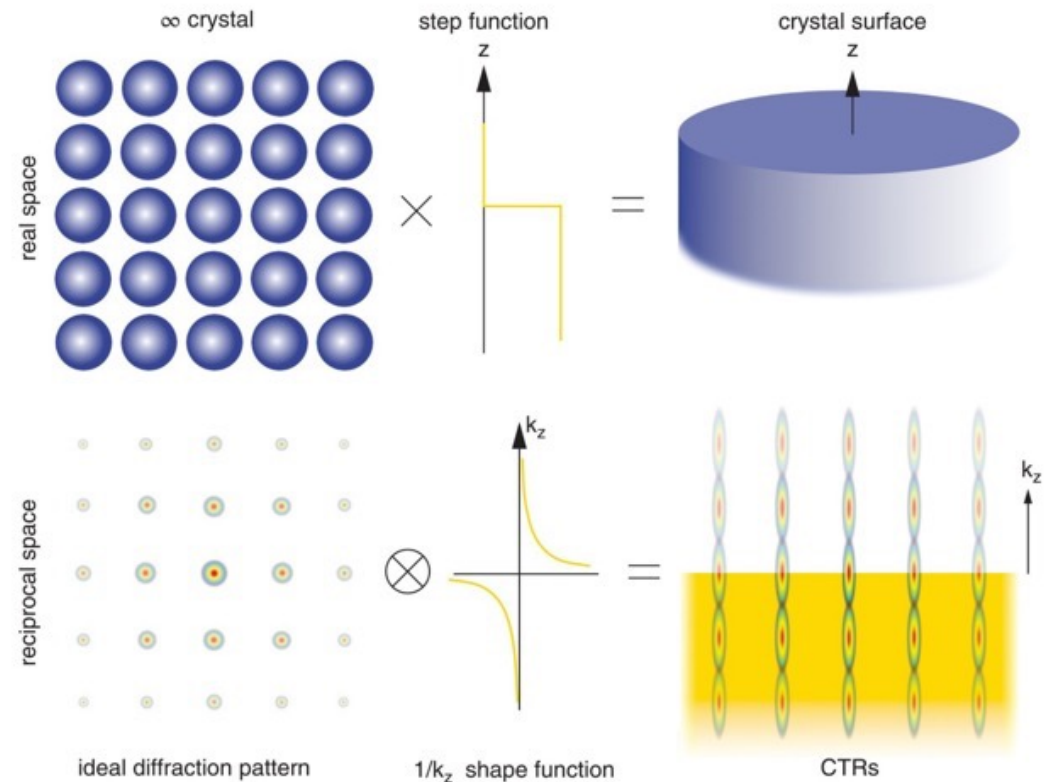
Surface X-ray diffraction

- In the simplest derivation of diffraction patterns, two assumptions are made – firstly, that one is operating in the kinematical limit (that is, single-scattering), and secondly, that the crystal is infinitely large. This results in the diffraction peaks being infinitely narrow (known as ‘delta functions’). In reality, of course, all diffraction spectra are smeared out to a certain degree because there is partial absorption and extinction.
- Crystals are finite in extent and one therefore measures a finite sample volume. The diffraction pattern of a finite crystal can be generated by convolving the Fourier transform of an infinitely large crystal structure (i.e. its ‘ideal’ diffraction pattern) with the Fourier transform of the function describing the boundary of the real crystal (called the ‘shape function’).

Surface X-ray diffraction

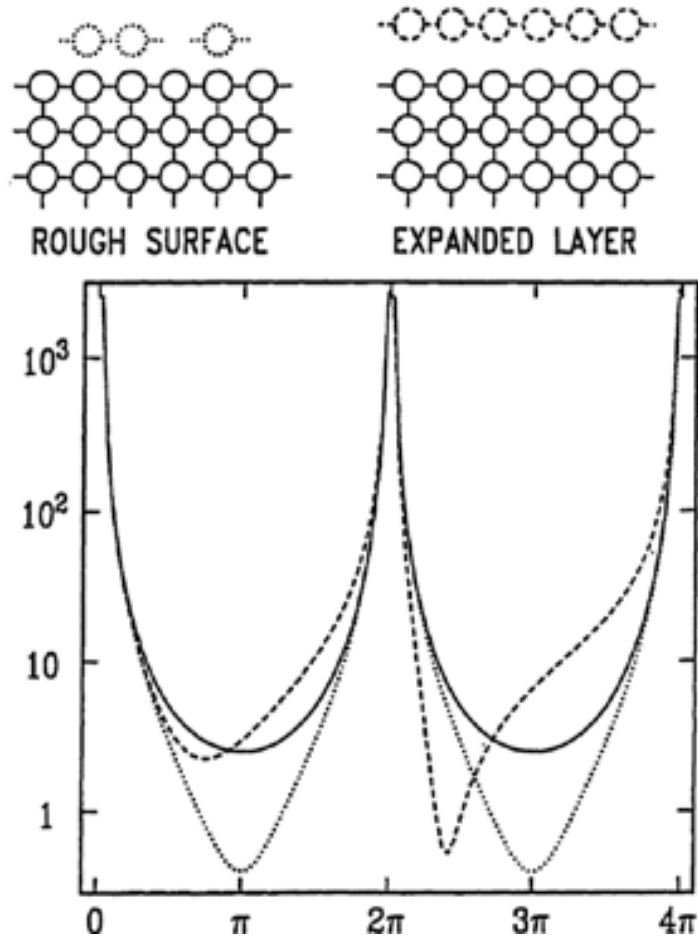
A single crystal terminated with an atomically flat surface has a step function as the boundary function. This has an FT showing a $1/k_z$ relationship that extends significantly in reciprocal space. The convolution of this with the 'ideal' diffraction pattern results in the latter being smeared out to produce a continuous signal in the direction perpendicular to the sample surface. These are crystal truncation rods (CTRs).

Any shifts in the atomic positions of the upper layers from their bulk positions, due to surface reconstructions and/or relaxations, will have a marked effect on the form and magnitude of the scattered amplitudes in portions of the CTRs away from the Bragg maxima. Recording CTRs therefore provides an exceptionally sensitive method for unravelling the structure of crystalline surfaces and interfaces.



Surface X-ray diffraction

- SXRD measurements are carried out using a grazing incident angle α , with respect to the sample surface. The choice of α depends on the experiment, sample quality, and scattering strength.
- For incident angles close to the critical angle α_c , the surface sensitivity increases rapidly. Exactly at α_c , the reflected wave is perfectly in phase with the incident wave, and the evanescent wave amplitude is approximately twice that of the incident wave. The evanescent *intensity* therefore approaches four times that of the incident beam. The penetration depth is low, and so the bulk contribution is suppressed. Hence, at α_c , the surface sensitivity is highest
- Disadvantage: large footprint on the sample and very sensitive to small changes (0.01 degrees) of the incoming angle.



- The full curve is for an ideally terminated simple-cubic lattice of atoms; its functional form is just $1/(\sin q_z)^2$, whose divergence at Bragg points $q = 2n\pi$ is clearly visible.
- The dashed curve corresponds to an outward displacement of a single layer of atoms at the surface; the intensity curve near the Bragg peaks, where there is little surface sensitivity, is barely changed, but the intensity at the CTR minimum is strongly modified.
- The dotted curve is for a rough surface, modeled by random omission of a fraction of the atoms in the top layer. The biggest effect is at the CTR minimum, this time with a symmetric drop of the intensity curve.